Washington University in St. Louis
Washington University Open Scholarship

All Theses and Dissertations (ETDs)

Spring 3-8-2014

The Role of FGF Signaling in the Regulation of Adult Murine Cardiomyocyte Contractility and Pathologic Hypertrophy

Sarah Nicole Cilvik
Washington University in St. Louis

Follow this and additional works at: https://openscholarship.wustl.edu/etd

Recommended Citation
Cilvik, Sarah Nicole, "The Role of FGF Signaling in the Regulation of Adult Murine Cardiomyocyte Contractility and Pathologic Hypertrophy" (2014). *All Theses and Dissertations (ETDs)*. 1231.
https://openscholarship.wustl.edu/etd/1231

This Dissertation is brought to you for free and open access by Washington University Open Scholarship. It has been accepted for inclusion in All Theses and Dissertations (ETDs) by an authorized administrator of Washington University Open Scholarship. For more information, please contact digital@wumail.wustl.edu.

WASHINGTON UNIVERSITY IN ST. LOUIS

Division of Biology & Biomedical Sciences
Developmental Biology

Dissertation Examination Committee:
David M. Ornitz, Chair
Kyunghee Choi
Peter Crawford
Patrick Jay
Robert Mecham
Jean Schaffer

The Role of FGF Signaling in the Regulation of Adult Murine Cardiomyocyte Contractility and Pathologic Hypertrophy

By

Sarah Nicole Cilvik

A dissertation presented to the
Graduate School of Arts and Sciences
of Washington University in
partial fulfillment of the
requirements for the degree
of Doctor of Philosophy

May 2014

St. Louis, Missouri

© 2014, Sarah Nicole Cilvik

Table of Contents

List of Figures iv

List of Tables vi

List of Abbreviations vii

Acknowledgements x

Abstract xi

Chapter 1 – Introduction: FGF Signaling in the Heart and Relevance to Postnatal Cardiac Remodeling 1

A. Significance 2

B. Cardiovascular Remodeling 2

C. Fibroblast Growth Factor Family 3

D. Fibroblast Growth Factor Signaling in Heart Development 4

E. Fibroblast Growth Factor Signaling in the Postnatal Heart 7

F. Implication of FGF-activated Signaling Pathways in Hypertrophy 12

G. Conclusions 16

H. Disclosure of co-authored works 17

Figures 18

Chapter 2 – Altered Gene Expression of FGF Ligands and Receptors in Postnatal Cardiac Remodeling 19

A. Introduction 20

B. Results 21

C. Discussion 28

Figures 33

Chapter 3 – Development of Hypercontractility and Hypertrophic Cardiomyopathy through Modulation of Sarcomere Mechanics 54

A. Introduction 55

B. Results 56

C. Discussion 65

Figures 71

Chapter 4 – Conclusions and Future Directions 90

Chapter 5 – Materials and Methods 96

Figures 104

Chapter 6 – References 107

List of Figures

Figure 1.1 FGF Signaling Pathway 18

Figure 2.1 Over-expression of FGF9 promotes transition from hypertrophy to heart failure 33

Figure 2.2 Cardiac-specific overexpression of FGF9 in the adult heart results in diastolic dysfunction with preservation of systolic function 35

Figure 2.3 Overexpression of FGF9 in the adult heart leads to increased fibrosis 36

Figure 2.4 Changes in gene expression following three weeks of cardiac FGF9 overexpression 37

Figure 2.5 Different gene expression profiles from exercise-induced versus caPI3K-induced physiological hypertrophy models 39

Figure 2.6 Gene expression changes one week post-aortic banding 40

Figure 2.7 Angiotensin Ii infusion induces hypertrophy, enhanced systolic function, and increased fibrosis in wild-type mice 41

Figure 2.8 Changes in gene expression following AngII treatment 42

Figure 2.9 Altered gene expression one week following MI 43

Figure 2.10 Possible mechanisms for FGF2-mediated cardioprotection 45

Figure 2.11 Tamoxifen-inducible cardiomyocyte-specific FGFR1/2 double conditional knockout (MHC-CreER DCKO) 47

Figure 2.12 MHC-CreER DCKO mice have a poorer response following myocardial infarction 49

Figure 2.13 MHC-CreER DCKO mice show increased expression of markers of pathological remodeling 50

Figure 2.14 Proposed models for regulation of paracrine FGF signaling in the adult heart 52

Figure 3.1 Inducible constitutively-active FGFR1 genetic system shows minimal baseline activity 71

Figure 3.2 Constitutively-active FGFR1-myc is rapidly inducible with consistently maintained levels of expression over time 73

Figure 3.3 Induction of caFGFR1 in adult cardiomyocytes results in the development of concentric hypertrophy with preservation of systolic function over time 74

Figure 3.4 *In vivo* induction of caFGFR1 in adult cardiomyocytes leads to a hypercontractile phenotype with the development of a dynamic obstruction in the proximal left ventricle 76

Figure 3.5 Chronic induction of caFGFR1 results in a pathologic state with molecular and histologic characteristics of hypertrophic cardiomyopathy 78

Figure 3.6 Chronic induction of caFGFR1 and significant concentric hypertrophy does not cause exercise intolerance in double transgenic mice 80

Figure 3.7 Transgene induction for 42 days, followed by DOX removal for 42 days leads to a partial phenotype reversal 81

Figure 3.8 Induction of caFGFR1 results in transient ERK1/2 activation and sustained downregulation of Akt activation 83

Figure 3.9 Double transgenic mice have significantly decreased troponin I phosphorylation and Serca2 expression 84

Figure 3.10 Ventricular myocytes from double transgenic mice have impaired relaxation and enhanced contraction 85

Figure 5.1 pTRE2-FGF2/EGFP plasmid 104

List of Tables

Table 2.1 Summary of notable gene expression changes in different models of cardiac remodeling 53

Table 3.1 Hemodynamic analysis of double transgenic and littermate control mice following 24 hours on DOX 86

Table 3.2 Hemodynamic analysis of double transgenic and littermate control mice following 42 days on DOX 87

Table 3.3 Blockade of FGFR tyrosine kinase partially ameliorates LV hypertrophy development in caFGFR1-expressing mice 88

Table 3.4 Blockade of beta-adrenergic and angiotensin receptors lessens phenotype development in caFGFR1-expressing mice 89

Table 5.1 Primary and secondary antibodies utilized for Western blotting 105

Table 5.2 ABI Taqman® gene expression assays for quantitative RT-PCR analysis 106

List of Abbreviations

AAC	Ascending aortic constriction
AngII	Angiotensin II
ANP	Atrial natriuretic peptide
BDM	2,3-Butanedione monoxime
βMHC	beta-myosin heavy chain
BNP	B-type natriuretic peptide
BPM	Beats per minute
ca	Constitutively-active
CFCS	Cardiofaciocutaneous syndrome
CM	Cardiomyocyte
CS	Costello syndrome
CsA	Cyclosporine A
Ctl	Control
CVD	Cardiovascular disease
DCKO	Double conditional knockout
DFF	Double floxed floxed
DOX	Doxycycline
DTG	Double transgenic
EC	Endothelial cell
EDP	End diastolic pressure
EDV	End diastolic volume
EF	Ejection fraction
EMT	Epithelial-mesenchymal transition
ERK	Extracellular-regulated kinase
ESP	End systolic pressure
ESPVR	End systolic pressure-volume relationship
ESV	End systolic volume

FGF	Fibroblast growth factor
FITC-WGA	Fluorescein-tagged wheat germ agglutinin
FRS2	FGFR substrate 2
FS	Fractional shortening
GAB1	GRB2-associated binding protein 1
GRB2	Growth factor receptor-bound 2
HCM	Hypertrophic cardiomyopathy
HR	Heart rat
HSPG	Heparan sulfate proteoglycan
HW/BW	Heart weight to body weight ratio
IGF1	Insulin-like growth factor-1
JNK	Jun N-terminal kinase
LS	LEOPARD syndrome
Los	Losartan
LV	Left Ventricle
LVAD	Left ventricular assist device
LVIDd	Left ventricular internal diastolic diameter
LVMI	Left ventricular mass index
LV POV	Left ventricular peak outflow velocity
LVPWd	LV diastolic posterior wall thickness
LW/BW	Lung weight to body weight ratio
MAPK	Mitogen-activated protein kinase
MEK	Mitogen-activated protein kinase kinase
MI	Myocardial infarction
NS	Noonan syndrome
PD17	PD173074
PKA	Protein kinase A
PKC	Protein kinase C

PLCγ	Phospholipase C-gamma
Pro	Propranolol
SEM	Subepicardial mesenchyme
Serca2	Sarcoplasmic reticulum ATPase 2
SHF	Second heart field
SHM	Sham
SHP2	Sh2 domain-containing protein tyrosine phosphatase
SOS	Son of sevenless
STAT	Signal transducer and activator of transcription
TAC	Transverse aortic constriction
TKD	Tyrosine kinase domain
TnI	Troponin I
VSMC	Vascular smooth muscle cell
Wort	Wortmannin

Acknowledgements

First and foremost, I would like to extend my sincerest thanks to my thesis advisor, David Ornitz, without whom I would not have made it through my PhD. His patience and kindness are true virtues, and his passion for science is aspirational. I greatly appreciate all of the time you devoted to me, making me into a better scientist and a stronger person. I would also like to thank Kory Lavine and Stacey House, two former MSTP students who gave much-needed advice and helped guide me through this process. You are both amazing physician scientists that anyone in our program should aspire to! Probably the most instrumental people to the completion of my thesis work were those in the Mouse Cardiovascular Phenotyping Core, especially Dr. Attila Kovacs, Carla Weinheimer. To Dr. Attila Kovacs, you taught me nearly everything I know about cardiovascular pathophysiology and echocardiography, and I know that I will continue to be grateful to you when I return to clinics this winter. To Carla Weinheimer, I am continually in awe of your surgical skills, and am so appreciative of everything you did for my project. Thank you to Angela Castro, Keita Uchida, and Colin Nichols, without whom I could not have achieved a satisfying end to my story. I am forever in your debt for your excellent advice and hard work right down to the wire! To my undergraduate student, Joy Wang, thank you for your excellent work, even on the most menial tasks, and thank you for always listening to me vent! Thank you to my thesis committee, Jean Schaffer, KC Choi, Bob Mecham, Patrick Jay, and Peter Crawford, for continued guidance throughout my PhD. To my great friends and MSTP classmates, Radhika Jagannathan and Gary Wang, you pulled me through when I wanted to quit, and I can't thank you enough for helping me to continually see the bigger picture! Most of all, thank you to my wonderful family and absolutely amazing husband. You were all there for me in my darkest hours and my brightest days. You believed in me when I didn't believe in myself. You fed me when I didn't have time to eat, and you listened to me rant when you had no idea what I was talking about. You will never know how much this unconditional love and support meant to me!

This work was supported by NIH grant HL105732 (D. Ornitz), American Heart Association grant 0910110G (S. Cilvik), and NIH grant HL45742 (C. Nichols). Transgenic mouse production was made possible through the Washington University Musculoskeletal Research Center (NIH grant P30 AR057235).

ABSTRACT OF THE DISSERTATION

The Role of FGF Signaling in the Regulation of Adult Murine Cardiomyocyte Contractility and Pathologic Hypertrophy

By

Sarah Nicole Cilvik

Doctor of Philosophy in Biology & Biomedical Sciences

Developmental Biology

Washington University School of Medicine, 2014

Professor David M. Ornitz, Chairperson

Cardiovascular diseases (CVDs) have been the leading cause of death in the United States for decades. They cause significant strain on the heart, resulting in an ongoing remodeling process that initially maintains cardiac function, but ultimately becomes maladaptive. The signaling pathways that drive cardiac remodeling are extremely complex and poorly understood, and therefore, a better understanding of the mechanisms involved in the development and progression of CVDs is essential in order to diagnose and treat these diseases more effectively. Fibroblast growth factors (FGFs) and their receptors are part of a large family of highly conserved signaling molecules that have been implicated in postnatal cardiac remodeling. FGF signaling increases following injury to the heart, and published studies demonstrate that FGF2 is cardioprotective following cardiac stress or injury. Despite the importance of FGF2 following injury, mice that lack or overexpress FGF2 develop normally and do not have any cardiac phenotype under homeostatic conditions. It is currently unknown how FGF signaling is regulated in the adult heart and why effects of FGF2 are only observed following injury. As a result, it was the goal of my thesis research to gain a better understanding of the role of FGF signaling in adult cardiac remodeling. I hypothesized that FGF signaling may be repressed in the adult heart under homeostatic conditions and becomes reactivated following injury. I utilized a doxycycline-inducible, cardiomyocyte-specific, constitutively-active FGF receptor (caFGFR1) mouse model to test whether the cardiomyocyte has the capacity to respond to a cell autonomous FGF signal. Induction of this transgene led to immediate changes in cardiac contractility and the eventual development of hypertrophic

cardiomyopathy (HCM) without progression to heart failure or premature death. Induction of caFGFR1 appears to increase the calcium sensitivity and decrease relaxation of the sarcomere through dephosphorylation of troponin I, and also by potentially increasing cytosolic calcium, mechanisms implicated in classic HCM models. Our doxycycline-inducible cardiomyocyte-specific caFGFR1 mouse provides a unique model of HCM that can be utilized to further characterize pathways that lead to phenotype development, as well as prevention or reversal.

Chapter 1

Introduction: FGF Signaling in the Heart and Relevance to Postnatal Cardiac Remodeling

A. Significance – The burden of cardiovascular disease in the United States

An estimated 82 million American adults have at least one type of cardiovascular disease, such as hypertension, myocardial infarction (MI), stroke, heart failure, and congenital cardiac defects. One out of every three deaths in the United States can be attributed to CVD, with an average of one American dying every 39 seconds [1]. CVD claims more lives than cancer, chronic lower respiratory disease and accidents combined, making it the leading cause of death in the United States in all but one year since 1900 [1]. Its total costs (direct and indirect) were estimated to be close to $500 billion in 2012, accounting for 16% of total health expenditures, more than any other disease [1]. The American Heart Association (AHA) predicts that more than 40% of Americans will have some form of CVD by the year 2030, with total costs increasing to more than $1.1 trillion [1]. As such, CVD represents a tremendous and continually increasing physical and financial burden to both Americans and the health care system. Therefore, a complete understanding of the mechanisms involved in the development and progression of CVD is essential in order to diagnose and treat these diseases more effectively, thus decreasing their morbidity and mortality.

B. Cardiovascular Remodeling

Cardiovascular diseases cause significant strain on the heart. For example, hypertension results in a pressure overload that the heart must overcome to effectively pump blood out of the ventricles, while myocardial infarction results in muscle death, leading to an increased workload for surviving muscle. In any event, the heart responds to such stress or injury by altering its myocardial structure and function, often through reactivation of developmental signaling pathways. Given the limited proliferative capacity of adult cardiomyocytes, the adult heart must rely on hypertrophy of existing myocytes in order to increase its size, which initially normalizes wall stress and maintains cardiac function. However, this pathological hypertrophy is characterized by predominantly increased myocyte width, fibrosis, and decreased ventricular chamber volume, and progressive remodeling inevitably leads to contractile dysfunction, ventricular dilatation, and heart failure [2-4]. In addition to pathological hypertrophy induced by an external cardiac stressor such as hypertension (secondary pathological hypertrophy), there is a primary myocardial disorder, hypertrophic cardiomyopathy (HCM), that is most often caused by mutations in

sarcomeric proteins. Like secondary hypertrophy, HCM is also pathological and characterized by increased myocyte width and fibrosis. However, what distinguishes HCM from other pathological hypertrophy is the presence of sarcomere disorganization and cardiomyocyte disarray. Additionally, the majority of patients with this type of primary pathological hypertrophy have maintained or even enhanced systolic function; only in rare cases does HCM progress to heart failure [5, 6].

In addition to primary and secondary pathological hypertrophy, there is a more beneficial (physiological) hypertrophy that allows the heart to increase in size in response to postnatal development (to adapt to the increasing size of the animal), as well as pregnancy or exercise (to adapt to increased workload demands). Physiological hypertrophy is characterized by a predominant increase in myocyte length, absence of fibrosis, maintenance of chamber dimension, and normal or enhanced cardiac function [2, 3, 7, 8]. Many studies have attempted to elucidate mechanisms that result in hypertrophy, but this process is extremely complex and remains poorly understood, particularly with regard to mechanisms that distinguish the advantageous physiological hypertrophy from the detrimental pathological hypertrophy. Evidence has shown that developmental pathways and re-expression of fetal genes are involved in regulating postnatal cardiac growth [9-11], and thus it is essential to understand the normal developmental pathways and how they can be reactivated and reused for growth of adult tissues in order to manipulate remodeling mechanisms in a beneficial way. As will be discussed below, fibroblast growth factor signaling is one such pathway that is crucial to various aspects of cardiac development, thus making it an excellent candidate for modulation of cardiac growth and physiology during the adult period.

C. Fibroblast Growth Factor Family

Fibroblast growth factors (FGFs) and their receptors are part of a large family of signaling molecules that are highly conserved and found in organisms ranging from *C. elegans* to humans [12-14]. This diverse family of polypeptide growth factors is vital during embryogenesis, controlling cell proliferation and migration, as well as mesoderm formation, neural induction, anterior-posterior patterning, and endoderm formation. In the adult, FGFs play an important role in the nervous system, in tissue healing and wound repair, and in tumor angiogenesis [15, 16]. These biological responses are mediated by the binding of FGFs to one of four distinct FGF receptor (FGFR) tyrosine kinases. Regulation of

binding affinity and ligand specificity is achieved by the binding of FGFs to heparin sulfate proteoglycans (HSPG) in the extracellular matrix, as well as by alternative mRNA splicing of FGFRs [15, 16]. This splicing is tissue-specific, producing epithelial forms (b splice variants) and mesenchymal forms (c splice variants) [17-20]. Binding of FGFs and HSPGs together to the receptor causes receptor dimerization and tyrosine kinase autophosphorylation of the intracellular domain. Downstream FGF signal transduction can proceed via three main pathways—Ras/MAP kinase pathway, phospholipase Cγ (PLCγ)/Ca^{2+} pathway, or PI3 kinase/Akt pathway—but activation of p38 MAPK, Jun N-terminal kinase (JNK), signal transducer and activator of transcription (STAT), and ribosomal protein S6 kinase 2 (RSK2) pathways can occur in certain cellular contexts (Figure 1.1) [15, 16, 21].

Most of the 22 FGFs identified in mammals are secreted proteins, and their expression is highly variable. Some are ubiquitously expressed throughout life, such as FGF1 and FGF2, while other FGFs are restricted to a particular cell type and/or particular developmental stage [22]. Of the 22 FGFs, several are expressed in the heart and have been shown to be important for both cardiac development and response to injury. However, the precise roles for FGF signaling during cardiovascular development, homeostasis, and response to injury, as well as how the FGF network interacts with other signaling pathways active in the heart, are only beginning to be elucidated.

D. Fibroblast Growth Factor Signaling in Heart Development

FGF ligands in the embryonic heart. Of the 22 known *Fgf* genes in mammals, several are expressed in the developing heart. The expression of both FGF ligands and receptors in cardiac and vascular mesoderm, in mesothelium, and in endoderm suggests an important role for these molecules in development. The first FGFs discovered in heart tissue were FGF1 and FGF2 (or acidic and basic FGF, respectively). Both ligands are expressed ubiquitously throughout development and adulthood, and, unlike other FGFs, they are not efficiently secreted [23]. Both *Fgf1* and *Fgf2* are expressed in cardiomyocytes and vascular endothelial cells and are capable of stimulating cardiomyocyte and endothelial cell proliferation [24-30]. Surprisingly, however, knockout of *Fgf1*, *Fgf2*, or both has little developmental consequence in the heart [23, 31, 32].

Fgf9, Fgf16, and *Fgf20* are closely related ligands that are expressed in the developing heart, specifically in the epicardium and endocardium during midgestation development [33-36]. My lab has shown previously that FGF9 is necessary for cardiomyocyte proliferation during embryonic heart development, as FGF9-knockout mice have smaller hearts than wild-type mice [36]. Studies examining FGF16 have indicated that this growth factor is expressed in and released from cardiomyocytes in both the embryonic and postnatal heart, and that knockout of FGF16 also results in significantly smaller hearts compared to WT mice, again as a result of decreased cardiomyocyte proliferation during embryonic development [37-39].

Several other FGFs are expressed in the second heart field (SHF), a population of cardiac progenitor cells in the pharyngeal mesoderm. These ligands have been shown to be important in the development cardiac outflow tract, right ventricle, and atrial myocardium [40]. FGF8 is the primary ligand involved in SHF development; it is expressed in a subset of primary heart field cells, throughout the SHF mesoderm, and in pharyngeal endoderm, where it has been shown to be chemotactic and chemokinetic for cardiac neural crest cells [40-42]. It is involved in left-right axis formation and normal looping of the heart tube [43], in addition to being required for expansion of the primary heart tube and for normal outflow tract development. *Fgf8* hypomorphs have disrupted right ventricle development and a spectrum of outflow tract defects, from hypoplastic outflow tracts to disrupted ventriculoarterial alignments (double outlet left ventricle, transposition of the great vessels) or failed septation of the outflow tract (persistent truncus arteriosus) [40, 41, 44-47].

Other FGF ligands, such as FGF10, cooperate with FGF8 in the SHF. *Fgf10* is expressed in the SHF, and loss of function of FGF10 in combination with conditional loss of FGF8 in pharyngeal mesoderm leads to more severe outflow tract alignment defects than seen in *Fgf8* mutants alone [48-51]. In addition, *Fgf10* is expressed in the developing myocardium, and our lab has shown recently that knockout of *Fgf10* leads to a thin-walled myocardium due to impaired migration of epicardial-derived fibroblasts and decreased cardiomyocyte proliferation [52].

FGF3 has also shown redundancy with FGF10 during early heart development. *Fgf3* is expressed in the lateral pharyngeal ectoderm and in the pharyngeal pouch, adjacent to *Fgf10* expression in the pharyngeal mesoderm [53]. Compound knockouts of *Fgf3* and *Fgf10* have a spectrum of defects

affecting the outflow tract, ventricular septum, atrioventricular cushions, ventricular myocardium, dorsal mesenchymal protrusion, pulmonary arteries, epicardium, and fourth pharyngeal arch artery, suggesting that these two ligands are essential for the normal developmental coordination of cardiovascular progenitors from the SHF and cardiac neural crest [53].

Fgf15 is another ligand expressed in the developing pharyngeal arches and is required for normal outflow tract development, as well as for ventricular septation [54, 55]. Loss of this protein results in alignment defects of the great vessels, overriding aorta or double outlet right ventricle, and ventricular septal defects, presumably through defective neural crest cell movement and accumulation during outflow tract remodeling [54, 55]. These findings may be applicable to *FGF19*, the human homolog of *Fgf15* [54].

Finally, *Fgf6*, *Fgf7, Fgf17*, and *Fgf18* are also expressed in the developing heart, but little is known regarding their functions [56-62].

FGF receptors in heart development. FGFs bind to one of four distinct FGF receptor (FGFR) tyrosine kinases, which undergo tissue-specific alternative mRNA splicing, producing epithelial forms (b splice variants) and mesenchymal forms (c splice variants) [17-20]. *Fgfrs* are widely expressed throughout development, and several *Fgfrs* are expressed in the developing heart, as identified by *in situ* hybridization and immunohistochemical studies [63-65]. *Fgfr1* is the primary *Fgfr* expressed in heart muscle. Consistent with the known tissue-specific alternative splicing of *Fgfrs*, the mesenchymal splice form (*Fgfr1c*) was the major form identified in both the embryonic and adult heart [66, 67]. In previous work, my lab has demonstrated myocardial expression of *Fgfr1* and *Fgfr2* during midgestation heart development, but was not able to detect expression of *Fgfr3* or *Fgfr4* in the embryonic heart [36].

In differing mouse models, all *Fgfrs* have been knocked out, but the phenotypes have not been informative with respect to heart development, either due to embryonic lethality prior to critical stages of heart development (*Fgfr1* and *Fgfr2*) or to lack of an obvious cardiac phenotype in viable mice (*Fgfr3* and *Fgfr4*) [68-72]. Chimera analysis, using embryonic stem cells lacking functional *Fgfr1,* showed a deficiency in the ability of *Fgfr1*$^{-/-}$ cells to contribute to the extra-embryonic, cephalic, heart, axial and paraxial mesoderm, and endoderm at E9.5, or to differentiate into cardiomyocytes *in vitro* [73, 74]. This suggested that FGFR1 may be required for neural crest cell migration, early patterning of the precardiac mesoderm, or cardiomyocyte differentiation. Our lab previously investigated the necessity for

cardiomyocyte FGF receptors through creation of a myocardial-specific knockout of both *Fgfr1* and *Fgfr2* (*Mlc2v-Cre DCKO*), and found a significant decrease in embryonic cardiomyocyte proliferation [36]. Additionally, recent evidence suggests that FGF receptors 1 and 2 are required in the SHF mesoderm (and not in endothelium or cardiac neural crest cells) for proper formation, alignment, and septation of the outflow tract [75].

Fgfr2 null embryos are not viable due to a placental defect [68], but targeted knockout of the b splice form of FGFR2 has yielded more useful information regarding the role of this receptor in heart development. While loss of the epithelial *Fgfr2b* results in severe defects incompatible with life beyond birth (lack of limbs, lungs, and anterior pituitary), closer analysis during embryonic development revealed that these mice have ventricular septal defects associated with overriding aorta or double outlet right ventricle, in addition to ventricular anomalies (thin myocardial wall, abnormal trabeculation [49, 76]. The ventricular defects were found to be the result of impaired migration of epicardial-derived fibroblasts and decreased cardiomyocyte proliferation, similar to the cardiac phenotype of *Fgf10* null mice [52]. This phenotype was recapitulated with an epicardial knockout of both *Fgfr1* and *Fgfr2*, suggesting that these receptors function redundantly in the epicardium to regulate fibroblast migration and myocardial growth [52].

E. Fibroblast Growth Factor Signaling in the Postnatal Heart

Clearly, a great deal is known about the expression, activity and function of FGF signaling during heart development, but there is much less knowledge about the expression and function of FGF ligands and receptors in the postnatal heart. FGF1 and FGF2 are the most extensively studied FGF ligands in the adult heart. As mentioned previously, both ligands are expressed ubiquitously throughout development and adulthood, but single knockout of either ligand or double knockout of both FGF1 and FGF2 has little or no consequence in the mouse heart [23, 31, 32]. Additionally, despite the ability of FGF1 and FGF2 to stimulate cardiomyocyte proliferation *in vitro*, cardiac-specific FGF1 or FGF2 transgenic mice, have normal postnatal development with no development of cardiac hypertrophy [26, 29, 30, 77, 78]. Cardiac-specific FGF1 overexpression, however, results in an altered vascular pattern and enhanced coronary flow [78].

Studies have strongly implicated FGF2 in the development of pathological hypertrophy in response to pressure overload in the adult heart. Addition of FGF2 to cultured neonatal rat cardiomyocytes leads to repression of adult cardiac genes and induction of embryonic genes, an expression profile characteristic of pressure overload-induced hypertrophy [10, 79-82]. Furthermore, the hypertrophy exhibited by paced adult rat cardiomyocytes is prevented by an anti-FGF2 antibody [83]. Thus, it is not surprising that mice lacking FGF2 develop significantly less hypertrophy than wild-type mice after being subjected to pressure overload by transverse aortic constriction (TAC) [31]. Many other studies have demonstrated that FGF2 is both necessary and sufficient for the development of pathological hypertrophy. Systemic administration of FGF2 following acute myocardial infarction in rats induces significant hypertrophy in non-infarcted myocardium [84]. Additionally, knockout of *Fgf2* prevented the development isoproterenol- and angiotensin II-induced pathological hypertrophy in the adult heart, while FGF2 transgenic hearts showed an exacerbated hypertrophic response to β-adrenergic stimulation, an effect mediated by signaling through ERK1/2 [85, 86].

Furthermore, studies have indicated that both FGF1 and FGF2 are protective against other types of injury to the adult heart, presumably through induction of angiogenesis. FGF1 is a potent angiogenic factor and has been shown in a variety of *in vivo* and *ex vivo* models of ischemia to improve collateral flow and LV function by induction of new vessel formation and reduction of apoptosis, effects mediated through induction of ERK1/2, protein kinase C, and inducible nitric oxide synthase (iNOS) [87-93]. Delivery of FGF2 to the heart has also been shown to enhance new vessel growth and collateral blood flow following myocardial ischemia or other injury [94-96]. Meanwhile, genetic models have demonstrated that FGF2-deficient mouse hearts have increased infarct sizes and reduced recovery of function following *ex vivo* ischemia-reperfusion injury compared to WT hearts, while cardiac-specific FGF2-overexpressing hearts exhibit decreased infarct sizes and increased recovery of function compared to WT [77]. Similarly, following induction of myocardial infarction (MI) by ligation of the left anterior descending (LAD) artery, *Fgf2*-knockout hearts have reduced fibroblast proliferation and collagen deposition, decreased endothelial proliferation and vascular density, decreased cardiomyocyte hypertrophy, increased final infarct size (infarct expansion), and impaired cardiac function compared to WT mice. In contrast, FGF2-overexpressing hearts show increased fibroblast proliferation and collagen

deposition, enhanced cardiomyocyte hypertrophy, and preserved function, as previously seen in the *ex vivo* work-performing heart model of ischemia-reperfusion [97].

In recent years, knowledge regarding the role of other FGF ligands in the adult heart has expanded significantly. *Fgf9* is expressed at low levels in the adult heart [98], and one study analyzing gene expression before and after implantation of a left ventricular assist device (LVAD) found that *Fgf9* expression is significantly decreased after mechanical unloading of the ventricle, suggesting that expression was increased in the failing heart [99]. The role of FGF9 in the postnatal heart was recently investigated utilizing a mouse model with inducible cardiomyocyte-specific expression of FGF9 [100]. These mice develop enhanced myocardial microvascular density and cardiac hypertrophy (increased LV wall thickness without increased cavity diameter) with normal diastolic and systolic function and no changes in the expression of pathological markers (*Anp*, *Bnp,* β*MHC*). Additionally, when subjected to myocardial infarction (MI), these mice develop increased hypertrophy, greater capillary density, decreased interstitial fibrosis, and attenuated induction of pathological markers compared to control mice. Adenoviral gene transfer of FGF9 by injection into the LV cavity immediately after ligation of the left anterior descending artery resulted in increased capillary density and LV wall thickness, improved systolic function, and reduction of post-MI mortality compared to control mice [100]. These findings suggest that FGF9 may be more beneficial and cardioprotective to the adult heart than FGF2, since induction of FGF9 did not result in increased interstitial fibrosis or upregulation of pathological markers.

In addition to FGF9, studies are beginning to shed some light on the role of the closely related FGF16. Unlike *Fgf9*, which decreases expression postnatally, *Fgf16* expression increases markedly during the early neonatal period and persists into adulthood [39]. In contrast to the postnatal effects of FGF9 and the role of FGF16 in regulating embryonic cardiac growth [37, 38], this ligand appears to block the FGF2-mediated growth and proliferation of cultured neonatal cardiomyocytes, through modulation of protein kinase C (PKC) activation [39]. However, no studies have investigated the *in vivo* functions of FGF16 in the postnatal heart.

Atypical FGFs and the adult heart. Most members of the FGF family signal over short distances, in an autocrine or paracrine fashion. However, there are a few FGFs that behave differently and are also significant in postnatal cardiac pathophysiology. FGF23, the most recently discovered

ligand, is a bone-derived endocrine hormone that regulates serum phosphate levels. Like other FGF ligands discussed above, systemic FGF23 expression has been found to lead to pathological cardiac hypertrophy [101].

Other atypical FGFs are the intracellular FGFs, or fibroblast growth factor homologous factors (FHFs). FGFs 11-14 lack signal sequences, are not secreted, and do not bind to FGF receptors. Instead, these four FGFs are intracellular proteins that bind to and modulate the activity of voltage-gated sodium channels. All of these FGFs are highly expressed in the developing heart [102], but FGF13 is the most abundant in the adult mouse heart [103, 104] and directly binds to the principal cardiac voltage-gated sodium channel, Nav1.5 [104]. Knockdown of FGF13 reduces sodium current and surface Nav1.5 expression, without affecting total Nav1.5 protein or gene expression, resulting in delayed channel recovery from inactivation and slowed conduction velocity [104]. These findings suggest that not-yet-recognized loss-of-function mutations in FGF13 may lead to cardiac arrhythmias, such as Long QT syndrome or Brugada syndrome [105].

FGF receptors in the adult heart. There is conflicting evidence regarding both the expression and function of FGF receptors in the adult heart. One study utilizing normal adult human heart samples found expression of all four FGFRs using immunohistochemistry [106]. FGFR1 was expressed at high levels in cardiomyocytes, along with FGFR2 and FGFR4. Meanwhile, coronary arteries, veins, and microvessels showed the highest expression of FGFR3 and lower levels of FGFR1 and FGFR2 [106]. In contrast, a study in rats utilizing quantitative *in vitro* autoradiography to image FGFRs that bind to a labeled FGF2 found very low levels of FGF receptor expression in the adult myocardium, with only the blood vessels showing a high density of receptors [107]. Yet another study demonstrated very low, but detectable, gene expression of *Fgfr1* in isolated adult rat cardiomyocytes [108].

Several studies have investigated changes in *Fgfr1* expression following hypertrophy or MI. In a rat model of hypertrophy, *Fgfr1* expression was upregulated in the heart one day following ligation of the abdominal aorta, but returned to basal levels at day six [109]. Meanwhile, in a rat MI model, *Fgfr1* gene expression was decreased three days after ligation of the left anterior descending artery (LAD), but increased in the border zone and noninfarcted myocardium at day seven and peaked at day 14. Expression remained elevated in the border zone for six weeks [110]. In contrast, another study

examining FGFR expression (as measured utilizing quantitative *in vitro* autoradiography for FGF-2 binding) following MI in rats found that expression started to increase at day three and remained elevated through the end of the study (day 14), although the earlier change in receptor expression in this study could reflect changes in the expression one or more of the other FGF receptors [107].

Limited functional studies have been performed to determine whether FGF receptors are necessary or sufficient for ventricular remodeling in the adult heart. Intramyocardial injection of an adenoviral FGFR1 dominant negative signaling construct abrogated FGF signaling and resulted in an intermediate degree of cardioprotection in an *ex vivo* ischemia-reperfusion model [111]. In contrast, endothelium-specific overexpression of constitutively-active FGFR2 resulted in a significant cardioprotective effect following myocardial infarction (reduced infarct size) via promotion of enhanced angiogenesis, anti-apoptotic effects on vascular smooth muscles cells and cardiomyocytes, and autocrine production of FGF2 [112]. Additionally, inhibition of FGFR1 abrogated the cardioprotective effects seen in an FGF1-transgenic mouse model of *ex vivo* ischemia-reperfusion [90].

These studies investigating FGF signaling in the adult heart provide useful insights for the potential roles of this developmental pathway in cardiac remodeling, but they also raise many questions. At present, only FGF2 is definitively both necessary and sufficient *in vivo* for cardiac remodeling following injury to the heart. FGF2 is capable of stimulating cardiomyocyte proliferation and hypertrophy *in vitro*, raising that question of why there is no growth deficiency in FGF2-knockout hearts or increased cardiac growth in FGF2-transgenic hearts. Additionally, many of the studies described above utilized transgenic models of ligand overexpression to demonstrate that FGF signaling is capable of inducing hypertrophy or other ventricular remodeling, but there is limited evidence regarding how expression of these ligands and receptors is altered following different cardiac stressors (exercise, pressure overload, MI, *etc.*) or whether these ligands are necessary to the remodeling process. My investigation into changes in cardiac gene expression in the FGF pathway in response to different stimuli (MI, aortic constriction, angiotensin II, swimming, and a genetic model of physiologic hypertrophy) will be presented in chapter two. Furthermore, there is a general lack of evidence regarding the cellular targets of FGF signaling; studies utilizing conditional knockouts of FGF receptors as well as ligands that are required to truly determine the necessity of these factors during the ventricular remodeling process. My preliminary studies investigating

the necessity for cardiomyocyte FGF receptors 1 and 2 for remodeling and cardiac function following MI will be presented in chapter two with a discussion of future loss of function studies in chapter five. Finally, FGF2, FGF9, and FGF23 were all sufficient to induce hypertrophy in either the uninjured (FGF9, FGF23) or injured (FGF2, FGF9) heart, but it is unclear whether these effects are due to a direct effect on the cardiomyocyte *in vivo*, or an indirect effect mediated by another cell type (as was proposed for FGF9). Chapter three will focus on my studies utilizing a cardiomyocyte-specific inducible constitutively-active FGFR1 to investigate the cell autonomous effects of FGF signaling, and address the question as to whether adult cardiomyocytes are competent to respond to an activated FGF receptor.

F. Implication of FGF-activated Signaling Pathways in Hypertrophy

Thus far, the discussion has focused on the functional effects of FGF signaling in the developing and adult heart. The more important discussion, however, is the downstream mechanisms through which FGFs exert their effects and the fact that many of these pathways are strongly implicated in the pathogenesis of ventricular remodeling, especially in the development of hypertrophy. As summarized above, ligand-dependent receptor dimerization results in a conformational change in receptor structure that activates the tyrosine kinase domain (TKD), resulting in transphosphorylation of the TKD and intracellular tail. These phosphorylated sites act as docking sites for adaptor proteins, such as FGFR substrate 2 (FRS2), which get directly phosphorylated by the receptor and drive activation of multiple signal transduction pathways, such Ras/MAP kinase, phospholipase Cγ (PLCγ) pathway, or PI3 kinase/Akt pathway (Figure 1.1) [15, 16, 21]. As will be discussed below, past literature suggests a paradigm in which pathological and physiological hypertrophy are mediated by distinct signaling pathways, with activation of the Ras/MAPK/ERK pathway resulting in pathological hypertrophy and activation of the PI3K/Akt pathway resulting physiological hypertrophy. However, recent reports present a much more complex picture in which the lines between beneficial physiological and maladaptive pathological hypertrophy are blurred.

"RASopathies" and Hypertrophic Cardiomyopathy. Phosphorylation of FRS2 recruits the adaptor proteins son of sevenless (SOS) and growth factor receptor-bound 2 (GRB2), which activate the small GTPase RAS [21]. Additionally, FRS2 forms a complex with and phosphorylates the SH2 domain-

containing protein tyrosine phosphatase, SHP2, which leads to the recruitment of an additional GRB2-SOS1 complex by FRS2. Recruitment of both GRB2 and SHP2 is essential for sustained activation of Ras [113]. RAS then activates RAF, which phosphorylates mitogen-activated protein kinase kinase (MEK), which finally phosphorylates and activates mitogen-activated protein kinases (MAPKs), most commonly ERK1/2. (Figure 1.1) [21, 114].

Recent evidence strongly suggests that aberrant RAS signaling can contribute to the pathogenesis of hypertrophic cardiomyopathy, which affects roughly one out of 500 adults and is the most common cardiovascular genetic disorder. While the majority of cases (45-70%) can be attributed to one of many possible mutations in sarcomeric proteins [6], there are also some syndromic diseases (the "RASopathies") in which patients can develop HCM [114-116]. Noonan (NS), Costello (CS), cardiofaciocutaneous syndrome (CFCS), and LEOPARD (LS) syndromes all have overlapping features of developmental delay, short stature, craniofacial defects, gastroesophageal dysmotility, and cardiac defects (including HCM) [116]. In 2001, it was discovered that gain-of-function missense mutations in SHP2 (encoded by *PTPN11*) accounted for nearly 50% of cases of Noonan syndrome [117], and nearly all patients with LEOPARD syndrome were found to harbor distinct dominant-negative mutations in the same gene [115, 118, 119]. In recent years, mutations in *KRAS, NRAS, SOS1, RAF1, BRAF, MEK1, MEK2, SHOC2, and CBL* have all been uncovered in patients with one of these "RASopathy" syndromes [115].

Interestingly, a cardiac-specific activated RAS mouse model actually pre-dated the discovery of the first mutation in SHP2. When oncogenic human *HRAS* was expressed *in vivo* in mouse cardiomyocytes under the control of the MLC-2v promoter, the result was a marked hypertrophic response, characterized by diastolic dysfunction, increased systolic Doppler velocities, intraventricular pressure gradients, increased expression of pathological markers, and myocyte disarray characteristic of human HCM [120, 121]. Additionally, when this gene was expressed postnatally under the control of the alpha-MHC promoter, mice developed significant hypertrophy and postnatal heart failure, presumably the result of impaired sarcoplasmic reticulum calcium uptake. Surprisingly, these mice did not show any activation of ERK1/2 or Akt signaling, suggesting the possibility that RAS can activate additional pathways.

The discovery of the “RASopathy” mutations inevitably led to the creation of more specific mouse models attempting to recapitulate the various syndromes and to determine the downstream signaling mechanisms responsible for the pathophysiology. Approximately 20% of patients with NS have HCM, and the likelihood of developing HCM is highly dependent on the particular mutation. Less than 10% of patients with SHP2 mutations and only 20% of patients with SOS1 mutations develop HCM, while HCM is found in nearly 95% of patients with RAF1 mutations, and mouse models recapitulate these trends [122-124]. Mice carrying a NS-associated mutation in SHP2 demonstrate specific ERK1/2 activation that was both necessary and sufficient during cardiac development to induce congenital heart defects, although this mutation was not associated with HCM [124]. In addition, induction of this gain-of-function mutation postnatally led to increased ERK1/2 activation in heart, but this was not associated with any cardiac pathology [124], indicating that postnatal activation of ERK1/2 signaling is not sufficient to induce hypertrophy or cardiac defects. Meanwhile, mice carrying the NS-associated SOS1 mutation develop pathological LV hypertrophy through activation of ERK1/2 and Stat3, and cardiac defects were prevented through inhibition of the MEK pathway [123]. A third mouse model of NS containing a gain-of-function mutation in RAF1 is highly associated with the development of HCM, and these pathological effects are reliant on enhanced MEK-ERK activity [122]. What is unclear regarding these three models is why enhanced ERK1/2 activation appears to be necessary and sufficient for HCM in RAF1 mutants, but not in SHP2 mutants.

In an attempt to better elucidate the role of ERK1/2 in the development of hypertrophy, a transgenic mouse model was used that overexpresses activated MEK1 in the heart. This led to activation of ERK1/2 signaling and concentric hypertrophy with impaired diastolic function, enhanced systolic function, and upregulation of the pathological markers ANP, BNP, skeletal α-actin, and β-MHC, suggesting that ERK1/2 activation is sufficient to induce hypertrophy [125]. However, a recent study demonstrated that ERK1/2 is not necessary for hypertrophy development *per se*, but rather for regulating the balance between concentric and eccentric hypertrophy [126]. Mice lacking both ERK1 and ERK2 in the heart developed spontaneous cardiac hypertrophy with aging and also in response to angiotensin II/phenylephrine infusion, but close inspection of cardiomyocytes revealed that double null myocytes lengthen and become thinner, leading to eccentric growth of the heart. In contrast, myocytes from hearts

expressing activated MEK1 to induce ERK1/2 signaling increased in width but not length, consistent with concentric hypertrophy [126]. Therefore, ERK1/2 signaling is not necessary for the development of hypertrophy, but it may affect the type of hypertrophy that results.

In contrast to NS, HCM is much more commonly associated with LS, which is characterized by dominant negative mutations that decrease the catalytic activity of SHP2 [114, 115]. Mice harboring one of the most common mutations in *Ptpn11* (Y279C) develop evidence of hypertrophic cardiomyopathy [127]. Additionally, mice overexpressing a cardiomyocyte-specific LEOPARD syndrome-associated loss-of-function mutation in SHP2 (Q510E) embryonically undergo significant cardiac hypertrophy, cardiomyocyte disarray, and depressed contractile function; induction of this mutated SHP2 postnatally did not result in HCM [128]. Both of these models showed increased Akt and mTOR activity, and HCM was reversed by treatment with rapamycin (mTOR inhibitor) [127-129]. The role of the PI3K/Akt pathway in cardiac hypertrophy will be discussed in more detail below.

What is clear from the "RASopathies" is that mutations within the same pathway can lead to very different (but also very similar) results. NS-associated gain-of-function mutations all induce activation of the ERK1/2 pathway, but not all of the mutations lead to HCM. Additionally LS-associated mutations have the opposite effect on SHP2 (dominant negative, or loss of function), are more likely to result in HCM through activation of the Akt/mTOR pathway. Finally, mouse models utilizing oncogenic human HRAS develop HCM without activation of either ERK1/2 or Akt, suggesting that another nonclassical pathway may be involved. Regardless of the final mechanism, it is evident that components immediately downstream of receptor tyrosine kinases (like FGFRs) are strongly implicated in the pathogenesis of hypertrophic cardiomyopathy. As will be discussed in chapter three, our lab has created an inducible cardiomyocyte-specific constitutively-active FGFR1 mouse model that rapidly develops HCM when induced in the adult heart. Although this HCM develops independent of ERK1/2 and Akt activation, based on the studies discussed above, it is likely that increased RAS activation is involved in the pathogenesis.

PI3K-Akt Signaling in Physiological versus Pathological Hypertrophy. In addition to activation of the Ras-MAPK pathway, phosphorylation of FRS2 and recruitment of GRB2 can also to the formation of another complex involving GRB2-associated binding protein 1 (GAB1) and activation of the PI3K-Akt pathway [21]. Evidence suggests that insulin-like growth factor-1 (IGF1) and PI3K-Akt signaling

mediate the development of physiological hypertrophy. Long-term training results in increased levels of free serum IGF-1 [130], and transgenic mice overexpressing the IGF1 receptor (IGF1R) specifically in cardiomyocytes develop compensated physiological hypertrophy that is dependent on signaling through PI3K(p110α) [131]. Further support for the involvement of the IGF1-PI3K-Akt signaling pathway exclusively in the development of physiological hypertrophy comes from knockout studies, in which mice lacking PI3K activity, Akt1 or IGF1R failed to develop exercise-induced hypertrophy, but still developed pathologic hypertrophy in response to pressure overload [3, 132-135]. Thus IGF1R and PI3K are both necessary and sufficient for physiologic but not pathologic hypertrophy.

Despite substantial evidence that IGF-1-mediated Akt activation is necessary for the development of physiologic hypertrophy, studies examining the role of Akt are less clear. While overexpression of the E40K (constitutively-active) Akt1 mutant results in physiologic hypertrophy (mild hypertrophy, enhanced contractility, no signs of cardiac pathology) [136], overexpression of myristoylated or phosphomimetic forms of Akt1 lead to pathologic hypertrophy (massive cardiac enlargement, impaired contractile function and interstitial fibrosis) [137, 138]. Yet another study demonstrated that acute activation of Akt1 resulted in adaptive hypertrophy with preserved contractility, while chronic activation resulted in a dilated cardiomyopathy with impaired cardiac function [139, 140]. These findings, in addition to those discussed above that LS-associated HCM is dependent on activation of Akt signaling, suggest the potential for overlapping mechanisms between physiologic and pathologic hypertrophy, further complicating our understanding of these processes.

G. Conclusions

The Ras-MAPK-ERK1/2 and PI3K-Akt pathways highlighted above are only two of several pathways that can be activated following FGFR dimerization and autophosphorylation. FGF binding has also been shown to activate several other pathways that are strongly implicated in cardiac hypertrophy and postnatal ventricular remodeling, including the p38 and JNK MAPK pathways, as well as the PLCγ pathway, which leads to activation of protein kinase C and increased cytosolic calcium [21, 141, 142]. The fact that FGFs are capable of activating so many different hypertrophy-inducing pathways underscores the necessity for further research examining the role of this growth factor family in the

postnatal heart. Thus far, most research has focused on FGF2. Limited studies have examined the roles of other FGF ligands or attempted to define the necessary cellular targets of FGF signaling. As such, my thesis work aims to increase understanding of FGF signaling in the adult heart, with the goal of better characterizing this pathway's involvement in ventricular remodeling, specifically hypertrophy.

H. Disclosure of co-authored works.

Chapter 2: Figure 2.1 and its associated legend were created by Kory Lavine and presented as preliminary data in his thesis in 2007. Additionally, echocardiography was performed by Attila Kovacs, while cardiac surgeries (aortic banding and MI) were performed by Carla Weinheimer in the Mouse Cardiovascular Phenotyping Core (mcpc.wustl.edu). Paraffin sections, H&E, and Trichrome staining were performed by the Developmental Biology Histology Core. cDNA samples from physiological hypertrophy models were provided by KC Yang in the lab of Jeanne Nerbonne.

Chapter 3: Kory Lavine created the TRE-caFGFR1 mouse line. As in Chapter 2, echocardiography was performed by Attila Kovacs while hemodynamic analysis was performed by Carla Weinheimer and analyzed by Carrie Giersach in the Mouse Cardiovascular Phenotyping Core. Paraffin sections and H&E staining were performed by the Developmental Biology Histology Core. Ventricular myocyte isolation and contractility assessment were performed by Keita Uchida in the lab of Colin Nichols. The data and information presented in this chapter have been published: Cilvik S, Wang J, Lavine K, Uchida K, Castro A, Gierasch C, Weinheimer C, Kovacs A, Nichols C, and D Ornitz. Fibroblast Growth Factor Receptor 1 signaling in adult cardiomyocytes increases contractility and results in a hypertrophic cardiomyopathy. *PLoS One* 2013, 8: e82979.

Chapter 5: Echocardiography, hemodynamic analysis, and exercise tolerance methods were written by Attila Kovacs and Carla Weinheimer. Ventricular isolation and myocyte contractility methods were written by Keita Uchida.

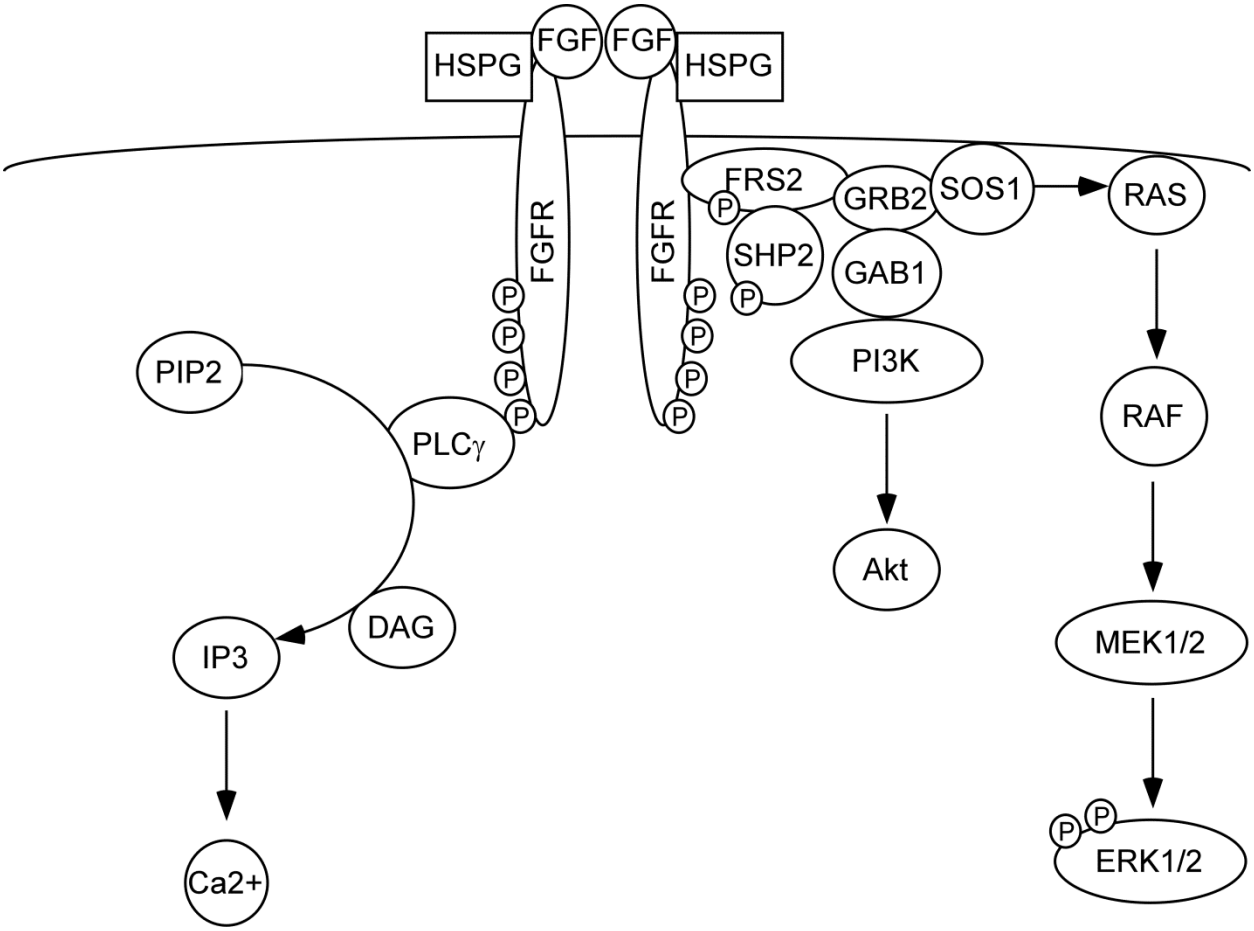

Figure 1.1 FGF Signaling Pathway. FGF ligands and heparin sulfate proteoglycans bind to the FGF receptors, causing receptor dimerization and activation through autophosphorylation. FGF signaling can then proceed via three main pathways: Ras-MAPK, PI3K-Akt, or PLCγ. Recreated from [21, 143].

Chapter 2

Altered Gene Expression of FGF Ligands and Receptors in Postnatal Cardiac Remodeling

A. Introduction

FGF2 has been clearly shown to be a cardioprotective factor involved in cardiac remodeling following stress or injury to the heart. In pressure overload models, it contributes to cardiomyocyte hypertrophy, while in MI models, it also causes increased fibroblast proliferation, prevents infarct expansion, and preserves cardiac function [31, 77, 85, 97]. Other FGF ligands, such as FGF1 and FGF9, and signaling pathways activated downstream of FGF receptors have also been implicated in postnatal cardiac remodeling. Additionally, pilot studies by Kory Lavine, a previous graduate student in our lab, utilizing an inducible cardiomyocyte-specific FGF9-overexpressing mouse line suggested that this ligand may play a role in the development of fibrosis in the adult heart. Induction of FGF9 overexpression concurrently with pressure-overload (TAC) resulted in a much more severe phenotype and rapid progression to heart failure (Figure 2.1). FGF9 has also been shown to be downregulated following LVAD placement in failing human hearts, suggesting that its expression is increased during pathological ventricular remodeling [99]. This led to the hypothesis that FGF9 expression may be increased following cardiac injury and that it is involved in the induction of fibrosis in pathological remodeling.

Furthermore, FGF2 is the only ligand that is well characterized in the adult heart. Very little is known regarding what ligands and receptors are expressed in the adult heart and how their expression changes following injury or stress. Also, despite the fact that FGFs are known to activate PI3K signaling [21], very little work has been done investigating whether FGF signaling plays a role in physiological remodeling. To better understand when and how FGF signaling may be involved in postnatal cardiac remodeling, I wanted to determine how gene expression changes with different types of pathological or physiological stressors. What are the commonalities between different types of injury, and perhaps more importantly, what are the significant differences between pathological and physiological remodeling?

Finally, due to the fact that knockout of *Fgfr1* is embryonic lethal [69, 70], very few studies have examined the role of this (or other) receptor(s) in the adult heart. As mentioned above, FGF2 has been shown to cause cardiomyocyte hypertrophy, as well as fibroblast and endothelial cell proliferation following MI [97], but it is not known whether this is a direct effect on each cell type or an indirect effect through one cell type that serves as a signaling center. As such, I started to address the potential cell-specific targets of FGF2 and downstream signaling mechanisms involved in cardioprotection, using a

tamoxifen-inducible cardiomyocyte-specific double knockout of *Fgfr1* and *Fgfr2* (*αMHC-CreER, FGFR1$^{f/f}$, FGFR2$^{f/f}$, R26R*, or MHC-CreER DCKO) and assess the response to injury from myocardial infarction (MI). Future completion of these studies by others in our lab will provide essential knowledge about cell-types that would be expected to show a beneficial response to FGF signaling versus those cell-types in which FGF signaling would lead to further pathological damage. They will facilitate future studies to address the mechanisms that regulate FGF activity in the context of physiological and pathological challenge. This knowledge will be essential to improve the design and implementation of FGF-based therapies for the treatment of human CVD.

B. Results

Inducible, Cardiac-Specific FGF9 Overexpression. Our lab has shown previously that FGF9 is essential to embryonic cardiac growth [36], and therefore we hypothesized that FGF9 may also be important in regulating postnatal cardiac growth or may be cardioprotective after injury, similar to FGF2. To investigate the role of FGF9 in the adult heart, our lab has utilized the doxycycline-regulatable TET-on system with the *αMHC-rtTA* mouse line. Expression of the reverse tetracycline transcriptional activator (rtTA) from the αMHC promoter leads to cardiomyocyte-specific expression of the rtTA protein [144]. To determine the effects of FGF9, our lab generated a tetracycline response element (TRE)-drivable FGF9-Ires-GFP transgene, which has been characterized previously [145]. Pilot studies presented in the thesis of Kory Lavine demonstrated that overexpression of FGF9 in the adult heart followed by pressure overload was severely maladaptive and led to rapid progression to heart failure (Figure 2.1). We hypothesized that FGF9 may be involved in more pathological aspects of remodeling, such as in the fibrotic response, and I thus continued experiments with this mouse line. Further characterization of this model revealed that after three weeks of transgene induction with doxycycline chow, double transgenic hearts had significantly reduced diastolic LV chamber dimension (as represented by LV internal diastolic diameter, 3.87 vs. 4.12 mm, p=0.02) (Figure 2.2A) and significantly increased E/e' ratios (46.6 vs. 29.7, p=0.05) (Figure 2.2B). The ratio of early mitral inflow velocity (E) to early diastolic mitral annular velocity (e') is well established as the best parameter to estimate LV filling pressure [146], so the significant elevation of this ratio is highly suggestive of a diastolic defect (impaired relaxation) in hearts

overexpressing FGF9. Despite the apparent diastolic dysfunction, systolic function, as measured by ejection fraction, is maintained in double transgenic mice (Figure 2.2C).

Following echocardiography, hearts were harvested for histological analysis, which revealed increased perivascular and interstitial fibrosis in double transgenic hearts (Figure 2.3), as well as quantitative RT-PCR analysis (Figure 2.4). Analysis of gene expression revealed that three weeks of DOX induction was sufficient for a 344-fold increase in *Fgf9* expression in double transgenic hearts ($p=0.001$) (Figure 2.4A). This degree of FGF9 overexpression resulted in significantly increased expression of *Fgf2* (2.4-fold increase, $p<0.001$) and *Fgfr1* (1.9-fold increase, $p=0.02$), while decreasing expression of *Fgf16* (2.5-fold decrease, $p<0.001$) and *Fgf10* (3.2-fold decrease, $p=0.10$) (Figure 2.4B). Markers of pathological remodeling are relatively unchanged, with the exception of *Col3a1*, which was significantly increased by FGF9 overexpression (2.9-fold increase, $p=0.03$) (Figure 2.4C). In addition to *Col3a1* upregulation, significantly increased expression of both *Tgfβ2* and *3* (*Tgfβ2*: 2.5-fold increase, $p=0.02$; *Tgfβ3*: 1.7-fold increase, $p=0.03$) supports the histological finding of increased fibrosis in double transgenic hearts [147]. Intriguingly, expression of *PdgfA* and *B*, which also play a critical role in the development of fibrosis similar to TGFβs [147], are decreased in double transgenic mice (*PdgfA*: 1.7-fold decrease, $p=0.01$; *PdgfB*: 2.3-fold decrease, $p=0.06$) (Figure 2.4E). Meanwhile, decreased expression of *VegfA* and *VegfR1/Flt1* (*VegfA*: 1.7-fold decrease, $p=0.05$; *VegfR1/Flt1*: 1.3-fold decrease, $p=0.17$) suggest the possibility that FGF9 overexpression may suppress angiogenesis (but at the very least does not increase angiogenesis) (Figure 2.4E).

Taken together, these results strongly implicate FGF9 in the activation of fibroblasts and maladaptive fibrotic remodeling in the heart. These findings are in stark contrast to a recent publication that demonstrated enhanced vascularization and cardiac hypertrophy with normal diastolic function following cardiac-specific overexpression of FGF9 [100], and thus it is evident that further analysis is necessary to elucidate the role that this ligand plays in adult cardiac remodeling. Based on our model of FGF9-overexpression, we hypothesized that FGF9 expression may be increased in hearts undergoing pathological remodeling.

FGF Expression in Physiological Hypertrophy. Samples were obtained from KC Yang in Jeanne Nerbonne's lab to analyze gene expression changes in two different models of physiological

hypertrophy. One group of eight- to 10-week-old mice were subjected to swim training for four weeks to induce physiological hypertrophy (n=6), while a second group of mice contained cardiac-specific constitutively-active PI3K, a genetic model of physiological hypertrophy (n=6) [148]. As expected, neither exercise nor caPI3K induced an increase in *ANP* expression (Figure 2.5A). Intriguingly, I observed a significant increase in *βMHC* in hearts expressing caPI3K (3.7-fold increase, p=0.03), in agreement with other published studies [148].

There were other important differences between exercise-induced and genetically-induced physiological hypertrophy, underscoring the complexity of this remodeling process. *Fgf2* expression was significantly downregulated in exercise-induced hypertrophic hearts (1.6-fold decrease, p=0.003), but unchanged in hearts from caPI3K mice. In addition, *Fgf10* was slightly, but not significantly, upregulated in exercise-induced hearts (1.2-fold increase, p=0.16), while *Fgf9* showed a similar trend in caPI3K hearts (1.2-fold increase, p=0.12). Additionally, *Fgfr1* was significantly downregulated in exercise-induced hypertrophy (1.2-fold decrease, p=0.02), but significantly increased in caPI3K-induced hypertrophy (1.7-fold increase, p<0.001) (Figure 2.5C).

One change that was common to both models of physiological hypertrophy was a significant increase in *Fgf16* expression. *Fgf16* was increased 1.2-fold in exercise-induced hearts (p=0.009) and 1.4-fold in caPI3K hearts (p=0.01) (Figure 2.5B). There were no significant changes in *Fgfr2* or *Fgfr3* (Figure 2.5C).

As noted above, this experiment highlighted some significant differences between actual physiological hypertrophy (as induced through exercise) and an established genetic model of physiological hypertrophy (utilizing constitutively-active PI3K). Even in this limited screen of FGF ligands and receptors, there were potentially important differences in gene expression that could be useful in further investigating the distinctions between pathological and physiological remodeling. No study to date has examined the necessity for FGF signaling in physiological hypertrophy, and based on the results of this screen, it would be worthwhile to examine the response to exercise in FGF2-knockout and FGF2-transgenic animals, as well as in FGF16-knockout and –transgenic mice.

FGF Expression in Pressure Overload-Induced Pathological Hypertrophy. To induce pathological remodeling, 8- to 10-week-old wild-type mice were subjected to ascending aortic constriction

(AAC) to cause significant pressure overload in the LV (performed by Carla Weinheimer in the Washington University Mouse Cardiovascular Phenotyping Core, http://mcpc.wustl.edu/). One week following surgery, hearts were harvested for gene expression analysis using quantitative RT-PCR (Figure 2.6). While there were trends toward upregulation of markers of pathological remodeling (Figure 2.6B-D), only *Fgf16* expression was significantly changed (2-fold decrease, p=0.02) (Figure 2.6A). The lack of significant changes in other genes studied was likely the result of the small sample size in this pilot experiment (n_{AAC}=2).

FGF Expression in Angiotensin II-Mediated Pathological Remodeling. It has long been known that the use of angiotensin converting enzyme (ACE) inhibitors and angiotensin receptor blockers is extremely beneficial in prolonging the progression of congestive heart failure. However, the mechanism by which angiotensin II (AngII) contributes to maladaptive heart remodeling is largely unknown. Several studies have shown that overactivation of the renin-angiotensin system (RAS) leads to cardiac fibrosis and diastolic dysfunction with no overt cardiac hypertrophy. In a mouse with a constitutively active form of AT1a, an angiotensin II receptor, the major cardiovascular modification was not cardiac hypertrophy or excessively high blood pressure, but rather, fibrosis, which appeared in early adulthood and progressed throughout the life of the mouse [149]. The cardiac fibrosis was primarily perivascular with some interstitial fibrosis, and the amount of fibrosis paralleled the functional cardiac alterations that occurred in these mice by 5 months of age (diastolic dysfunction with subsequent evolution toward heart failure) [149]. Similarly, mice with cardiac-specific expression of a transgene fusion protein that releases AngII from cardiomyocytes (without involvement of systemic RAS) had increased collagen deposition and no hypertrophy in the heart under basal conditions [150]. These mice were subjected to ligation of the LAD to induce an MI, and the transgenic mice had a more profound hypertrophic response, a significantly increased LV internal diastolic diameter, and a significantly decreased ejection fraction compared to their WT littermates [150]. Furthermore, mice with a targeted deletion of the angiotensin II receptor, AT1, had virtually no interstitial fibrosis in response to severe chronic aortic regurgitation, a model of LV volume overload. In contrast, WT mice in this same experiment had extensive progressive interstitial fibrosis that led to severe diastolic dysfunction and congestive heart failure [151].

These results are very similar to what we have seen when FGF9 expression is induced in the adult myocardium, as described above. As a result, I hypothesized that there is a link between the cardiac fibrosis seen in these models of AngII and FGF9 overexpression. It has been demonstrated that angiotensin II is able to upregulate expression of FGF2, FGFR1, and HSPG in cultured human cardiac smooth muscle cells [152], and thus is may be possible that AngII also increases the expression of FGF9.

To determine if there is a connection between AngII- and FGF9-mediated fibrosis, we inserted mini-osmostic pumps containing angiotensin II (2ug/kg/min) into wild-type mice, allowing AngII to be released at a rate of 0.5 μl/h for 14 days. Echocardiography was performed at the end of the two-week infusion to assess *in vivo* LV mass and cardiac function (Figure 2.7A and B). Angiotensin II resulted in a moderate, but insignificant, increase in LV mass index (6.3 vs. 4.0 mg/g, p=0.2) (Figure 2.7A) and a significant increase in systolic function, as measured by ejection fraction (EF, 0.75 vs. 0.59, p=0.002). In agreement with *in vivo* measurement of LV mass, postmortem assessment of cardiac mass, determined by the ratio of heart weight (biventricular mass) vs. body weight (HW/BW ratio), was significantly increased in mice that received AngII compared to vehicle-treated controls (5.9 vs. 4.6 mg/g, p=0.02) (Figure 2.7C). Additionally, histologic analysis displayed increased fibrosis in mice treated with AngII (Figure 2.7D). Furthermore, analysis of gene expression using quantitative RT-PCR revealed significant reduction in the expression of *Fgfr2* (1.5-fold decrease, p=0.005), *Fgf7* (1.4-fold decrease, p=0.02), and *Fgf16* (2.9-fold decrease, p=0.004), with near significant reduction of *Fgf10* (3.4-fold decrease, p=0.06) (Figure 2.8 A and B). There were trends toward upregulation of *Anp*, *Bnp*, *Col3a1*, and *Tgfβ3* (Figure 2.8 C and D). Intriguingly, expression of *βMHC* was not increased despite the appearance of pathological hypertrophy (Figure 2.8C).

Myocardial Infarction. Eight- to 12-week-old mice were subjected to LAD ligation to induce myocardial infarction (performed by Carla Weinheimer in the Washington University Mouse Cardiovascular Phenotyping Core, http://mcpc.wustl.edu/) [153, 154]. One week following MI, hearts were removed and dissected into two pieces, infarcted tissue and non-infarcted tissue. Both pieces likely included infarct border zone. RNA was extracted and quantitative RT-PCR was utilized to compare gene expression between non-surgical controls, non-infarcted myocardium, and infarcted myocardium. Consistent with published studies [107, 110], *Fgf2* expression was significantly increased in infarcted

myocardium (1.8-fold versus nonsurgical control, p=0.03) (Figure 2.3A). *Fgfr1* and *Fgfr2,* and a downstream effector of FGF signaling, *Etv4 (Pea3)*, were also significantly upregulated in the infarct region one week following MI (*Fgfr1*: 5.6-fold increase, p=0.001; *Fgfr2*: 25.9-fold increase, p=0.02; *Etv4/Pea3*: 11.3-fold, p=0.004). *Fgfr2* was also significantly increased to a lesser degree in the non-infarcted myocardium (9.5-fold increase, p=0.03), while *Fgfr1* and a different downstream effector, *Etv5* (*Erm*), were nearly significantly increased (*Fgfr1*: 2.2-fold increase, p=0.06; *Etv5/Erm*: 2.0-fold increase, p=0.06) (Figure 2.3B).

Surprisingly, there was significant downregulation of *Fgf9* and *Fgf16* in both the infarcted and non-infarcted myocardium compared to nonsurgical controls (*Fgf9* infarct: 5-fold decrease, p<0.001; *Fgf9* non-infarct: 3.3-fold decrease, p=0.004; *Fgf16* infarct: 12.5-fold decrease, p<0.001; *Fgf16* non-infarct: 3.3-fold decrease, p=0.001) (Figure 2.3A). Gene expression was present, but unchanged for *Fgfr3*, *Fgf7, Fgf10,* and *Fgf17*. Expression of *Fgf20* and *Fgfr4* could not be detected, and other FGF ligands were not examined.

Expression of other genes involved in cardiac remodeling are presented in Figure 2.3 (C-E). All pathological markers were trending towards upregulation, with significant increases noted for *Anp* in the non-infarcted myocardium (9.6-fold increase, p=0.04) and *Col1a1* in the infarcted tissue (3.6-fold increase, p=0.009) (Figure 2.3C). Meanwhile, *TGFβ1-3* were all significantly upregulated in the infarct region (*TGFβ1*: 2.6-fold increase, p=0.05; *TGFβ2*: 3.5-fold increase, p=0.04; *TGFβ3*: 7.4-fold increase, p=0.005), and non-significantly increased in non-infarcted tissue (Figure 2.3D). Additionally, there was a trend towards upregulation of *PdgfA* in both the infarcted and non-infarcted wall, while *PdgfC* was significantly upregulated in the infarct zone (12.7-fold increase, p=0.05) (Figure 2.3 E).

I have also noted significant upregulation of the epicardial marker *Tbx18* and increased expression of the EMT marker *Slug* in the infarct region (Figure 2.3F), consistent with previous studies [155]. Published studies have shown that myocardial and vascular precursor cells reside within the epicardium, that these cells can migrate into the damaged tissue following MI [156, 157], and that FGF2 can induce epicardial EMT in the developing chick heart [60]. I hypothesize that one function of FGF2 upregulation in response to MI is signaling to FGFRs in the epicardium to stimulate EMT and migration of EPDCs into the infarcted tissue to promote healing. Similar to the mechanism proposed in zebrafish to

regenerate heart tissue [158], EPDCs could then differentiate into vascular and myocardial progenitor cells and help to repopulate and repair infarcted tissue. However, it is additionally possible that FGF2 signals directly to the cardiomyocyte where it could have a direct cardioprotective role by inducing hypertrophy or promoting cell survival, or to the endothelial or perivascular cell, where it could function in neo-angiogenic pathways that are necessary for the myocardial response to injury. Another, more likely, alternative is that one of these cell types (epicardial, endothelial, fibroblast, or myocyte) receives the FGF signal and serves as a signaling center, releasing other factors that promote the remodeling effects in other cells (Figure 2.10).

While one recent study has constitutively overexpressed an activated FGFR2 in endothelial cells and shown an improved response to MI [112], no studies have addressed the potential cellular targets of FGF2 (or any other FGF) in the mature heart by examining cell-specific requirements for FGFR expression/function in response to injury or physiological challenge.

Response to MI in a Tamoxifen-Inducible Cardiomyocyte-Specific FGFR1/2 Double Conditional Knockout. To determine if FGF signaling in the cardiomyocyte is directly responsible for any of FGF2's cardioprotective effects, I have used a tamoxifen-inducible cardiomyocyte-specific FGFR1/2 double conditional knockout mouse line (*αMHC-CreER, FGFR1$^{f/f}$, FGFR2$^{f/f}$, R26R*, or MHC-CreER DCKO) (Figure 2.11A). Twelve- to fourteen-week-old MHC-CreER DCKO mice and their littermate *FGFR1$^{f/f}$, FGFR2$^{f/f}$, R26R* (DFF) controls, as well as *αMHC-CreER, R26R* control (Cre control) mice, were injected IP with 40mg/kg tamoxifen daily for six days to induce Cre activity. One week later, mice were harvested either for examination of heart weight-to-body weight (HW/BW) ratios, β-galactosidase staining, and quantitative RT-PCR analysis, or subjected to ligation of the left anterior descending (LAD) artery to induce myocardial infarction (performed by Carla Weinheimer in the Washington University Mouse Cardiovascular Phenotyping Core, http://mcpc.wustl.edu/).

One week following tamoxifen injections, MHC-CreER DCKO mice expressed LacZ in nearly all cardiomyocytes, with no expression seen around the vasculature, in the epicardium, or in DFF controls, indicating sufficient Cre activation following six days of tamoxifen injections (Figure 2.11B**)**. MHC-CreER DCKO and littermate control mice (with or without Cre) had comparable HW/BW ratios (Figure 2.11C), indicating that one week following tamoxifen injections, there is no apparent tamoxifen- or Cre-induced

toxicity and that acute inactivation of FGF receptors 1 and 2 from the myocardium does not affect cardiac mass.

Eight- to 12-week-old mice received MI surgery one week following tamoxifen injections, and were followed by echocardiography at one week and one month post-MI. Serial short-axis slices were used to measure ejection fraction and percentage of infarcted tissue at both time points using VisualSonics Vevo770 software. MHC-CreER DCKO mice showed a trend towards decreased ejection fractions and increased infarct sizes compared to their littermate controls (Figure 2.12C and D). When harvested one month post-MI, DCKO mice had elevated lung weight-to-body weight ratios (LW/BW) (Figure 2.12A), as well as higher expression of both *Anp, Bnp* and *βMHC* in non-infarcted tissue (opposite wall) compared to DFF littermate controls (Figure 2.13), indicating a higher degree of heart failure in these mice. Though myocyte size was not measured in these experiments, the fact that *βMHC* expression increases significantly suggests that the hypertrophic remodeling program is still induced. As a result, I hypothesize that cardiomyocyte FGF receptors play a role in cardiomyocyte survival rather than hypertrophy, and that increased cell death may be responsible for the larger infarct sizes and poorer function post-MI.

These studies were eventually discontinued for several reasons. Progress was slowed significantly with higher than normal mortality for MI studies for both genotypes (~50%), a problem that was encountered by other mouse lines in our lab undergoing different cardiac surgeries, such as closed-chest ischemia-reperfusion. During the troubleshooting process, we determined that transfer stress was the most likely cause of our mortality issues, and have since moved our cardiac colony adjacent to the Mouse Cardiovascular Phenotyping Core, resulting in normal rates of postsurgical mortality. Meanwhile, the closed-chest ischemia-reperfusion model had been recently established in the Mouse Cardiovascular Phenotyping Core, and since this model was more clinically relevant [159], we decided to continue future experiments using this model instead of the chronic MI model.

C. Discussion

As mentioned previously, most studies examining FGF signaling in the adult heart have revolved around FGF2, but very little work has been done investigating other FGF ligands or receptors in the

postnatal heart. It was the goal of these experiments to increase our knowledge of how FGF signaling molecules change in different models of cardiac remodeling, both pathological and physiological. Notable findings from these gene expression analysis experiments are summarized in Table 2.1. The most striking findings were the very dramatic changes in *Fgf16* expression, in addition to the fact that the expression pattern was reversed between physiological and pathological hypertrophy. *Fgf16* expression was significantly increased following exercise- or caPI3K-induced hypertrophy, but significantly decreased in every pathological model examined (pressure overload, AngII, MI). Changes in *Fgf16* expression were far less variable than changes in other genes, achieving significant results in some cases with a sample size of only two animals.

Recent publications have begun to examine the role of FGF16 in the postnatal heart. Lu *et al*. examined the expression and functions of FGF16 and found that FGF16 expression markedly increases during the early neonatal period compared to expression levels in the embryonic heart, and that these high levels of expression persist into adulthood [39]. Using cultured neonatal cardiomyocytes, they discovered that FGF16 abrogates FGF2-induced myocyte proliferation and upregulation of cell cycle genes, but that FGF16 treatment alone has no effects on cardiomyocytes or cell cycle gene expression [39]. The authors note that the increasing FGF16 expression in cardiomyocytes during the neonatal period corresponds with the loss of proliferative capacity in these cells. Therefore they postulate that FGF16 negatively regulates proliferation of neonatal cardiomyocytes, possibly through receptor competition with FGF2 or via downstream effects on PKC signaling [39].

This finding is very interesting, because it suggests the possibility that FGF16 may also negatively regulate growth, or hypertrophy, of adult cardiomyocytes. Intriguingly, my work has indicated that this growth factor is significantly downregulated when the heart is stressed, and in situations where FGF2 has been shown to be necessary for remodeling. Thus, I hypothesize that FGF16 opposes the actions of FGF2 under normal conditions, and that its expression is downregulated when the heart is under stress to allow FGF2-mediated hypertrophy and cardiac remodeling to occur in order to preserve heart function.

While expression of FGF9, which is closely related to FGF16 [160], follows similar trends, it is clearly not as tightly regulated as FGF16. Additionally, despite our hypothesis that FGF9 contributes to

pathological fibrotic remodeling, we did not see upregulation of this ligand in any of the heart failure models, suggesting that it is not an essential signal for the development of fibrosis. Studies are being continued in our lab to further address the roles of FGF9 and FGF16 in the postnatal heart.

Another interesting finding from this gene expression analysis was the significant upregulation of both *Fgfr1* and *Fgfr2* one week following myocardial infarction in both the infarcted and non-infarcted myocardium. Very little is known about the *in vivo* expression patterns of FGF receptors and ligands in adult heart tissue due to a lack of suitable antibodies and difficulty immunostaining adult cardiac sections. In addition, despite the clear necessity for FGF2 in ventricular remodeling, no study has addressed the potential cellular targets of FGF2 (or other FGF ligands) in the mature heart by examining cell-specific requirements for FGFR expression/function in response to injury or physiological challenge. We hypothesized several models (discussed above and presented in Figure 2.10) of direct and indirect signaling, and I began breeding our DFF mouse line into various tissue-specific Cre lines, such as the αMHC-CreER [161], Gata5-Cre [162], and Tie2-Cre [163] lines, in order to test the different models. MHC-CreER DCKO mice showed trends toward increased infarct sizes, poorer function, and higher levels of pathological gene expression in the MI model, suggesting that FGF signaling is necessary in cardiomyocytes for proper remodeling and maintenance of function after injury, although the precise mechanism is still being investigated using the more clinically relevant closed-chest ischemia-reperfusion model. Based on these results, we also hypothesized that FGFR gain-of-function in cardiomyocytes would be cardioprotective following cardiac injury.

Finally, the findings presented in this chapter also suggest potential mechanisms for regulation of FGF signaling in the adult heart. As discussed in the introduction, FGFs are potent mitogenic factors that are essential for embryonic cardiac growth and capable of stimulating proliferation and cell growth in cultured myocytes. As such, it is only logical that FGF signaling would be repressed (or maintained at low levels) in the adult heart in order to maintain proper cardiac size, and that this pathway would be induced following injury or stress to allow for postnatal cardiac growth. This would explain why cardiac-specific overexpression of FGF2 does not result in spontaneous hypertrophy; however, the mechanisms for this repression are unknown. By combining the findings of these studies with previously published work, I

propose four potential models by which FGF signaling can be kept in check in the postnatal heart until required following stress, presented in Figure 2.14.

The first model states that FGF2 is sequestered in the cell in which it is made and only released following injury. It is well established that FGF2 is not efficiently secreted [23], and further support for this model comes from a previous publication examining a cardiac-specific FGF2-transgenic mouse line, in which FGF2 protein expression was increased 25-fold, but only a 2-fold increase was observed in the coronary effluent [77]. It has also been demonstrated previously that FGF2 is able to stimulate the expression of cell cycle and hypertrophy markers *in vitro* in isolated ventricular myocytes [83, 164], suggesting that if FGF2 were available to myocytes *in vivo*, it would stimulate a hypertrophic response. Furthermore, recent work suggests that caspase-1 can mediate the secretion of FGF2, providing a potential mechanism for stress-induced release of this ligand [165].

The second model I hypothesize states that FGF2 is released from the cell but sequestered in the extracellular matrix until injury occurs, when it is freed to reach the target cell. It is known that FGF2 can be retained in the extracellular matrix by binding to heparin sulfate proteoglycans [13, 166], but recent evidence also suggests that other FGF ligands, such as FGF16, can modulate the activity FGF2 [39]. The results of my studies support a model in which FGF16 and FGF2 are tightly and reciprocally regulated, suggesting the possibility that FGF16 levels must be reduced in order for FGF2-mediated remodeling to occur. Studies are ongoing in our lab to further investigate the interactions between FGF2 and other FGF ligands.

The third model proposes that regulation of FGF signaling occurs at the level of the receptors on the target cell; I hypothesize that receptors may be present at a low level basally with their expression upregulated following injury. As discussed in chapter 1, there is conflicting evidence regarding both the expression of FGF receptors in the adult heart. One study found expression of FGFR1, 2, and 4 in cardiomyocytes, and expression of FGFR1, 2, and 3 in the vasculature in human samples using immunohistochemistry [106]. In contrast, a study in rats utilizing quantitative *in vitro* autoradiography to image FGFRs that bind to a labeled FGF2 found very low levels of FGF receptor expression in the adult myocardium, with only the blood vessels showing a high density of receptors [107], while yet another study demonstrated very low, but detectable, gene expression of *Fgfr1* in isolated adult rat

cardiomyocytes [108]. The robust increase the expression of *Fgfr1* and *Fgfr2* following injury in my studies supports the possibility that regulation of FGF signaling is at least partially mediated at the level of receptor expression.

Finally, the fourth potential model purports that downstream components of the FGF signaling pathway are repressed basally and induced under injury conditions. This would seemingly contradict *in vitro* studies that indicate that adult cardiomyocytes are competent to respond to an FGF signal [164], but one cannot refute the possibility that the act of isolating and culturing adult ventricular myocytes constitutes a cardiac injury capable of altering gene expression. As such, only *in vivo* studies utilizing cell autonomous activation of FGF signaling can rule out this model. These studies will be the focus of Chapter 3.

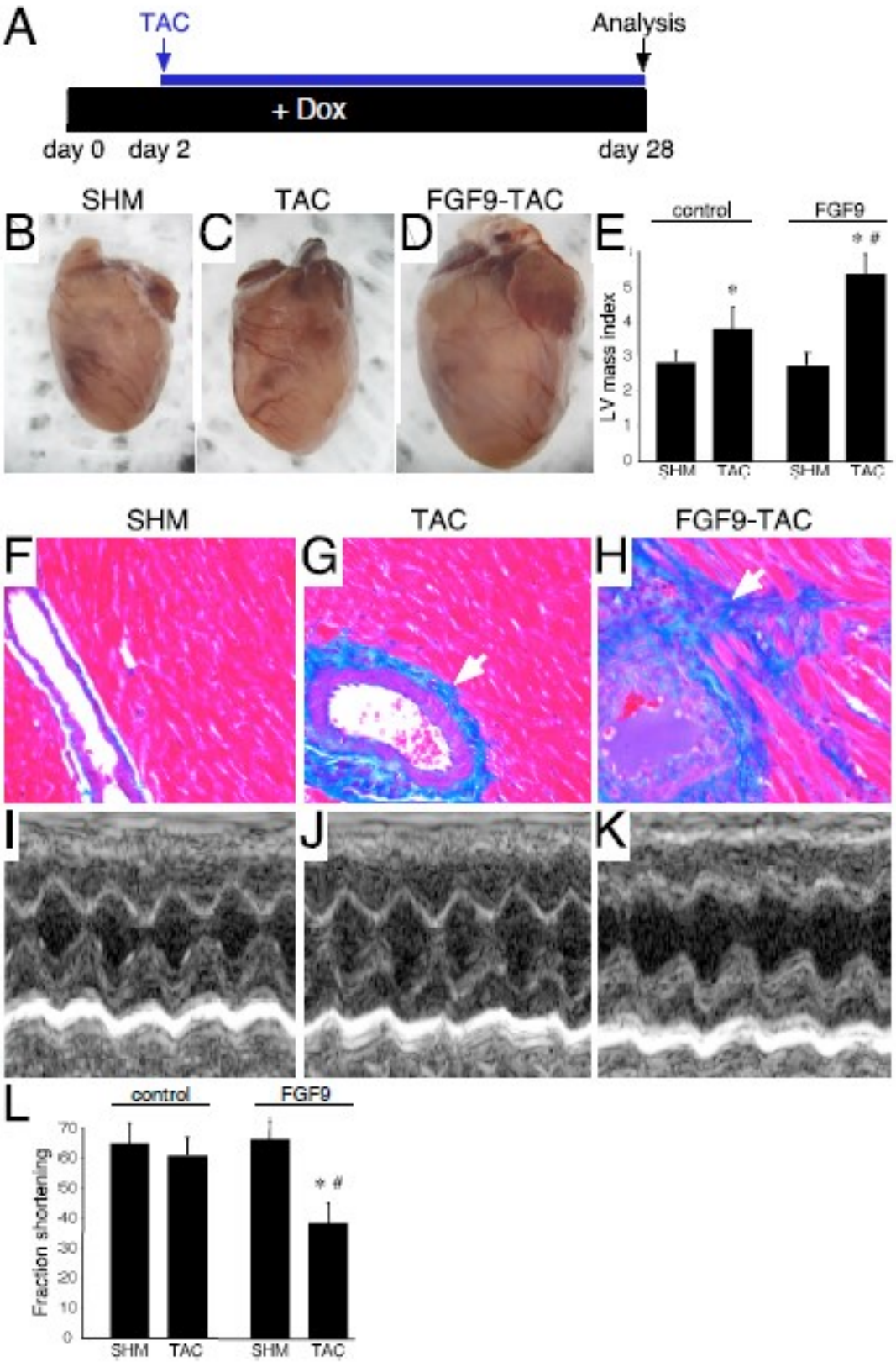
A
TAC
Analysis
+ Dox
day 0
day 2
day 28
SHM
TAC
FGF9-TAC
B
C
D
E
control
FGF9
LV mass index
SHM
TAC
SHM
TAC
F
G
H
I
J
K
L
control
FGF9
Fraction shortening
SHM
TAC
SHM
TAC

Figure 2.1 Over-expression of FGF9 promotes transition from hypertrophy to heart failure. (A) Schematic depicting timing of transgene activation and transaortic constriction (TAC). (B-D) Whole mount photographs of control sham (B), control TAC (C), and FGF9 over-expressing TAC (D) hearts demonstrating marked cardiomegaly in banded (TAC) FGF9 hearts. 4X magnification. E, Quantitation of LV mass index in control and FGF9 over-expressing hearts reveals that for both genotypes banded hearts show increased LV mass index. Banded FGF9 over-expressing hearts have a significantly increased LV mass index compared to banded control hearts. (F-H) Trichrome staining of control sham (F), control TAC (G), and FGF9 over-expressing (H) hearts demonstrates that over expression of FGF9 enhances cardiac fibrosis seen in control TAC hearts. I-K, Echocardiographic analysis of control sham (I), control TAC (J), and FGF9 over expressing (K) hearts reveals that while control sham and control TAC hearts display normal systolic function, FGF9 over-expressing hearts have diminished contractile function, K, Quantitation of fractional shortening shows that FGF9 over-expressing TAC hearts have a statistically significant decrease in fractional shortening compared to both control sham, control TAC, and FGF9 over-expressing sham mice. Asterisk denotes a statistically significant difference between sham and TAC mice and # denotes a statistically significant difference control TAC and FGF9 over-expressing TAC mice. (Experiments performed and figure/legend created by Kory Lavine, a past graduate student in the Ornitz lab.)

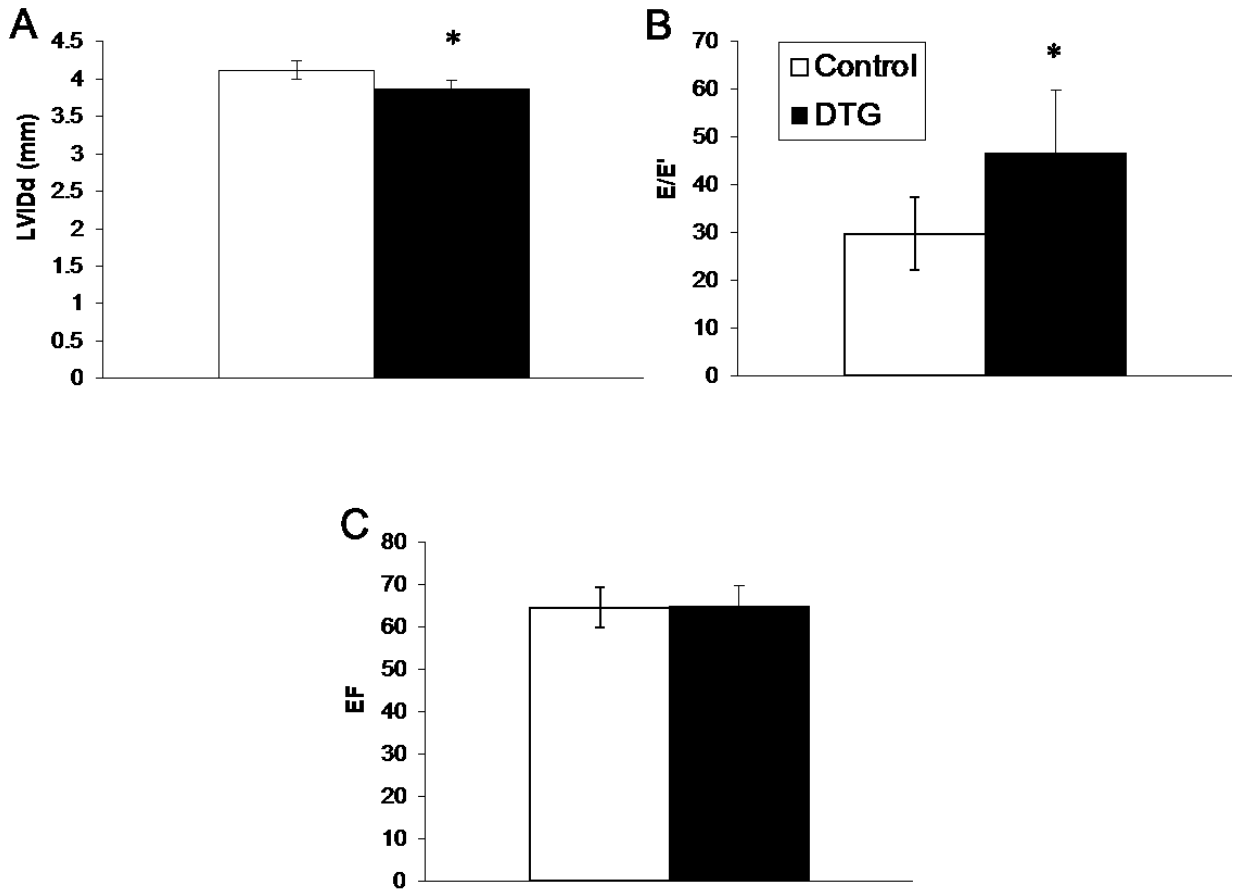

Figure 2.2 Cardiac-specific overexpression of FGF9 in the adult heart results in diastolic dysfunction with preservation of systolic function. αMHC-rtTA, TRE-FGF9 double transgenic (DTG) and littermate controls were fed doxycycline chow for 20 days to induce transgene expression, and then echocardiography was utilized to measure cardiac function. (A) Double transgenic hearts had significantly smaller LV internal diastolic diameter (LVIDd) than littermate controls. (B) DTG mice also had significantly higher E/E' ratios, indicating higher filling pressure compared to control hearts. (C) Despite apparent diastolic defects, systolic function, as measured by ejection fraction (EF), was normal in DTG mice. $n_{control}=4$, $n_{DTG}=5$. Error bars = standard deviation. *$p<0.05$.

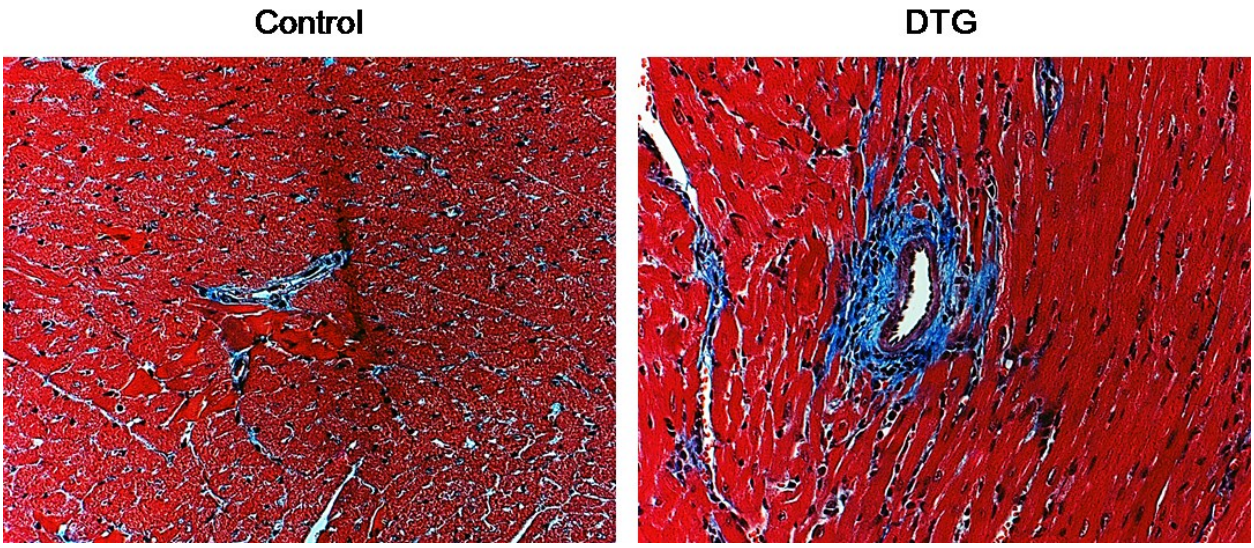

Figure 2.3 Overexpression of FGF9 in the adult heart leads to increased fibrosis. αMHC-rtTA, TRE-FGF9 double transgenic (DTG) and littermate controls were fed doxycycline chow for 20 days to induce transgene expression, and then hearts were harvested for histological analysis. Trichrome staining of control (left) and double transgenic hearts (DTG) reveals areas of increased perivascular and interstitial fibrosis, likely accounting for the diastolic defects seen on echocardiography.

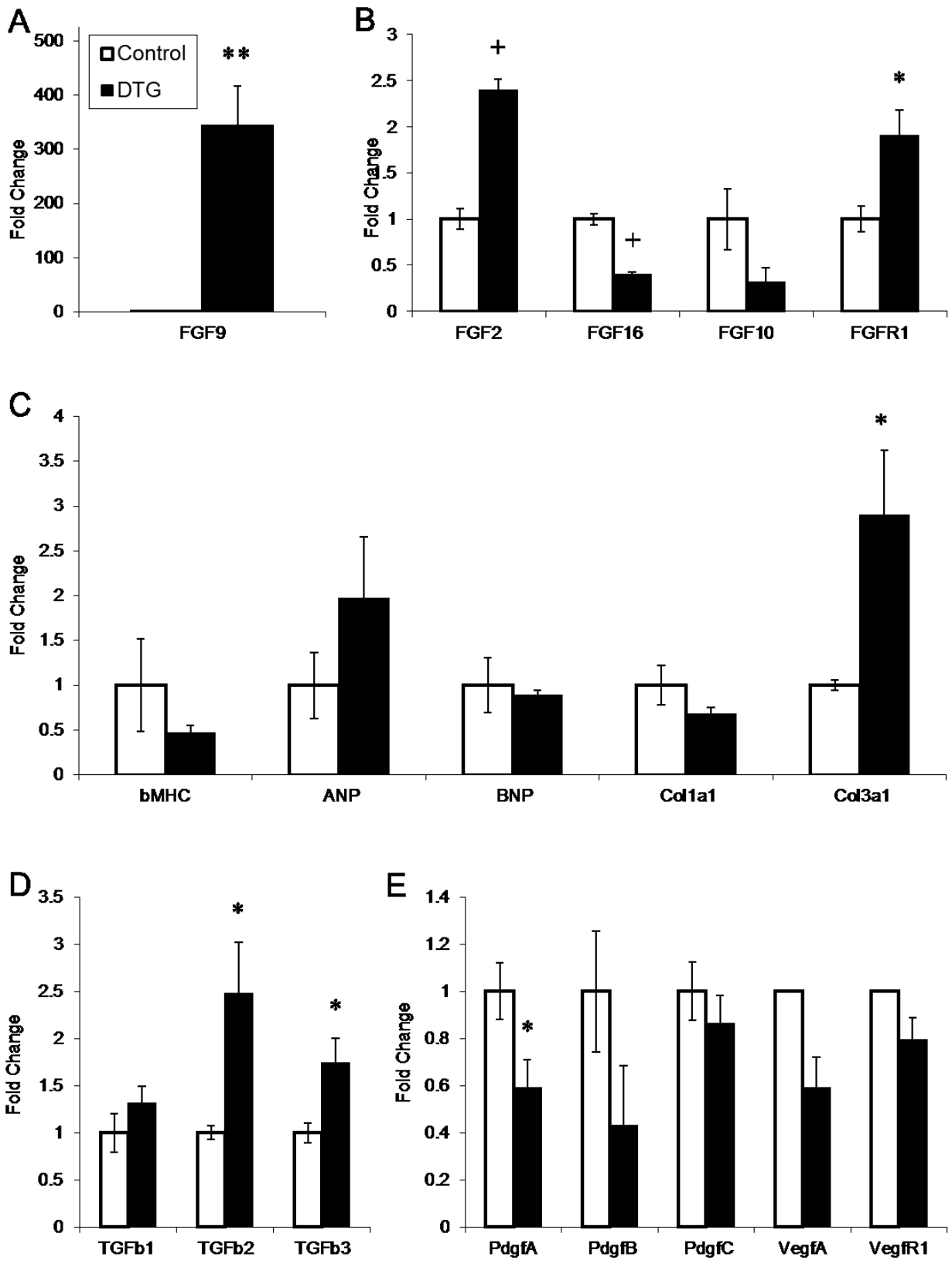
A
Control
DTG
**
Fold Change
500
400
300
200
100
0
FGF9
B
+
+
*
Fold Change
3
2.5
2
1.5
1
0.5
0
FGF2
FGF16
FGF10
FGFR1
C
*
Fold Change
4
3.5
3
2.5
2
1.5
1
0.5
0
bMHC
ANP
BNP
Col1a1
Col3a1
D
*
*
Fold Change
3.5
3
2.5
2
1.5
1
0.5
0
TGFb1
TGFb2
TGFb3
E
*
Fold Change
1.4
1.2
1
0.8
0.6
0.4
0.2
0
PdgfA
PdgfB
PdgfC
VegfA
VegfR1

Figure 2.4 Changes in gene expression following three weeks of cardiac FGF9 overexpression. αMHC-rtTA, TRE-FGF9 double transgenic (DTG) and littermate controls were fed doxycycline chow for 20 days to induce transgene expression, and then hearts were harvested for quantitative RT-PCR analysis. (A) Feeding of DOX chow for 20 days leads to 340-fold upregulation in *Fgf9* expression in DTG hearts. (B) Overexpression of FGF9 for 3 weeks leads to significant upregulation of *Fgf2* and *Fgfr1*, and significant downregulation of *Fgf16*. (C) Markers of pathological cardiac remodeling are relatively unchanged, with the exception of *Col3a1*, which is significantly upregulated. (D) *Tgfβ1* and *2* are also significantly upregulated, supporting histologic findings of increased fibrosis in FGF9-overexpressing hearts. (E) *PdgfA* expression is significantly decreased, and there is a trend towards decreased *PdgfB, VegfA,* and *VegfR1*, indicating that vascularization is not increased following FGF9 induction. $n_{control}$=5, n_{DTG}=5. Error bars=SEM. *p<0.05, **p<0.01, +p<0.001.

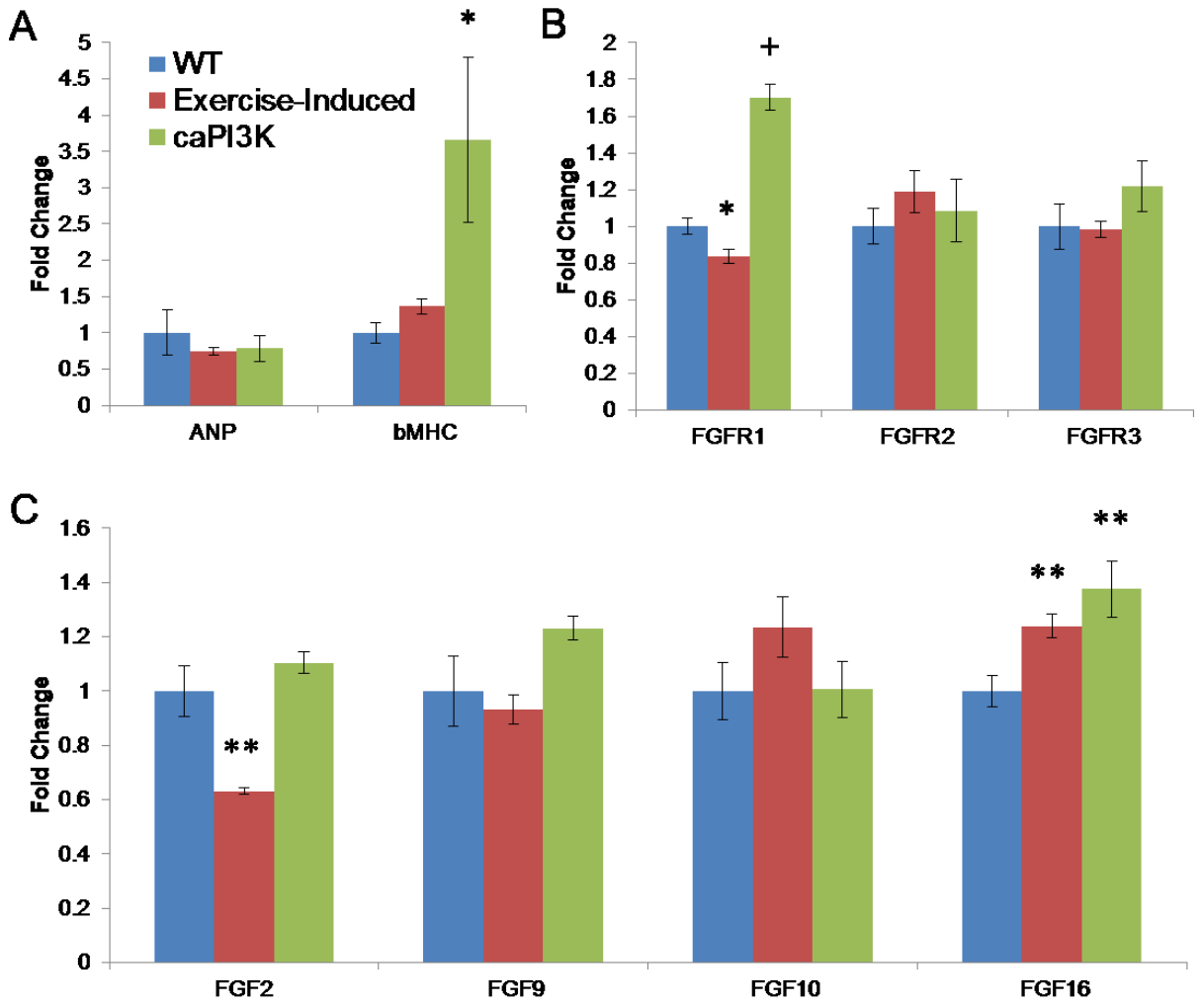

Figure 2.5 Different gene expression profiles from exercise-induced versus caPI3K-induced physiological hypertrophy models. (A) As expected, neither model showed an increase in *ANP* expression, supporting the notion that the hypertrophy is physiological. Constitutively-active PI3K, however, did induce significant upregulation of *βMHC*, an intriguing finding that has been noted previously [148]. (B) *Fgfr1* expression was significantly decreased in exercise-induced hypertrophy but significantly increased in caPI3K hearts. (C) *Fgf2* expression was significantly decreased in exercise-induced hypertrophy, but unchanged in hearts expressing caPI3K, while *Fgf16* expression was significantly increased in both conditions. n=6 for all groups. Error bars = SEM. *p<0.05, **p<0.01, +p<0.001.

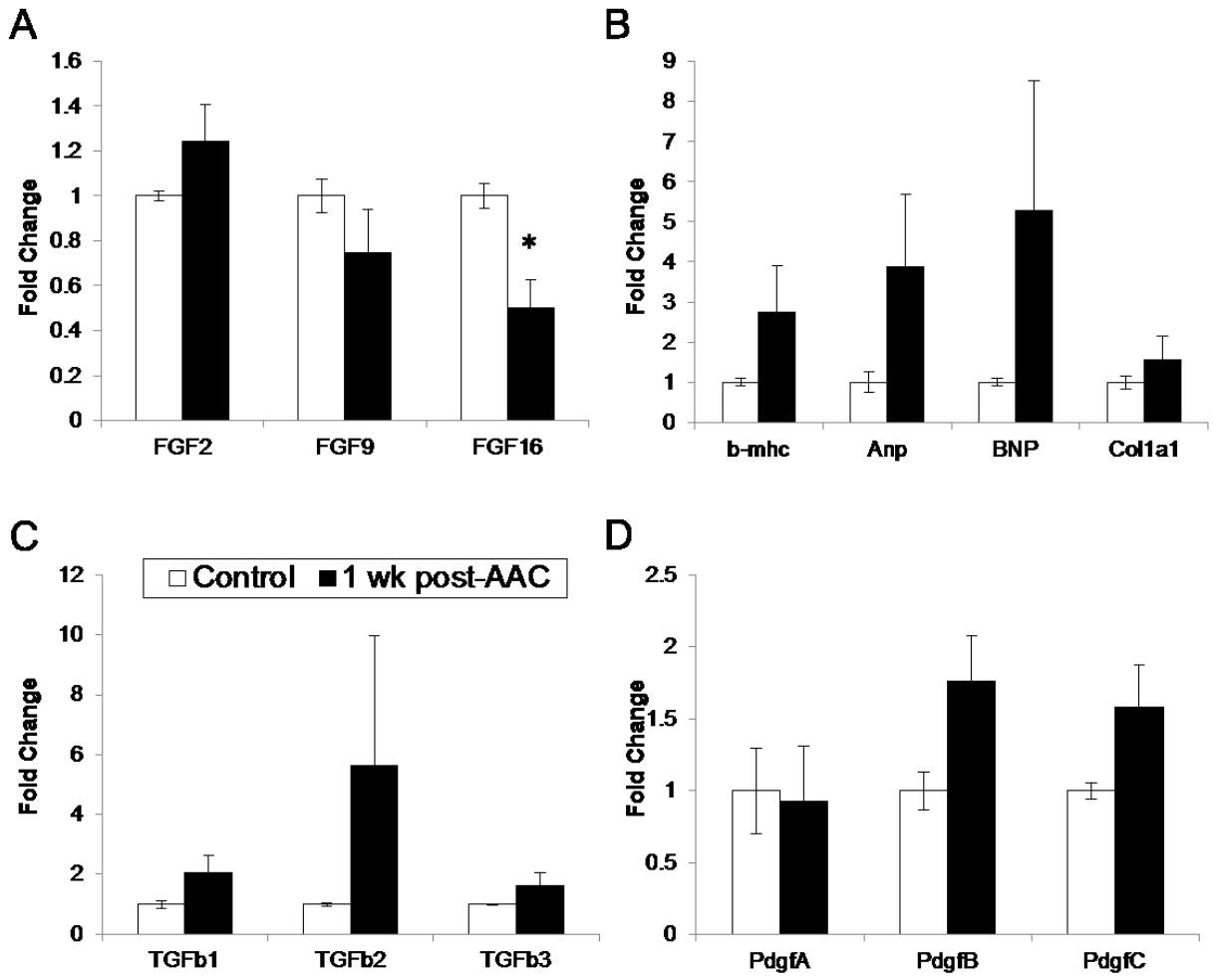

Figure 2.6 Gene expression changes one week post-aortic banding. Eight- to 10-week-old mice were subjected to ascending aortic constriction (AAC) to induce pressure overload and pathological hypertrophy. (A) There was a slight increase in *Fgf2* expression one week after aortic banding and a significant decrease in *Fgf16* expression. (B) There was a trend towards upregulation of markers of pathological remodeling, (C) *Tgfβ* expression, and (D) *Pdgf* expression one week after AAC. $n_{control}$=3, n_{AAC}=2. Error bars=SEM.

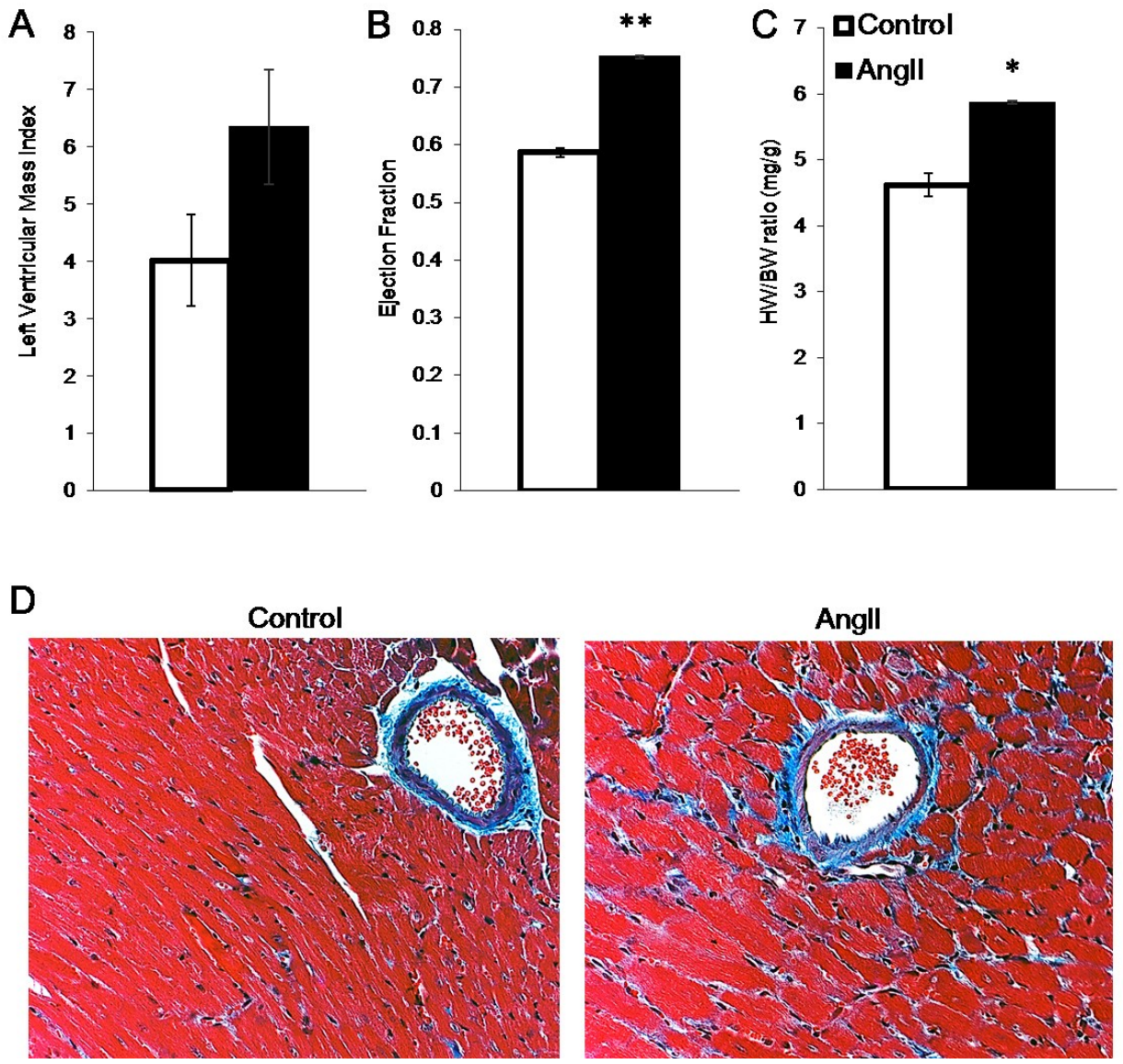

Figure 2.7 Angiotensin II infusion induces hypertrophy, enhanced systolic function, and increased fibrosis in wild-type mice. Angiotensin II- (AngII-) containing osmotic minipumps were implanted in wild-type mice, allowing for continual delivery of AngII for two weeks. (A) After two weeks of AngII infusion, echocardiography revealed increased LV mass index, and (B) significantly enhanced systolic function. (C) Postmortem analysis revealed significantly increased cardiac mass, as measured by heart weight (biventricular weight) to body weight ratio (HW/BW). (D) Histological analysis using Trichrome staining illustrates the presence of increased fibrosis in mice that received AngII (right) compared to vehicle controls (left). n=2 for both groups. Error bars=SEM. *p<0.05, **p<0.01.

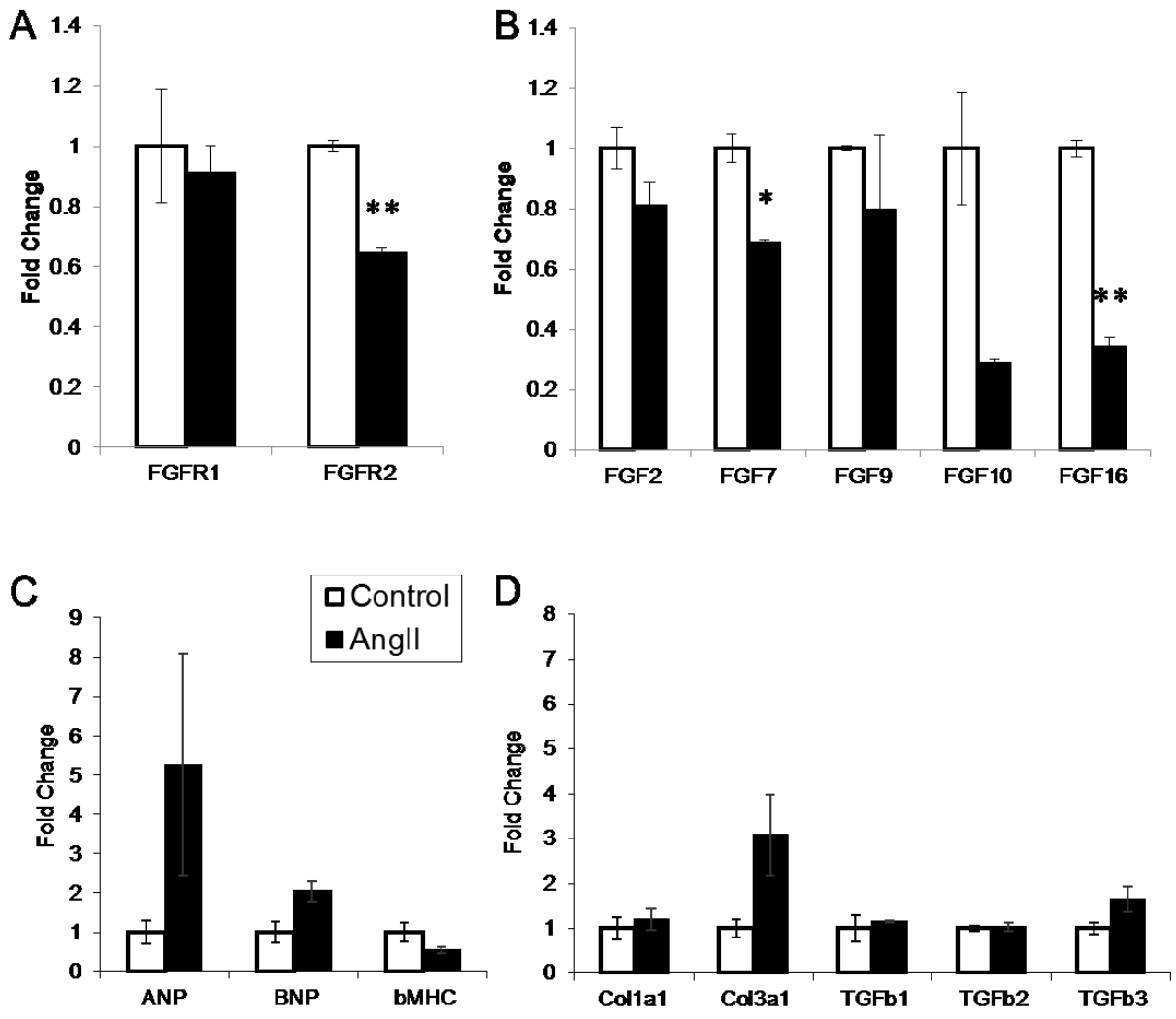

Figure 2.8 Changes in gene expression following AngII treatment. Wild-type mice were infused with AngII or vehicle via osmotic minipumps for two weeks, and then hearts were harvested for quantitative RT-PCR analysis. (A) *Fgfr2* was significantly downregulated following AngII treatment. (B) *Fgf7* and *Fgf16* were also significantly decreased in mice receiving AngII. (C) Expression of *Anp* and *Bnp* are increased following AngII infusion (not significant), and despite the presence of hypertrophy, *βMHC* expression is actually decreased (not significant). (D) Despite the appearance of increased fibrosis on histology, expression of fibrotic markers is not significantly upregulated. n=2 for both groups. Error bars=SEM. *p<0.05, **p<0.01.

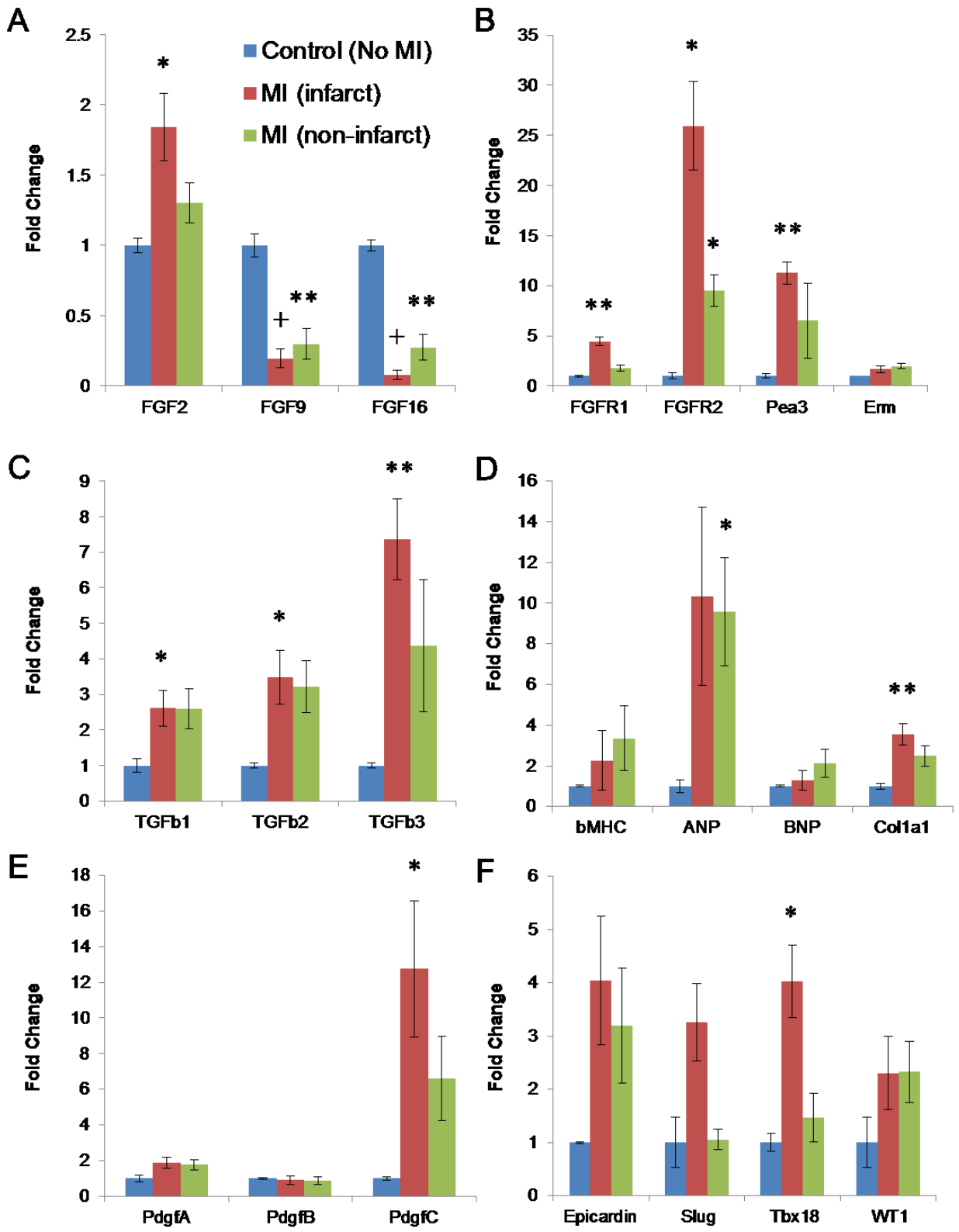
A
Control (No MI)
MI (infarct)
MI (non-infarct)
Fold Change
FGF2
FGF9
FGF16
B
Fold Change
FGFR1
FGFR2
Pea3
Erm
C
Fold Change
TGFb1
TGFb2
TGFb3
D
Fold Change
bMHC
ANP
BNP
Col1a1
E
Fold Change
PdgfA
PdgfB
PdgfC
F
Fold Change
Epicardin
Slug
Tbx18
WT1

Figure 2.9 Altered gene expression one week following MI. The left anterior descending artery was ligated to induce myocardial infarction. Quantitative RT-PCR was used to examine gene expression of FGF ligands and receptors and other markers of pathological remodeling in infarcted and non-infarcted regions from the same heart compared to nonsurgical controls. (A) *Fgf2* is significantly increased in infarcted tissue, while expression of *Fgf9* and *Fgf16* is significantly repressed in both infarct and non-infarct regions. (B) *Fgfr1, Fgfr2*, and a downstream mediator of FGF signaling, *Etv4/Pea3* are significantly upregulated in the infarct zone, while *Fgfr2* is also significantly increased in non-infarcted myocardium. (C) *ANP* expression is significantly increased in non-infarcted tissue, while *Col1a1* is significantly upregulated in the infarct region. (D) *Tgfβ1-3* are all increased in infarcted tissue. (E) *PdgfC* is also significantly increased in the infarct zone. (F) There is a trend for increased expression of epicardial markers following MI, though only *Tbx18* shows significant upregulation in the infarct region. $n_{control}=3$, $n_{MI}=4$. Error bars = SEM. *$p<0.05$, **$p<0.01$, +$p<0.001$.

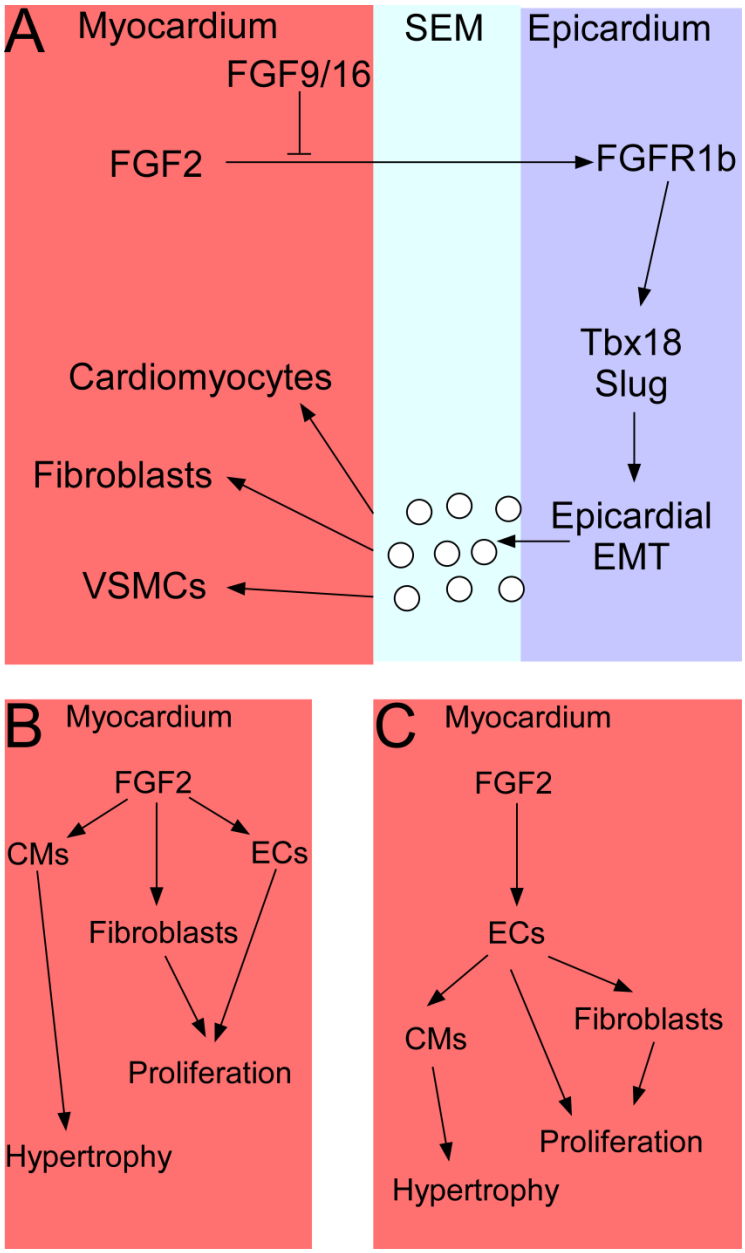

Figure 2.10 Possible Mechanisms for FGF2-Mediated Cardioprotection. (A) I hypothesize that one function of FGF2 upregulation in response to MI is signaling to FGFRs in the epicardium to stimulate EMT and migration of EPDCs into the infarcted tissue to promote healing. Similar to the mechanism proposed in zebrafish to regenerate heart tissue [158], EPDCs could then differentiate into vascular and myocardial progenitor cells and help to repopulate and repair infarcted tissue. (B) Another possibility is that FGF2 signals directly to the cardiomyocyte where it could have a direct cardioprotective role by inducing hypertrophy or promoting cell survival, or to the endothelial or perivascular cell, where it could function in

angiogenic pathways that are necessary for the myocardial response to injury. (C) Another, more likely, alternative is that one of these cell types (epicardial, endothelial, fibroblast, or myocyte) receives the FGF signal and serves as a signaling center, releasing other factors that promote the remodeling effects in other cells. ECs=endothelial cells, CMs=cardiomyocytes, VSMCs=vascular smooth muscle cells, SEM=subepicardial mesenchyme, EMT=epithelial-mesenchymal transition.

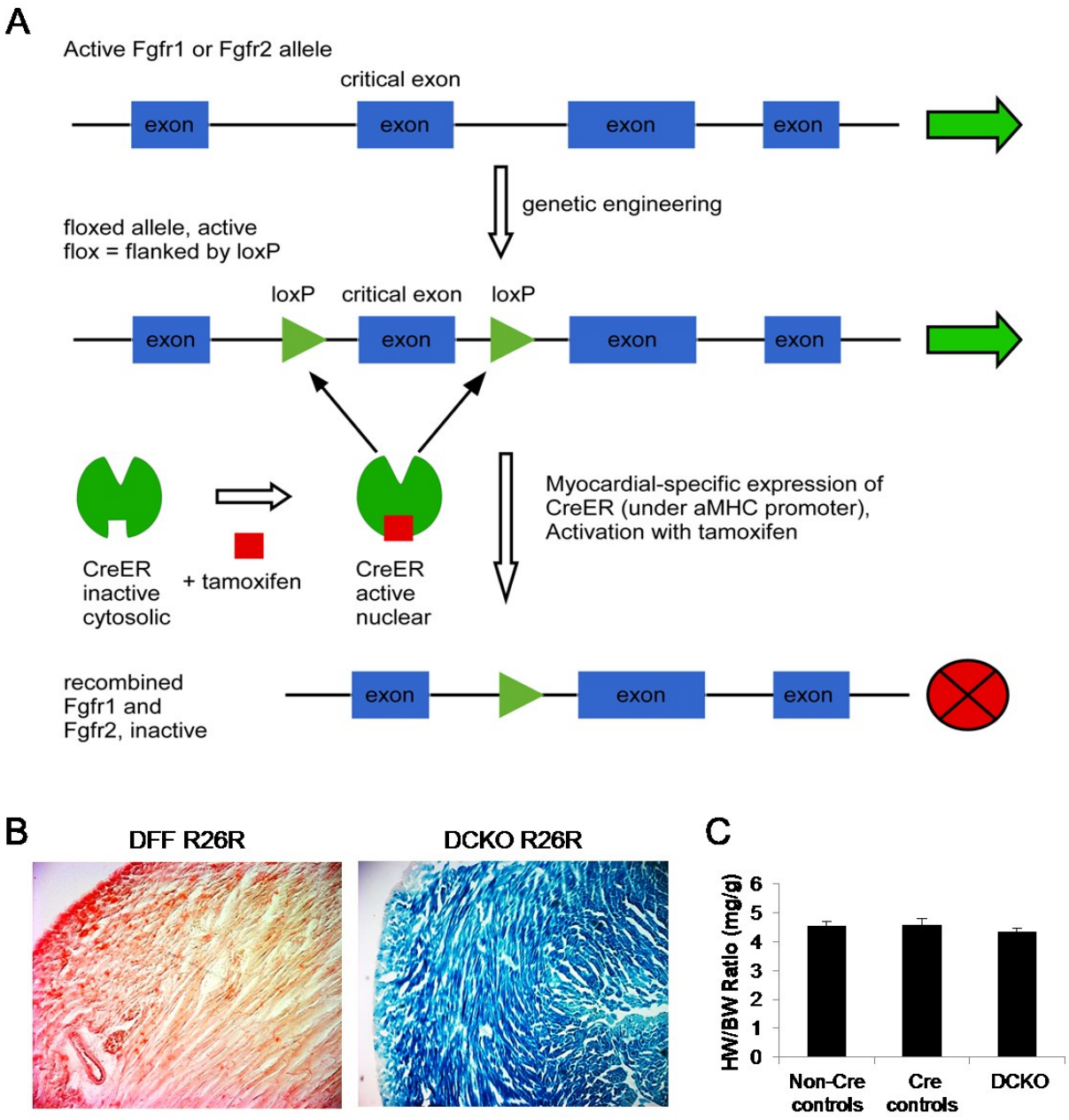

Figure 2.11 Tamoxifen-inducible cardiomyocyte-specific FGFR1/2 double conditional knockout (MHC-CreER DCKO). (A) Schematic of the double conditional knockout system, showing that following tamoxifen injections (6 days, 40 mg/kg IP), Cre becomes active in cardiomyocytes and deletes floxed alleles of FGF receptors 1 and 2. (B) β-galactosidase staining one week following the sixth tamoxifen injection shows LacZ expression in nearly all cardiomyocytes, with no expression around vasculature, in the epicardium (DCKO R26R) or in littermate controls (DFF R26R). (C) HW/BW ratios suggest equivalent

cardiac mass in DCKO and littermate control (with or without Cre) mice. Error bars=SEM. DFF=double floxed-floxed (*Fgfr1*$^{f/f}$, *Fgfr2*$^{f/f}$), DCKO=double conditional knockout (*αMHC-CreER*, *Fgfr1*$^{f/f}$, *Fgfr2*$^{f/f}$).

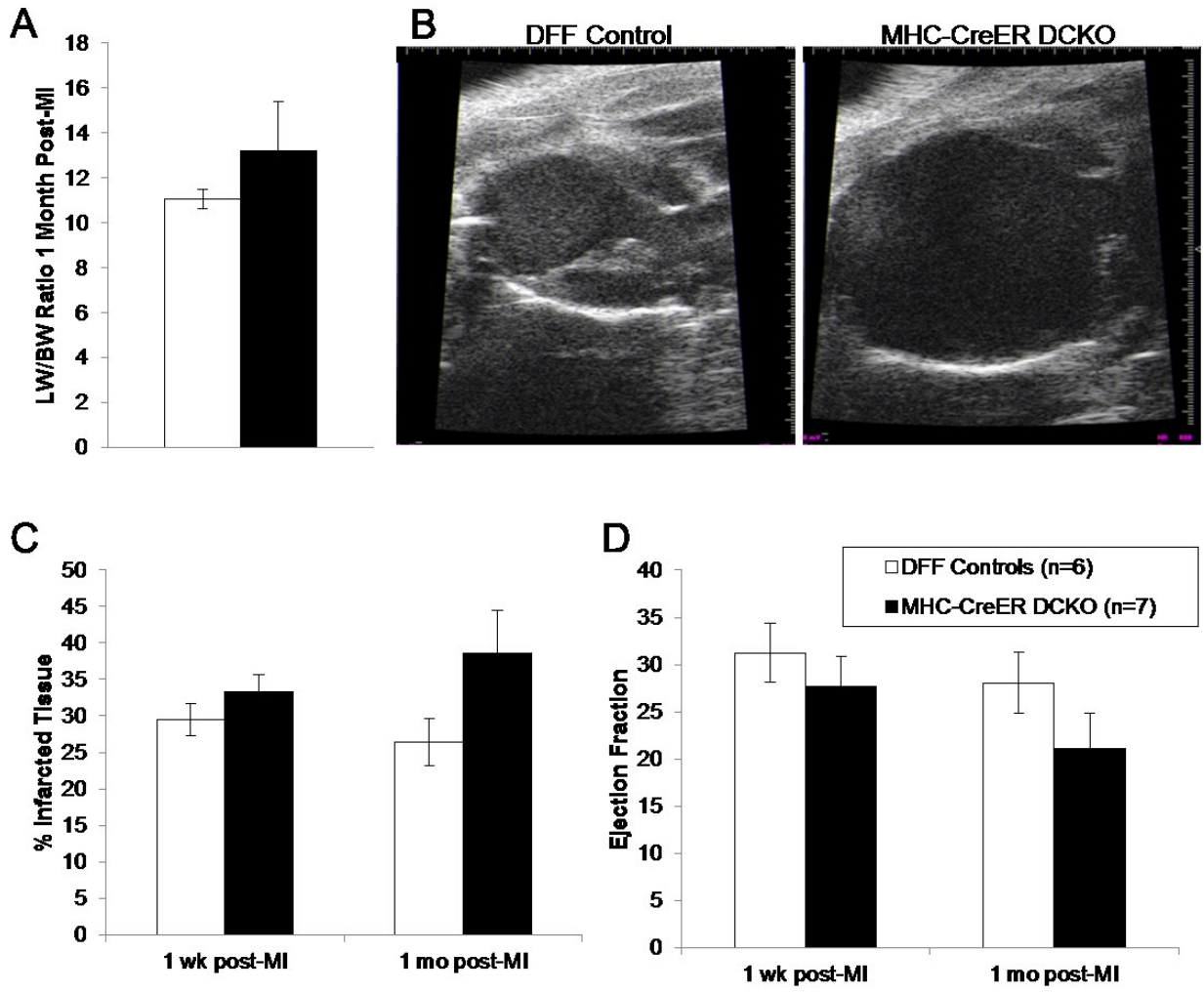

Figure 2.12 MHC-CreER DCKO mice have a poorer response following myocardial infarction. (A) DCKO mice have higher lung weight to body weight ratios (LW/BW), suggesting a high degree of cardiac dysfunction. (B) Representative echo images illustrating larger infarct size in DCKO mice. (C) DCKO hearts trend towards increased infarct sizes and (D) poorer systolic function compared to littermate controls at both one week and one month following MI. Ejection fraction and % infarcted tissue were measured using serial short-axis echocardiographic slices and Vevo770 software. n_{DFF}=6, n_{DCKO}=7. Error bars=SEM.

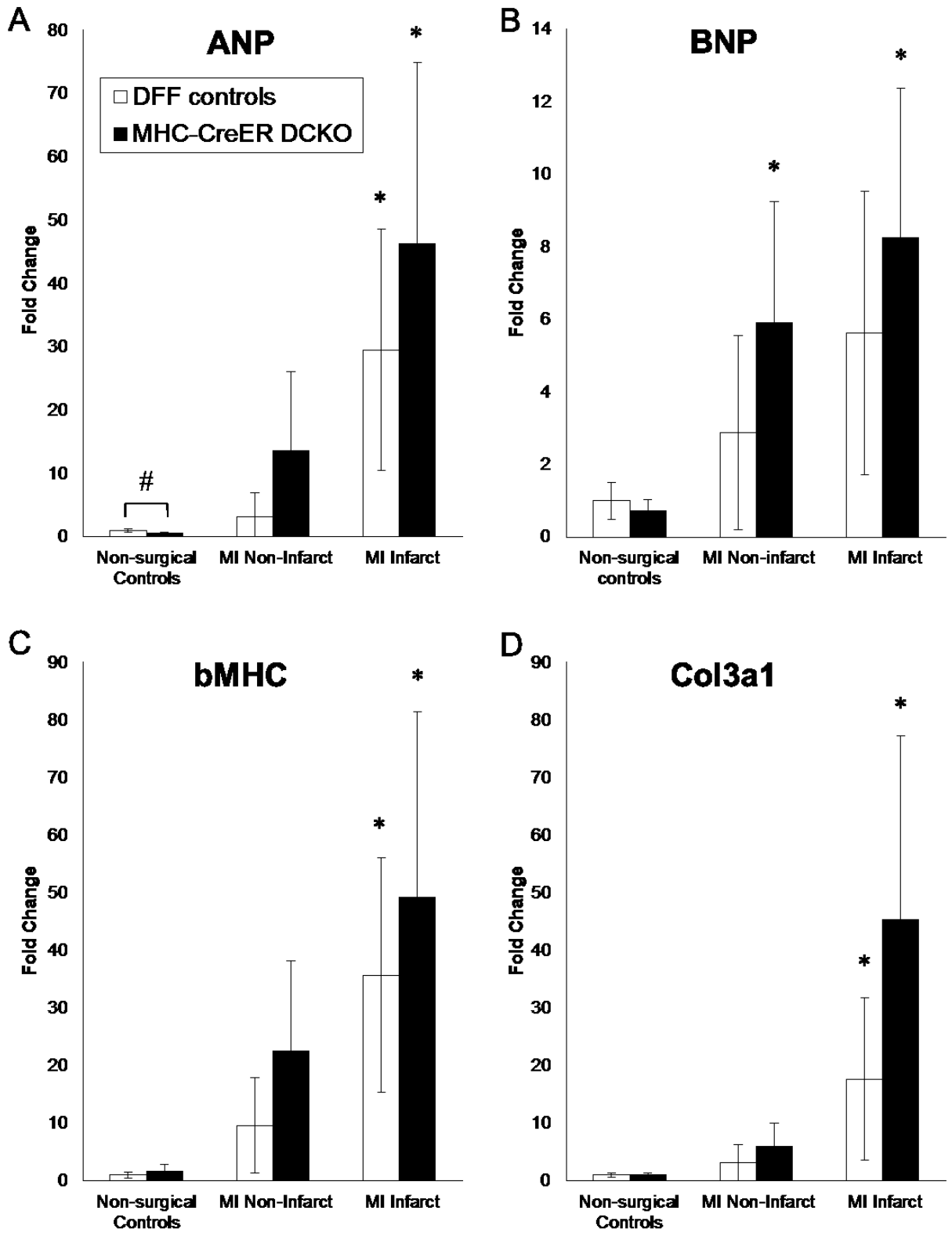

Figure 2.13 MHC-CreER DCKO mice show increased expression of markers of pathological remodeling. One month following MI, hearts were harvested and dissected into infarcted tissue and non-

infarcted tissue. DCKO hearts showed trends toward increased expression of (A) *Anp*, (B) *Bnp*, (C) *βMHC*, and (D) *Col3a1* in both infarct and non-infarct regions. In addition, non-surgical DCKO mice had significantly decreased expression of *Anp* compared to littermate controls (A). Nonsurgical: n_{DFF}=4, n_{DCKO}=3; MI: n_{DFF}=6, n_{DCKO}=7. Error bars=SEM. *p<0.05 vs. respective nonsurgical controls. #p<0.05 vs. DFF littermate controls.

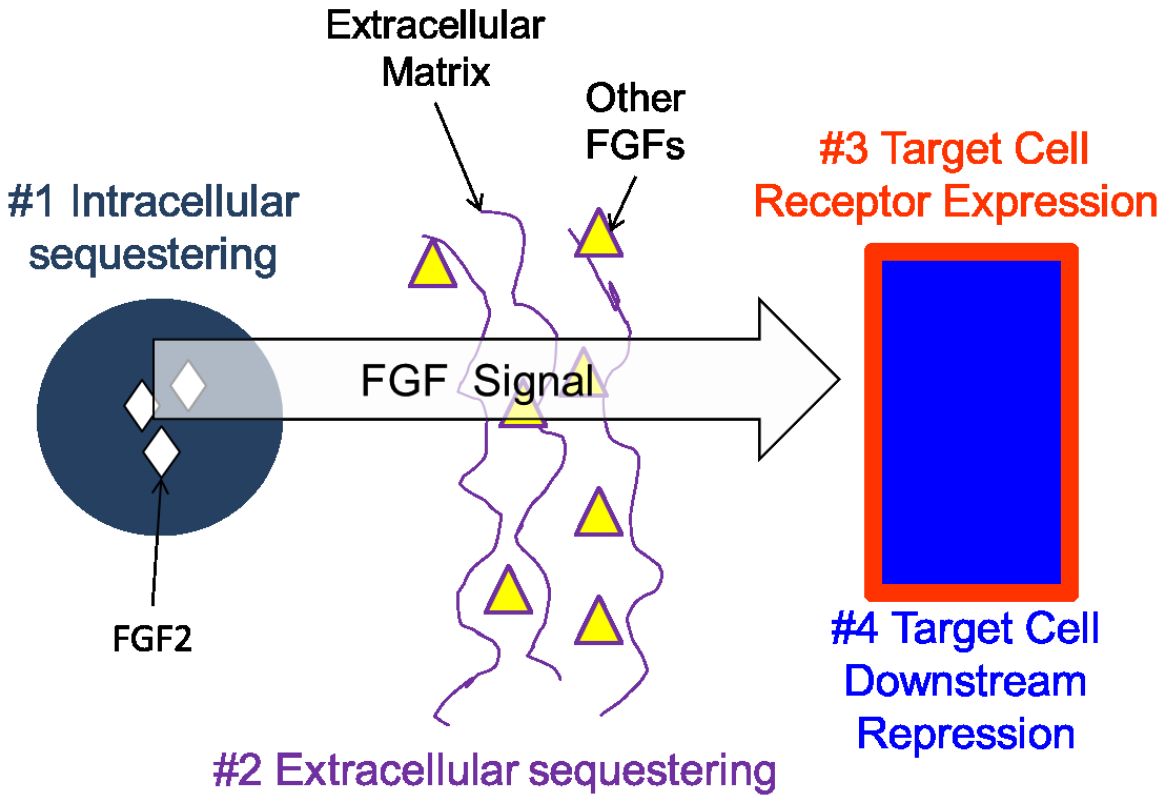

Figure 2.14 Proposed models for regulation of paracrine FGF signaling in the adult heart. We propose four potential models to address why FGF2 loss- and gain-of-function mice do not have a cardiac phenotype under homeostatic conditions. In model #1, FGF2 is sequestered in the cell in which it is made and only released following injury. In model #2, FGF2 is released from the cell but sequestered in the extracellular matrix until injury occurs, when it is freed to reach the target cell. In model #3, regulation of FGF signaling occurs at the level of the receptors on the target cell; we hypothesize receptors may be present at a low level basally with their expression upregulated following injury. Finally, in model #4, downstream components of the FGF signaling pathway are repressed basally and induced under injury conditions.

Gene	Exercise-Induced Hypertrophy	caPI3K Hypertrophy	Aortic Constriction	MI	AngII
ANP	Normal	Normal	UP 3.9-fold 1 week post banding (NS)	UP 10.3-fold in infarct (p=0.12), 9.6-fold in non-infarct (p=0.04)	Up 5-fold (NS)
bMHC	UP 1.36-fold (NS)	UP 3.66-fold (p=0.03)	UP 2.7-fold 1 wpb (NS)	Up slightly (NS)	Down slightly (NS)
FGF2	DOWN 1.6-fold (p=0.003)	Normal	UP 1.2-fold 1wpb (NS)	UP 1.8-fold in infarct (p=0.03)	Normal
FGF9	Normal	UP 1.2-fold (NS)	DOWN 1.3-fold 1wpb (NS)	DOWN 5-fold in infarct (p=0.0007), 3.3-fold in non-infarct (p=0.004)	Down slightly (NS)
FGF10	Up slightly (NS)	Normal	not assessed	Down slightly (NS)	DOWN 3.4-fold (p=0.06)
FGF16	UP 1.24-fold (p=0.009)	UP 1.38-fold (p=0.01)	DOWN 2-fold 1 wpb (p=0.02)	DOWN 12.5-fold in infarct (p=0.000008), 3.7-fold in non-infarct (p=0.001)	DOWN 2.9-fold (p=0.004)
FGFR1	DOWN 1.2-fold (p=0.02)	UP 1.7-fold (p=0.000007)	not assessed	UP 5.6-fold in infarct (p=0.001), 2.2-fold in non-infarct (p=0.06)	Normal
FGFR2	Normal	Normal	not assessed	UP 30-fold in infarct (p=0.02), 9.5-fold in non-infarct (p=0.03)	DOWN 1.5-fold (p=0.005)
FGFR3	Normal	Normal	not assessed	DOWN 2-fold in infarct (p=0.04)	Not assessed

Table 2.1 Summary of notable gene expression changes in different models of cardiac remodeling. Cells highlighted in green represent genes that were significantly upregulated, while cells highlighted in red represent genes that were significantly downregulated. Note that *Fgf16* expression displays a distinct expression pattern, in which it is upregulated in models of physiological hypertrophy and downregulated in models of pathological hypertrophy.

Chapter 3

In Vivo Induction of Constitutively-Active FGFR1 in Adult Cardiomyocytes Leads to the Rapid Development of Hypercontractility and Hypertrophic Cardiomyopathy through Modulation of Sarcomere Mechanics

A. Introduction

Hypertrophy is an adaptive mechanism by which the heart can respond to stress or injury. In response to postnatal development, pregnancy, or exercise, the heart undergoes physiological hypertrophy, characterized by a predominant increase in myocyte length, absence of fibrosis, maintenance of chamber dimension, and normal cardiac function. In response to injury or stress, such as a myocardial infarction or an increase in afterload due to hypertension, functional heart muscle will compensate with hypertrophy, which initially maintains cardiac function. This pathological hypertrophy is characterized by predominantly increased myocyte width, fibrosis, decreased ventricular chamber volume, and eventual cardiac dysfunction and failure [2, 3]. Additionally, there is a primary myocardial disorder, hypertrophic cardiomyopathy (HCM), most often caused by dominant mutations in sarcomeric proteins. HCM is a pathologic condition characterized by myocyte hypertrophy and disarray, fibrosis, and maintenance or even enhancement of systolic function [5, 167]. Many studies have attempted to elucidate mechanisms that result in hypertrophy, but this process remains poorly understood, particularly with regard to mechanisms that distinguish the advantageous physiologic hypertrophy from the detrimental pathologic hypertrophy.

Previous studies have indicated that while not essential for development, FGF2 is upregulated and is vital to the pathologic hypertrophic response to cardiac pressure overload, as well as the remodeling response to chronic myocardial infarction (MI) [31, 32, 77, 97]. *Fgf2*$^{-/-}$ mice develop significantly less hypertrophy compared with *Fgf2*$^{+/+}$ mice following transverse aortic constriction (TAC) [32], and, compared to controls, they also show larger infarct sizes and poorer function following MI [77, 97]. Gain-of-function studies in mice in which FGF2 is constitutively overexpressed, either ubiquitously or in cardiomyocytes, demonstrate that FGF2 can promote cardiomyocyte hypertrophy only in times of cardiac stress, as FGF2-overexpressing transgenic mice do not experience spontaneous hypertrophy or changes in vascular density [77, 85, 97]. Additionally, overexpression of FGF2 results in proliferation of both endothelial cells and fibroblasts following injury to the heart, but not under baseline conditions, as FGF2-transgenic mice do not have excess extracellular matrix production or vascular formations [97]. However, following MI or *ex vivo* ischemia-reperfusion, FGF2-overexpressing mice show decreased infarct size and improved cardiac function [77, 97].

In this study, we aimed to understand the mechanisms governing FGF signaling in the development of cardiac hypertrophy and why FGF2 overexpression is not sufficient to induce hypertrophy under homeostatic conditions. We hypothesized that adult cardiomyocytes are not competent to respond to an FGF signal, that the FGF signaling pathway is repressed in cardiomyocytes under baseline conditions, and that this repression is relieved following injury or stress to the heart.

To directly test this model, we engineered a transgenic mouse line in which we could cell-autonomously induce expression of a ligand-independent constitutively-active FGF receptor (caFGFR1-myc) specifically in cardiomyocytes through doxycycline administration to α*MHC-rtTA, TRE-caFgfr1-myc* double transgenic mice (DTG, Figure 1A). We found that *in vivo* induction of caFGFR1 in adult cardiomyocytes leads to rapid changes in cardiomyocyte contractile dynamics and a dynamic obstruction in the proximal left ventricle. This acute pathology is followed by the progressive development of concentric hypertrophy with significantly increased cardiac mass and cardiomyocyte size, interstitial fibrosis, and myocyte disarray characteristic of hypertrophic cardiomyopathy. Interestingly, systolic function is preserved, even after six months of transgene induction. Examination of signaling pathways strongly suggests a mechanism in which activation of FGF signaling in cardiomyocytes leads to both an increase in myofilament calcium sensitivity and a reduction in calcium recycling into the sarcoplasmic reticulum. Calcium dysregulation and alterations and myofilament calcium sensitivity are common mechanisms implicated in the pathogenesis of familial hypertrophic cardiomyopathy, and as a result, this novel model of caFGFR1-induced HCM may be useful for further investigation into the mechanisms involved in HCM development and studies aimed at its reversal.

B. Results

Doxycycline-inducible cardiomyocyte-specific constitutively-active FGF receptor 1 mouse model. To investigate the potential function of FGF signaling in adult cardiomyocytes, we utilized the doxycycline-regulatable TET-on system with the *αMHC-rtTA* mouse line. Expression of the reverse tetracycline transcriptional activator (rtTA) from the αMHC promoter leads to cardiomyocyte-specific expression of the rtTA protein [144]. To determine the effects of cell autonomous activation of FGF signaling, we generated a tetracycline response element (TRE)-drivable FGFR31c(R248C)-c-myc

transgene, in which FGFR31c(R248C) is a chimeric receptor consisting of the FGFR3c(R248C) mutant extracellular and transmembrane domains fused to the FGFR1 tyrosine kinase domain (Figure 3.1A). The FGFR3c(R248C) mutation confers ligand-independent constitutive activity [168]. By fusing this mutant FGFR3c receptor to the FGFR1 tyrosine kinase domain, one can produce a receptor that constitutively activates FGFR1 signaling in the absence of ligand (caFGFR1). A c-myc tag was placed at the C-terminal tail of caFGFR1 to allow detection of mutant receptor expression. Addition of this epitope did not affect the activity of the mutant receptor (data not shown). For simplicity the *Tre-Fgfr31c(R248C)-c-myc* transgene will be referred to as *Tre-caFgfr1*.

αMHC-rtTA/TRE-caFGFR1 double transgenic mice (DTG) were examined expression of the c-myc tag (transgenic caFGFR1 expression only) and FGFR1 (both transgenic caFGFR1 and native FGFR1 expression) in the absence of doxycycline to determine the basal level of transgene activation in our genetic system, as well as the level of native FGFR1 protein expression in the adult mouse heart. Double transgenic animals displayed very low levels of c-myc and FGFR1 protein expression (Figure 1G, DTG 0d), while single transgenic TRE-caFGFR1 animals did not show any expression of the transgene or native FGFR1 (Figure 3.1B, control 0d). To determine if this level of basal transgene expression led to a cardiac phenotype, we measured the ratio of biventricular weight and total body weight (HW/BW ratio, Figure 3.1C), as well as mean cardiomyocyte cross-sectional area (Figure 3.1D) and *in vivo* left ventricle (LV) diastolic posterior wall thickness (LVPWd, Figure 3.1E) and proximal LV peak outflow velocity (LV POV, Figure 3.1F) in 12- to 14-week-old mice. Cardiac mass, myocyte size, and LV wall thickness were comparable between double transgenic mice and littermate controls, while a small, but significant, increase was observed in peak outflow velocity (1.01 ± 0.61 m/s vs. 0.57 ± 0.18 m/s, p=0.0002).

To further investigate whether a pathologic cardiac phenotype was present at baseline, we utilized quantitative RT-PCR to examine the gene expression of established markers heart failure, hypertrophy, and fibrosis (Figure 3.1G) [9-11, 79]. While the expression of b-type natriuretic peptide (*bnp*) was slightly elevated (2.1 ± 1.2-fold vs. control, not significant), levels of atrial natriuretic peptide (*anp*), beta-myosin heavy chain (*βmhc*), and collagens 1 and 3 (*col1a1*, *col3a1*) were unchanged in double transgenic hearts at baseline. In all studies, littermate controls included single transgenic mice (αMHC-rtTA only, TRE-caFGFR1 only) or wild-type mice. No significant differences were observed

between the three control genotypes in any of the analyzed parameters, and as a result, control data were pooled.

To test whether αMHC-rtTA can confer inducible expression of caFGFR1 in the heart, we examined c-myc and FGFR1 expression following the administration of doxycycline (DOX) chow (Figure 3.2A). One day of DOX was sufficient to induce robust expression of the transgene (Figure 3.2A, DTG 1d), which was maintained at consistent levels with chronic feeding of DOX chow (Figure 3.2A, DTG 7d, 21d, 168d). No transgene activation or native FGFR1 expression was visible in littermate control animals (Figure 3.2A, control 1d, 7d, 21d, 168d). We also utilized quantitative RT-PCR to measure the fold change in *Fgfr1* gene expression (Figure 3.2B). While *Fgfr1* mRNA expression was significantly increased at baseline (0d) in double transgenic mice (19.6 ± 6.6-fold vs. control, $p=0.001$), expression increased dramatically after one day on DOX chow (199.2 ± 79.5-fold vs. control, $p<0.001$) and was maintained at these high levels with chronic DOX feeding. Additionally, we monitored gene expression of the ETS transcription factors *Etv4* and *Etv5* (Figure 3.2C), which have been shown to be activated by FGF signaling [15, 169]. Despite the increased *Fgfr1* expression, *Etv5* and *Etv4* gene expression remained unchanged at baseline (0d) in double transgenic mice compared to littermate controls. Expression of both transcription factors increased significantly after one day of transgene induction (*Etv5*: 2.98 ± 0.89-fold vs. control, $p<0.001$; *Etv4*: 2.63 ± 1.06 vs. control, $p<0.01$), and they remained elevated with chronic expression of caFGFR1. Fold change and statistical analysis depicted in Figures 3.2B and 3.2C was calculated compared to corresponding time-matched littermate controls (not shown for simplicity).

In vivo characterization of phenotype development in αMHC-rtTA, TRE-caFGFR1 mice. To determine the effect of activating FGF signaling specifically in cardiomyocytes, 12- to 14-week-old double transgenic animals and littermate controls were fed doxycycline (DOX)-containing chow for varying lengths of time to induce transgene expression, and cardiac function was monitored over time with echocardiography. LV diastolic posterior wall thickness was significantly elevated in double transgenic mice within one day of DOX induction (0.99 ± 0.20 vs. 0.88 ± 0.02 mm, $p=0.001$, LVPWd) (Figure 3.3A), and LV mass index was significantly elevated by one week of induction (5.3 ± 1.0 vs. 4.2 ± 0.5, $p=0.02$, LVMI) (Figure 3.3C). Both parameters continued to increase throughout six months of induction.

Meanwhile, LV internal diastolic diameter was significantly decreased within one week of transgene induction (3.04 ± 0.26 vs. 3.47 ± 0.21 mm, p=0.001, LVIDd) (Figure 3.3B) and remained relatively constant throughout the length of the study. Systolic function, as measured by ejection fraction (not shown) or fractional shortening (Figure 3.3D) remained comparable between double transgenic animals and littermate controls throughout the length of the study, and was even significantly increased at three time points (1d, 42d, 126d). Heart rates were slightly, but not significantly, decreased at all time points in double transgenic mice (data not shown). Representative diastolic mid-ventricle short-axis still images from double transgenic animals are presented in Figure 3.3E. Note the concentric and symmetrical increase in wall thickness and the decreased chamber volume.

To determine the effects of caFGFR1 on the relaxation and contractile properties of the adult heart, we performed *in vivo* hemodynamic analysis after one day (Figure 3.4A, Table 3.1) and six weeks (Figure 3.4B, Table 3.1) of transgene induction. Following one day of induction, no significant differences were observed in heart rate, dP_{max}, dP_{min}, end systolic or diastolic pressure (ESP, EDP), or tau (Glantz) values of relaxation (Table 3.1). However, end systolic volume was greatly reduced (18.2 ± 3.3 vs. 31.7 ± 4.5 mL, p=0.051), and end diastolic volume was significantly decreased in double transgenic mice compared to littermate controls (31.8 ± 2.8 vs. 51.2 ± 4.5 mL, p=0.01). In order to more accurately assess the contractility and stiffness of the ventricle, we increased the afterload of the heart by briefly constricting the transverse aorta and examining the end-systolic pressure-volume relationship (ESPVR) between the baseline and increased afterload pressure-volume (PV) loops. The slope of the ESPVR is an excellent indicator of the contractility of the heart, and it is clearly elevated following 24 hours of caFGFR1 induction (10.4 ± 1.6 vs. 3.6 ± 1.1, p=0.004, Figure 3.4A).

Six weeks of transgene induction resulted in an obstructive phenotype, as indicated by the altered appearance of the pressure and dP/dt tracings (Figure 3.4B) and the significantly elevated end systolic pressures seen in double transgenic animals compared to littermate controls (191.6 ± 21.2 vs. 105.8 ± 2.7 mmHg, p=0.01, Figure 3.4B). Additionally, there was a significant increase in tau (Glantz) in double transgenic hearts (Table 3.2), suggesting the presence of a relaxation defect. Due to the dynamic obstruction, the shape of the PV loop of the double transgenic mice was significantly altered, making it difficult to directly compare other parameters to littermate controls.

Echocardiographic Doppler analysis supported the findings from the hemodynamic studies. Representative color Doppler images from double transgenic mice (Figure 3.4C, bottom) showed a very distinctive point of flow convergence (Venturi effect) in the mid- to proximal-LV that was never seen in control mice (Figure 3.4C, top). Doppler tracings revealed significantly elevated outflow velocities at the point of the flow convergence (Figure 3.4D), which, when quantified, were more than four times higher than control values (>3.0 vs. <1.0 m/s, $p<0.001$ at all time points, Figure 3.4E). As stated previously and shown in Figure 3.1F, double transgenic mice also showed significantly elevated proximal-LV outflow velocities at baseline; however, these values were significantly lower than velocities seen after 24 hours of transgene induction (0d: 1.01 ± 0.61 vs. 1d: 2.98 ± 0.80 m/s, $p<0.001$), and did not affect phenotype development. However, where possible, mice with peak outflow velocities greater than 1.0 m/s at baseline were not utilized for further analysis.

***Histologic characterization of phenotype and pathological gene expression analysis*.** To further characterize the hypertrophy phenotype in double transgenic mice, we performed gross and histological analysis of hearts from double transgenic and littermate control mice. Following 42 days of caFGFR1 induction, hearts were visibly larger in double transgenic animals (Figure 3.5A). This difference was even more apparent after 300 days of transgene expression, as demonstrated in Trichrome-stained cardiac cross-sections from control (Figure 3.5B, top) and double transgenic hearts (Figure 3.5B, bottom). Also note that even after ten months of caFGFR1 expression, concentric hypertrophy was still present, and none of the six hearts examined showed signs of progressing to a dilated state. Histologic analysis of LV cross-sections induced with DOX for 42 days showed patchy areas of myocyte disarray (H&E staining, Figure 3.5C) and increased interstitial fibrosis (Picrosirius red staining, Figure 3.5D). Fluorescein-tagged wheat germ agglutinin (FITC-WGA) was utilized to label all cell membranes in sections of the adult heart. Following six months of transgene induction, FITC-WGA staining clearly illuminated large patches of increased interstitial cells, which were never seen in littermate controls (Figure 3.5E). FITC-WGA staining from representative double transgenic mice, shown in Figure 3.5F, illustrates the progressive enlargement of myocytes (cut in cross section) from baseline (0d) to six months (168d) of transgene induction. Cardiomyocyte cross-sectional area was significantly increased by one

week of caFGFR1 induction (287.8 ± 15.4 vs. 229.2 ± 31.5 μm^2, p=0.002) and continued to increase through six months of induction (512.0 ± 152.2 vs. 271.3 ± 30.1 μm^2, p=0.02, Figure 3.5G).

To confirm that the hypertrophy seen in double transgenic mice was pathologic, quantitative RT-PCR was used to examined the expression of markers of pathological ventricular remodeling (Figure 3.5H & I). The antihypertrophic and antifibrotic natriuretic peptides, A*np* and *Bnp*, were significantly elevated in double transgenic mice after one day of caFGFR1 induction (*Anp*: 3.2 ± 1.7-fold vs. control, p=0.01; *Bnp*: 7.7 ± 4.2-fold vs. control, p=0.003), while the fetal hypertrophy marker β-myosin heavy chain and the fibrotic markers collagens 1 and 3 were not significantly elevated until 42 days of transgene induction (*βMHC*: 7.9 ± 5.2-fold vs. control, p=0.02; *Col1a1*: 1.5 ± 0.4-fold vs. control, p=0.04; *Col3a1*: 4.4 ± 2.3-fold vs. control, p=0.01).

Exercise tolerance. Double transgenic mice expressing caFGFR1 exhibited all of the pathophysiological characteristics of hypertrophic cardiomyopathy (HCM). Because one of the most common clinical manifestations of HCM is exercise intolerance [170], it was important to determine if chronic induction of caFGFR1 and the resulting concentric hypertrophy would result in impair performance during forced exercise. Adult mice were fed DOX chow for six months and then subjected to an acute treadmill stress test, where their exercise tolerance was measured by the length of time they were able to run unassisted (time to failure). Interestingly, double transgenic mice with chronic caFGFR1 expression did not display any signs of exercise intolerance and were capable of running for the same length of time as their littermate controls (24.4 ± 1.0 vs. 21.5 ± 4.7 minutes, not significant, Figure 3.6).

Reversibility of phenotype. One of the advantages of the Tet-on system is its reversibility. Just as addition of DOX leads to the translocation of the rtTA to the nucleus and the binding to the TRE, the removal of DOX inactivates the rtTA and halts transcription of the transgene. To assess the reversibility of the caFGFR1-induced phenotype, 12- to 14-week old αMHC-rtTA, TRE-caFGFR1 mice and littermate controls were induced with DOX chow for six weeks and fed normal chow for six weeks. Development and reversal of hypertrophy was evaluated using *in vivo* echocardiography and postmortem histological and protein or gene expression analysis. LV mass index (LVMI, Figure 3.7C) was significantly reduced by 16.5% from the LVMI observed following six weeks on DOX chow (5.48 ± 0.72 vs. 6.57 ± 0.85 mg/g, p=0.007), although it remained slightly elevated compared to control mice after six weeks off DOX (5.48 ±

0.72 vs. 4.60 ± 0.51 mg/g, not significant). Similarly, LV internal diastolic diameter (LVIDd, Figure 3.7B) was significantly increased by 12% from the LVIDd observed before DOX removal (3.44 ± 0.21 vs. 3.07 ± 0.11 mm, p=0.01), and it returned to near control levels following DOX removal (3.44 ± 0.21 vs. 3.61 ± 0.38 mm, not significant). LV diastolic posterior wall thickness (LVPWd, Figure 3.7A) was also reduced by 16% from the wall thickness observed after six weeks on DOX (1.14 ± 0.16 vs. 1.36 ± 0.25 mm, p=0.007), but remained significantly elevated over littermate controls after six weeks off DOX (1.14 ± 0.16 vs. 0.85 ± 0.09 mm, p=0.01). LV peak outflow velocity (LV POV, Figure 3.7D), measured at the point of flow convergence in the mid-ventricle, was the most resistant to reversal. While outflow velocity was significantly decreased by 20% following removal of DOX (3.17 ± 0.58 vs. 3.99 ± 0.0 m/s, p=0.02), it remained significantly elevated compared to littermate controls (3.17 ± 0.58 vs. 0.66 ± 0.20 m/s, p<0.001). Consistent with the *in vivo* wall thickness, mean cardiomyocyte cross-sectional area remained significantly larger than littermate controls following DOX removal for six weeks (332 ± 21 vs. 233 ± 32 μm^2, p=0.005; Figure 3.7E), despite decreasing by 24% compared to pooled data from two independent cohorts of double transgenic mice induced for six weeks (332 ± 21 vs. 435 ± 102 μm^2, n=4 and 7, p=0.08).

To determine whether the continued presence of phenotype was the result of resistance to reversibility or continued expression of caFGFR1, Western blot analysis of c-myc expression (Figure 3.7F) and quantitative RT-PCR analysis for *Fgfr1* gene expression (Figure 3.7G) were performed. The transgene, as measured by its c-myc tag, was still expressed at relatively high levels after 42 days of DOX removal (DTG 42d ON, 42d OFF; Figure 3.7F), although expression was significantly reduced compared to transgene expression following three weeks of DOX induction (DTG 21d; Figure 3.7F). As expected, no transgene expression was observed in littermate control animals (Control 21d; Figure 3.7F). This continued expression of the c-myc tag following DOX removal corresponded to a 54 ± 13-fold increase of *Fgfr1* compared to littermate controls (p=0.0002), down 82% from the 299 ± 60-fold seen following transgene induction for 42 days. Despite continued transgene expression, levels of expression of downstream mediators of FGF signaling, *Etv5* and *Etv4* (Figure 3.7H), and markers of pathological ventricular remodeling (Figure 3.7I) returned to normal levels following 42 days off DOX.

Mechanisms involved in phenotype development following induction of caFGFR1. FGF receptors can activate a variety of pathways, including MAPK/ERK, PI3K/Akt, PLCγ, and STATs. In an effort to elucidate the mechanisms involved in the development of the hypercontractility and hypertrophy seen in double transgenic mice, we analyzed protein expression throughout the time course of caFGFR1 induction. While there was a trend towards transient 2-fold increase in ERK1/2 activation after one day of induction, this change was not consistent enough to achieve significance (n_{DTG}=8, $n_{control}$=5; Figure 3.8), and no changes were apparent beyond 24 hours of caFGFR1 induction. We also examined the activation of other MAPKs (p38, JNK), as well as Akt, PLCγ, and STATs (Stat3, Stat5), none of which showed any trends toward activation following induction of FGF signaling in cardiomyocytes (Figure 3.8). Additionally, pharmacologic inhibitors of MEK1/2 (U0126), PI3K (Wortmannin), and Calcineurin (Cyclosporine A) were tested *in vivo* and none were able to inhibit phenotype development (Table 3.3).

Because there was no clear activation of a pathway, or pathways, directly downstream of the FGF receptor (despite increased expression of *Etv4* and *Etv5*), we examined other signaling pathways that could result in hypertrophy or hypercontractility. We hypothesized that induction of caFGFR1 could lead to increased sensitization of cardiomyocytes to sympathetic signaling, since adrenergic activation in the heart has been shown to both increase contractility and cause hypertrophy in cardiomyocytes [171]. As a result, we examined the phosphorylation of targets downstream of adrenergic receptors, such as protein kinase A (PKA), troponin I (TnI), and phospholamban. No changes in activation of PKA at any time during caFGFR1 induction were observed. However, in contrast to what we would expect if adrenergic signaling were increased, phosphorylation of TnI was significantly decreased by one week of transgene expression (0.26 ± 0.21 vs. control, p=0.01, Figure 3.9). There was also a trend towards decreased phosphorylation of phospholamban, but this result was much more variable than TnI phosphorylation (data not shown). In addition to increased adrenergic signaling, alterations in calcium handling are a common mechanism in the development of hypertrophy [5, 6]. Western blot analysis revealed significant downregulation of Serca2, the calcium ATPase that recycles calcium back into the sarcoplasmic reticulum, by seven days of transgene induction (0.40 ± 0.24 vs. control, p=0.03, Figure 3.9).

Assessment of cardiomyocyte contractile properties. To determine whether changes in cardiac contractility seen *in vivo* were due to cell autonomous effects on the cardiomyocyte, 10- to 12-week-old double transgenic and littermate control mice were induced with doxycycline for 24-48 hours, and then unloaded cell shortening was assessed in freshly isolated ventricular myocytes paced at 0.5 Hz. Representative traces of myocyte contraction (Figure 3.10A) and quantitation of myocyte length demonstrate that myocytes isolated from double transgenic hearts had significantly shorter sarcomeric lengths at both diastole and systole (Figure 3.10B), with an overall increase in fractional shortening (Figure 3.10C) compared to myocytes from littermate controls, suggesting that caFGFR1 leads to both impaired relaxation and enhanced contraction in cardiomyocytes.

To determine if the failure to fully relax was due to inherent changes in sarcomeric proteins, 2,3-butanedione monoxime (BDM), which inhibits actin-myosin interactions and slows cross bridge cycling [172, 173], was added to isolated ventricular myocytes, and led to significant lengthening of both control and double transgenic sarcomeres (Figure 3.10D). More importantly, myocytes from double transgenic mice experienced a significantly greater change in sarcomere length and approached the same final relaxed sarcomere length as their littermate controls following BDM addition (Figure 3.10E).

To determine if the altered contractile properties in double transgenic myocytes were the result of increased intracellular calcium concentration (due to decreased calcium recycling), myocytes were loaded with BAPTA-AM, an intracellular calcium chelator [173]. In contrast to BDM, there was no change in final relaxed sarcomere length in either control or double transgenic myocytes, suggesting that increased intracellular calcium is likely not involved in the altered relaxation of double transgenic cardiomyocytes (data not shown).

Clinical usefulness. Two classes of drugs that have been proven to reverse pathological remodeling and improve cardiac function in heart failure are angiotensin receptor blockers, such as losartan, and beta-blockers, such as propranolol [174]. While the precise mechanisms by which beta-blockers improve cardiac function and promote reverse remodeling are unknown, this treatment is one of the mainstays for the symptomatic relief of obstructive HCM due to its ability to decrease the outflow gradient [174, 175]. Meanwhile, losartan is contraindicated in patients with LV outflow obstruction due to its effect on blood pressure (which can increase outflow gradient) [176], but recent studies have indicated

that blockade of angiotensin signaling can prevent much of the pathological remodeling in animal models of HCM [177].

To examine the clinical usefulness of this new model of hypertrophic cardiomyopathy, double transgenic mice were given losartan (80 mg/kg/d) or propranolol (67 mg/kg/d) in their drinking water in an attempt to determine if these drugs could prevent or lessen phenotype development (Table 3.4). Treatment began one week prior to the start of DOX chow, and continued throughout one week of transgene induction. Both drugs significantly abrogated the hypertrophic response seen in untreated DTG mice (induced for one week, DTG 7d), as assessed by *in vivo* LV mass index (losartan DTG: 4.3 ± 0.6 mg/g, propranolol DTG: 4.0 ± 0.7 mg/g, DTG 7d: 5.3 ± 1.0, DTG 0d: 4.0 ± 0.4 mg/g). The increase in LV posterior wall thickness was also moderately blocked with both drugs, though neither treatment caused a significant reduction (losartan DTG: 0.97 ± 0.06 mm, propranolol DTG: 0.95 ± 0.16 mm, DTG 7d: 1.14 ± 0.27 mm, DTG 0d: 0.85 ± 0.09 mm). Only propranolol significantly reduced the LV outflow velocity, though it was still significantly elevated compared to measurements taken prior to drug treatment and caFGFR1 induction (DTG 0d) (losartan DTG: 4.8 ± 0.2 m/s, propranolol DTG: 2.3 ± 1.2 m/s, DTG 7d: 4.1 ± 0.8, DTG 0d: 0.9 ± 0.4). These studies suggest that this model of caFGFR1-induced HCM may prove useful to evaluate other treatments aimed at preventing or reversing the course of this pathological condition.

C. Discussion

Induction of caFGFR1 in adult cardiomyocytes results in hypercontractility and a hypertrophic cardiomyopathy. In this study, we created a new mouse model in which we could induce FGF receptor signaling specifically in cardiomyocytes in an attempt to better understand the relationship between FGF signaling and the development of hypertrophy. We hypothesized that adult cardiomyocytes are not competent to respond to an FGF signal due to repression of the FGF signaling pathway under homeostatic conditions. However, we discovered that cell autonomous activation of FGF signaling, via a constitutively active FGF receptor, is sufficient to induce significant hypertrophy within seven days of transgene expression (Figures 3.3 and 3.5). This hypertrophy is concentric, leading to significantly increased wall thickness (Figure 3.3A) and reduced chamber volume (Figure 3.3B). Cardiac mass

(Figure 3.3C) and cardiomyocyte cross sectional area (Figure 3.5C) progressively increased throughout six months of caFGFR1 induction (illustrated in Figures 3.3E and 3.3F). Patchy areas of fibrosis, elevated expression of pathologic cardiac markers, and particularly myocyte disarray (Figure 3.5) and maintenance or enhancement of systolic function (Figure 3.3D) support the notion that sustained activation of FGF signaling in adult cardiomyocytes leads to a hypertrophic cardiomyopathy.

In addition to the development of HCM, we discovered that inducing caFGFR1 can rapidly increase the contractility of the heart within 24 hours of exposure to DOX, as evidenced by the significantly elevated slope of the end-systolic pressure-volume relationship curve following an increase in the afterload of the heart (Figure 3.4A). This hypercontractility results in the narrowing of the ventricle during systole, leading to a high velocity jet of blood flowing past the papillary muscles in the mid- to proximal-ventricle (Figure 3.4C-E). This effect is further amplified to the point of a dynamic obstruction following the development of concentric hypertrophy, as evidenced by the significant elevation in end systolic pressure in the distal ventricle (Figure 3B). The hypercontractility phenotype is also extremely sensitive to activation of FGF signaling, as it is significantly elevated even at baseline due to a small amount of leakiness and minimal transgene expression in double transgenic mice (Figure 3.1B, DTG 0d). It is also resistant to reversal following removal of DOX (Figure 3.7D). Hypertrophic parameters approached near control levels after six weeks off DOX, while peak outflow velocity in the mid-ventricle remained significantly elevated compared to littermate controls. The fact that double transgenic mice at baseline do not show signs of hypertrophy despite having increased contractility suggests that a low level of activated FGFR1 in cardiomyocytes directly regulates cardiac contractility, while prolonged exposure to high levels of activated FGFR1 leads to the development of HCM. These data, showing a rapid and significant increase in myocyte contractility in response to FGF pathway activation, reveal at least one component of potential cardioprotection by FGF following myocardial injury.

Constitutively-active FGFR1 in cardiomyocytes alters mechanisms common to HCM pathophysiology. Hypertrophic cardiomyopathy affects roughly one out of 500 adults and is the most common cardiovascular genetic disorder. The majority of cases (45-70%) can be attributed to one of many possible dominant mutations in sarcomeric proteins (over 800 mutations in 11 different contractile genes [6]. However, a fairly large number of patients develop HCM and lack one of these known

mutations. In addition, this is a complex and heterogeneous disease, and the correlations between genotype and phenotype remain poorly understood. To our knowledge, no study has shown that overactivation of FGFR1 is linked to HCM. However, mutations that lead to increased Ras activity, a known mediator of the FGF signaling cascade, are associated with the development of HCM (as well as a host of other cardiac and syndromic defects) [116]. In an effort to determine the mechanisms that lead to hypercontractility and the development of HCM in our mouse model, we examined pathways known to be activated by FGF receptor tyrosine kinases. While there were some trends (transient activation of ERK1/2 after one day of induction, decreased Akt activation), activation of downstream pathways (ERK1/2, p38, JNK, Akt, PLCg1, Stat3, Stat5) tended to be inconsistent and thus inconclusive in both double transgenic hearts and controls. However, the downstream FGF-responsive target genes *Etv4* and *Etv5*, were consistently and persistently increased. Given the lack of clear activation of one particular pathway, or pathways, it does not appear that these classical downstream signaling pathways are directly involved in the development of hypercontractility or progression of hypertrophy seen in this model. Similar to our findings, there was no increase in phosphorylated ERK or Akt in a Ras-induced HCM mouse model [178], suggesting that a novel or nonclassical pathway was responsible for development of the HCM phenotype.

As a result, we turned our attention to other possible mechanisms for the development of hypercontractility and HCM, and hypothesized that expression of caFGFR1 resulted in cardiomyocytes that were hypersensitive to sympathetic stimulation. Norepinephrine or epinephrine bind to beta-adrenergic receptors (G-protein coupled receptors) on cardiomyocytes, leading to synthesis of cAMP and activation of protein kinase A (PKA), which phosphorylates a variety of downstream targets, including myofilament proteins (such as troponin I and myosin binding protein C), ion channels, and proteins involved in calcium handling (phospholamban). Phosphorylation of these targets leads to increased inotropy (contractility) and increased lusitropy (relaxation) in cardiomyocytes [171]. However, caFGFR1-expressing hearts showed no increase in PKA activation, and significantly decreased phosphorylation of troponin I (TnI) by one week of DOX induction, suggesting that sympathetic hypersensitization was not the mechanism for the increased contractility.

However, decreased TnI phosphorylation has important implications for the mechanism of phenotype development in these mice. TnI is a regulatory protein in the sarcomere that plays a key role in cardiomyocyte contraction and relaxation. TnI inhibits the interaction between actin and myosin during diastole, when cytosolic calcium concentration is low. During systole, calcium concentration rises, binds to troponin C (TnC) and leads to a conformational change in the troponin complex that removes TnI inhibition of cross bridge formation and promotes sarcomere contraction. Phosphorylation of TnI by protein kinase A or C (PKA, PKC) represents an important regulatory mechanism to modulate the contractile properties of the myofilament, as it increases the amount of calcium necessary for activation of contraction (*i.e.,* it decreases the calcium sensitivity of the sarcomere) and increases the rate of calcium dissociation [179, 180]. This ultimately results in accelerated relaxation and increased crossbridge cycling. Therefore, the decrease in TnI phosphorylation seen in this model would result in increased calcium sensitivity of the sarcomere, leading to contraction at lower calcium concentrations, and ultimately to impaired relaxation. Mechanisms governing the dephosphorylation process are much less clear, although it has been demonstrated that protein phosphatases 1 or 2A (PP1, PP2A) are capable of dephosphorylating TnI [180-184]. Importantly, activation of PP2A has been implicated as a feedback mechanism downstream of FGF receptor activation [185-187], making this one possible mechanism by which caFGFR1 could have direct effects on myofilament physiology. The potential involvement of protein phosphatases in the pathology of hypertrophic cardiomyopathy was further implicated in a study utilizing a transgenic mouse model of activated Ras, a small G-protein downstream of the FGF receptor [178]. Regardless of the specific mechanism, decreased phosphorylation of TnI and the resulting increased myofilament calcium sensitivity provides a common link between this caFGFR1 expression model of HCM and classical models involving sarcomere mutations. At least 62 mutations have been identified in thin filament regulatory proteins (tropomyosin, troponin T, and troponin I), many of which have been shown to increase myofilament calcium binding affinity and one of which prevents PKA-mediated phosphorylation [188, 189].

Another proposed model for the development and progression of HCM is abnormal intracellular calcium handling [5, 6]. Several studies of mouse models of HCM have demonstrated decreasing levels of calcium handling proteins, as well as diminished calcium transients and release of calcium from the

sarcoplasmic reticulum [178, 190]. One study even demonstrated that administration of diltiazem, an L-type calcium channel blocker, before the emergence of hypertrophy was sufficient to maintain normal levels of calcium handling proteins and prevent phenotype development [190]. As a result, we examined the expression levels of various calcium handling proteins, and found that Serca2, the calcium ATPase responsible for recycling calcium back into the sarcoplasmic reticulum, was significantly reduced following induction of caFGFR1 for one week (Figure 3.9). Downregulation of Serca2 would be expected to result in decreased sarcoplasmic reticulum calcium concentration and potentially higher cytosolic calcium concentration, leading to both stronger sarcomere contraction as well as an inability to relax.

In an attempt to further characterize the mechanisms involved in the development of hypercontractility and HCM in our genetic model, we examined the contractility of isolated cardiomyocytes from double transgenic and littermate control mice induced with DOX for 24-48 hours. Baseline recordings revealed that double transgenic myocytes were significantly shorter during diastole than control myocytes, suggesting the presence of a relaxation defect. Double transgenic myocytes also had significantly increased contractility (fractional shortening), suggesting that caFGFR1 leads to intrinsic changes in cardiomyocyte contractile properties. To define the relative contribution of cytosolic calcium versus changes in myofilament contractile properties, we then subjected these myocytes from DOX-induced double transgenic and littermate controls to 2,3-Butanedione monoxime (BDM), an inhibitor of myosin-actin interactions, or BAPTA-AM, a membrane-permeable calcium chelator. BDM was able to significantly increase diastolic sarcomere length in both control and DTG myocytes. While DTG myocytes experienced a greater overall change in sarcomere length, they remained significantly shorter than control myocytes, indicating a partial reversal of the relaxation defect. BAPTA-AM, however, had little effect on sarcomere length in control or DTG myocytes. These data strongly suggest that alterations in cardiomyocyte contractility (specifically relaxation) that result from expression of caFGFR1 are due to changes within the myofilament and not from a rise in cytosolic calcium concentration. Further studies are necessary to determine precisely how FGF signaling affects myofilament physiology. While it is likely that decreased TnI phosphorylation plays a role in the pathophysiology of our model, we did not observe significant changes in p-TnI until seven days of transgene induction, suggesting that other modifications to the contractile apparatus may occur earlier.

In conclusion, the doxycycline-inducible cardiomyocyte-specific caFGFR1 mouse provides a unique model of HCM that can be utilized to examine the common pathways that lead to phenotype development, as well as the extent of phenotype prevention and/or reversibility. This model also suggests the possibility that activating mutations in FGFR1 may directly lead to HCM or may modify the phenotype when combined with mutations in other proteins. Finally, perhaps the most striking finding from these studies is that low levels of activated FGFR1 have rapid and potent effects on cardiac contractility without any pathological effects, suggesting that targeted activation of the FGF signaling pathway may be beneficial to patients with heart failure and poor systolic function. Further investigation is necessary to more precisely elucidate the mechanisms responsible for the increased contractility following expression of caFGFR1, as well as pathways involved in the rapid progression from hypercontractility to HCM.

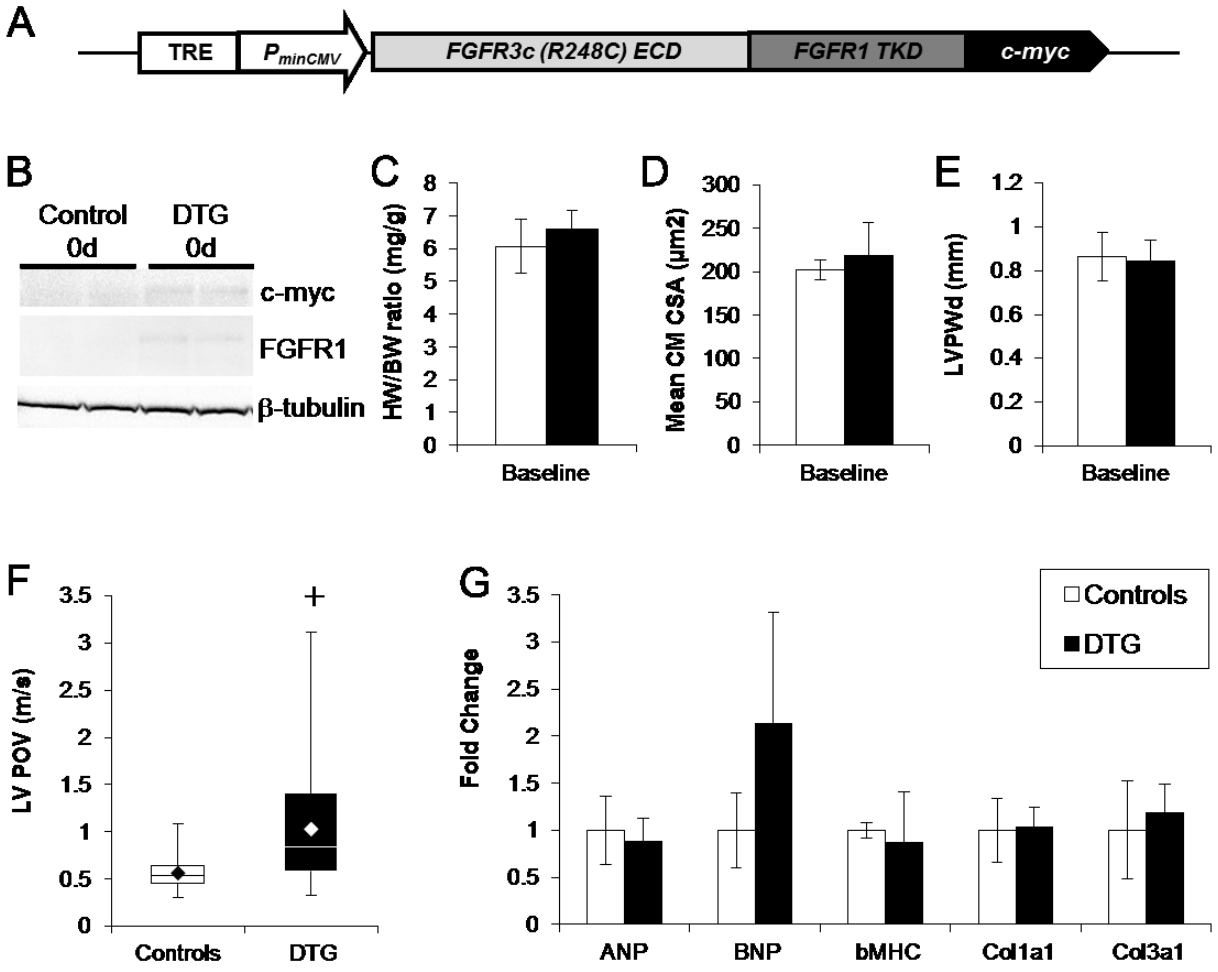

Figure 3.1 Inducible constitutively-active FGFR1 genetic system shows minimal baseline activity. (A) We generated a tetracycline response element (TRE)-drivable FGFR31c(R248C)-c-myc transgene, in which FGFR31c(R248C) is a chimeric receptor consisting of the FGFR3c(R248C) mutant extracellular and transmembrane domains (which confer ligand-independent constitutive activity) fused to the FGFR1 tyrosine kinase domain. (B) Western blot demonstrating minimal expression of c-myc tag and FGFR1 in double transgenic animals (DTG) not exposed to DOX (0d). No transgene or FGFR1 expression is visible in single transgenic controls (TRE). β-tubulin expression demonstrates equal protein loading. (C-E) Twelve- to 14-week-old mice show no evidence of hypertrophy on gross measurement of biventricular weight/body weight ratio (HW/BW, C; n_{DTG}=7, $n_{control}$=7), histological measurement of mean

cardiomyocyte cross sectional area (CM CSA, D; n_{DTG}=5, $n_{control}$=5), or echocardiographic measurement of diastolic left ventricular posterior wall thickness (LVPWd, E; n_{DTG}=47, $n_{control}$=23). No differences were observed between littermate controls (αMHC-rtTA only, TRE-caFGFR1 only, or wild-type), so results were pooled for analysis. (F) Minimal expression of caFGFR1 is sufficient to induce a small, but significant, increase in outflow velocity from the proximal LV. (G) Quantitative RT-PCR analysis showing no significant changes in markers of pathologic cardiac remodeling (n=4 for DTG and controls). Error bars = standard deviation. + $p<0.001$.

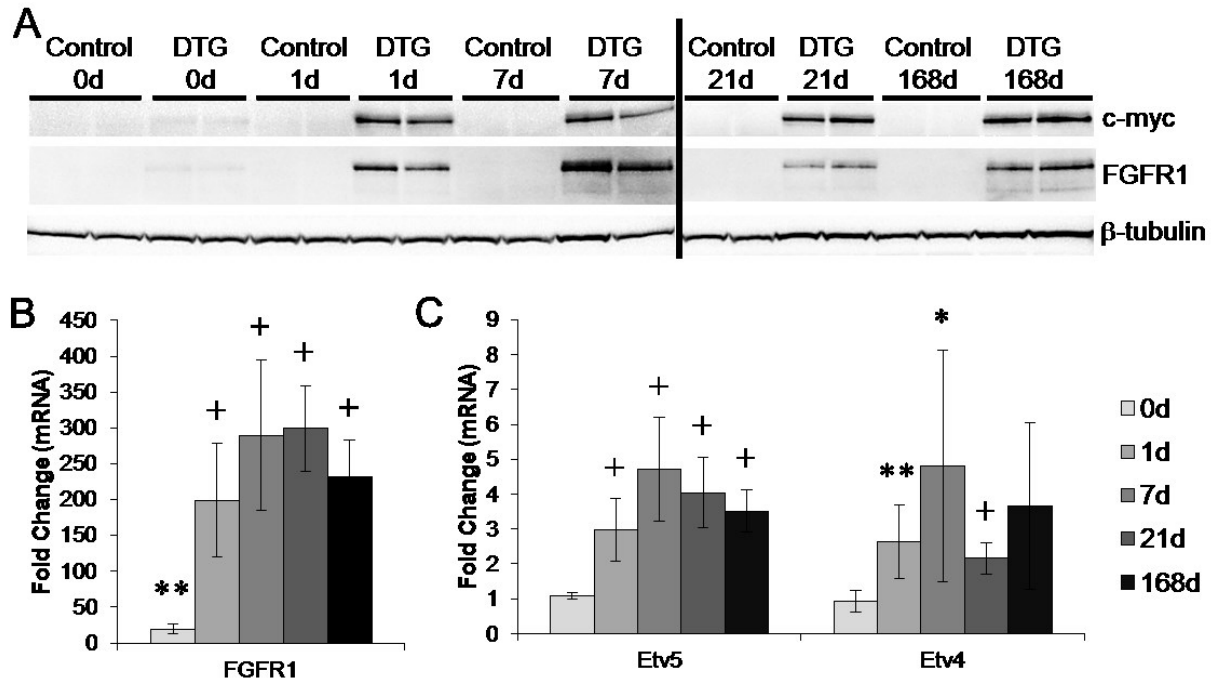

Figure 3.2 Constitutively-active FGFR1-myc is rapidly inducible with consistently maintained levels of expression over time. (A) Western blots showing expression of FGFR1 and the c-myc tag (with β-tubulin loading control). Little to no FGFR1 expression is observed in single transgenic controls. A small amount of c-myc and FGFR1 expression is observed in DTG hearts at baseline (0d), and level of caFGFR1-myc transgene expression increases dramatically following feeding of DOX chow for as little as 24 hours (DTG 1d). Transgene protein expression remains relatively constant with chronic activation (DTG 7d, 21d, and 168d). (B) Quantitative RT-PCR analysis (DTG: n_{0d}=4, n_{1d}=7, n_{7d}=5, n_{21d}=6, n_{168d}=4) showing a significant 19-fold increase in *Fgfr1* mRNA in uninduced DTG animals (0d) that rises to a 200-fold increase within one day of transgene induction (1d). FGFR1 gene expression remains relatively constant with chronic DOX chow feeding. (C) No significant changes in downstream transcription factors *Etv5* or *Etv4* were measured at baseline (0d), but significant and consistent induction was observed after one day of feeding DOX chow (1d). Fold change is versus corresponding time-matched littermate controls (not shown; n_{0d}=4, n_{1d}=6, n_{7d}=4, n_{21d}=5, n_{168d}=4). Error bars = standard deviation. *p<0.05, ** p<0.01, + p<0.001.

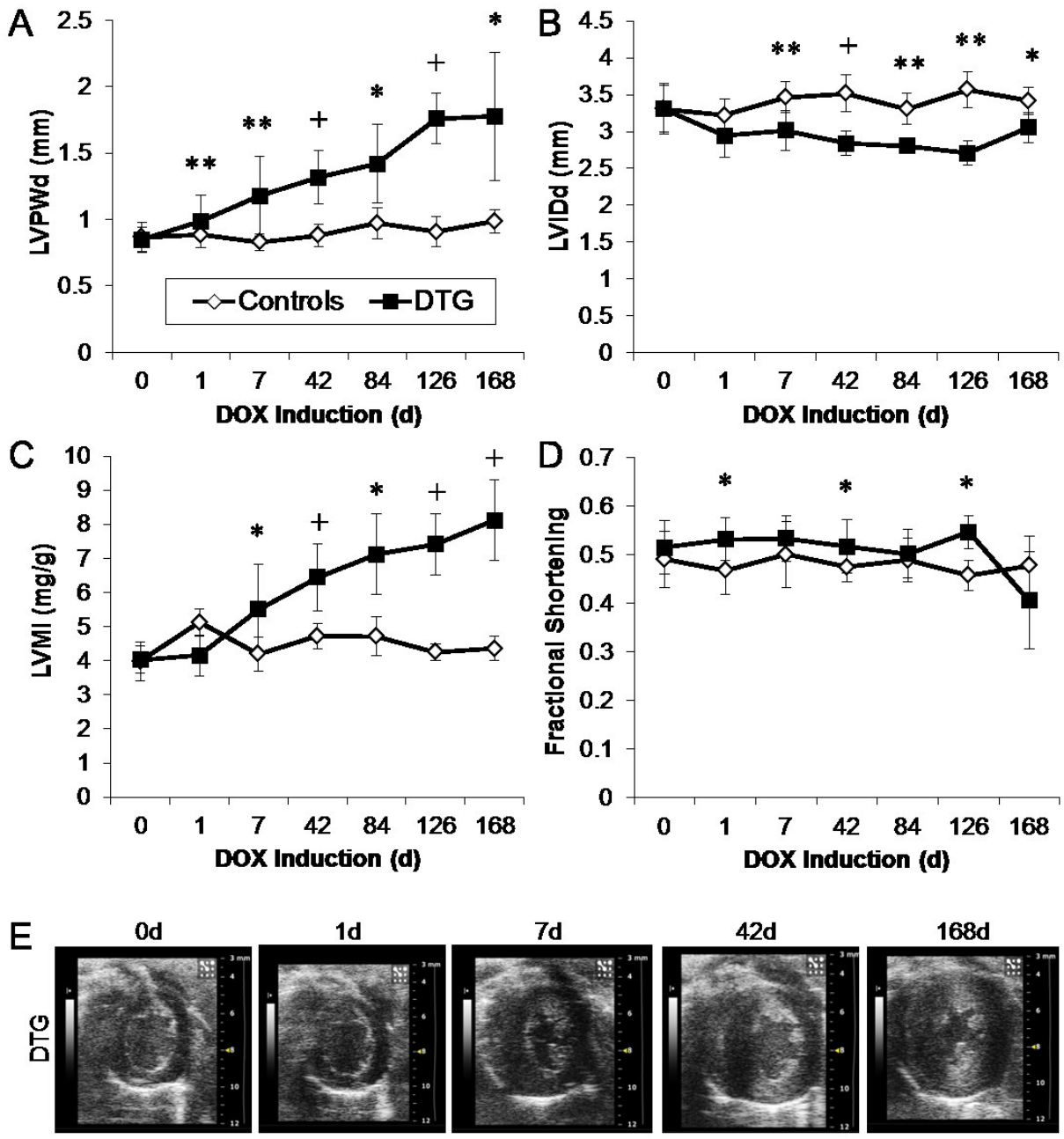

Figure 3.3 Induction of caFGFR1 in adult cardiomyocytes results in the development of concentric hypertrophy with preservation of systolic function over time. Twelve- to 14-week-old mice were induced with DOX chow for varying lengths of time and cardiac function was monitored using echocardiography. (A) Left ventricular (LV) diastolic posterior wall thickness (LVPWd, A) was significantly elevated by one day of induction, while LV mass index was significantly elevated (LVMI, C) and LV internal diastolic diameter significantly decreased (LVIDd, B) within seven days of DOX induction. (D)

Systolic function was maintained throughout 6 months of transgene induction. Littermate controls represent single transgenic (αMHC-rtTA or TRE-caFGFR1) or wild-type littermates; no genotype-specific differences were observed and thus controls were pooled for analysis. Error bars = standard deviation. *p<0.05, **p<0.01, +p<0.001. 0d: n_{DTG}=47, $n_{control}$=23; 1d: n_{DTG}=8, $n_{control}$=4; 7d: n_{DTG}=17, $n_{control}$=7; 42d: n_{DTG}=14, $n_{control}$=12; 84d: n_{DTG}=4, $n_{control}$=4; 126d: n_{DTG}=4, $n_{control}$=4; 168d: n_{DTG}=4, $n_{control}$=4. (E) Representative short axis echocardiographic images depicting the progression of hypertrophy in double transgenic animals (DTG) from baseline to 168 days (six months) of induction.

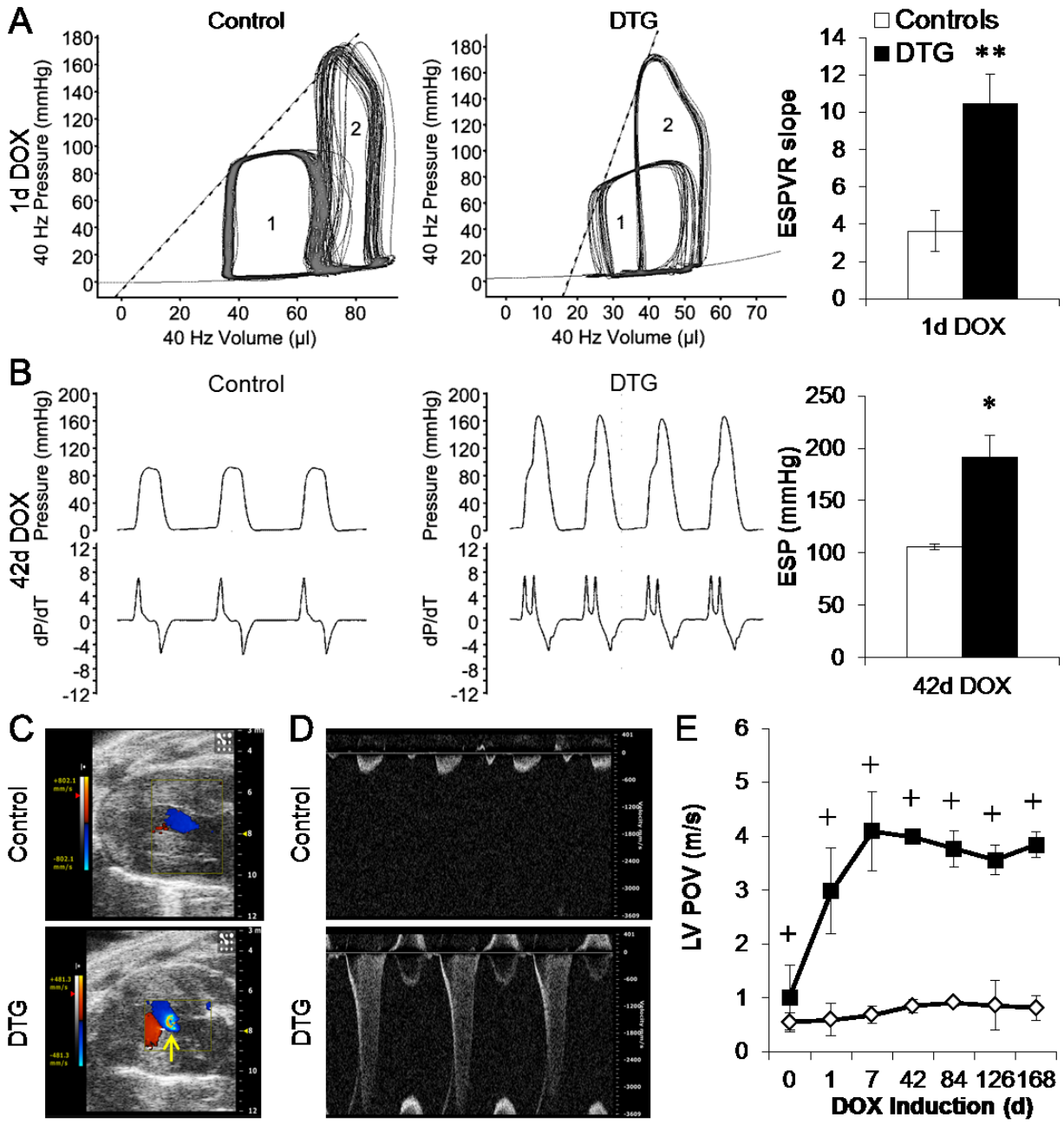

Figure 3.4 *In vivo* induction of caFGFR1 in adult cardiomyocytes leads to a hypercontractile phenotype with the development of a dynamic obstruction in the proximal left ventricle. (A) Representative pressure-volume (PV) loops from hemodynamic analysis of double transgenic adult mice (DTG) induced with DOX for one day compared to littermate controls (1). To examine the contractility of the heart, afterload was increased by briefly occluding the aorta, causing an increase in the end systolic pressure and volume in both cohorts (2). The slope of the end systolic pressure-volume relationship

(ESPVR, dotted line) is significantly elevated in double transgenic mice (n=3 for DTG and control). (B) Representative pressure (top) and dP/dt (bottom) tracings indicating significantly elevated end systolic pressure (ESP) and the presence of a dynamic obstruction in DTG mice induced with DOX for 42 days (n_{DTG}=3, $n_{control}$=2). (C) Representative color Doppler images (blue = blood outflow, red = blood inflow) and (D) proximal LV Doppler tracings illustrating flow convergence characteristic of the Venturi effect (yellow arrow) and elevated outflow velocity at the point of obstruction in the proximal LV in DTG mice. (E) Quantitation of outflow velocity at the point of flow convergence, indicating that a dynamic obstruction is present at baseline in DTG mice, increases significantly with one day of transgene induction, and reaches the maximum measurable velocity by seven days of induction. Error bars = standard deviation. *p<0.05, **p<0.01, +p<0.001.

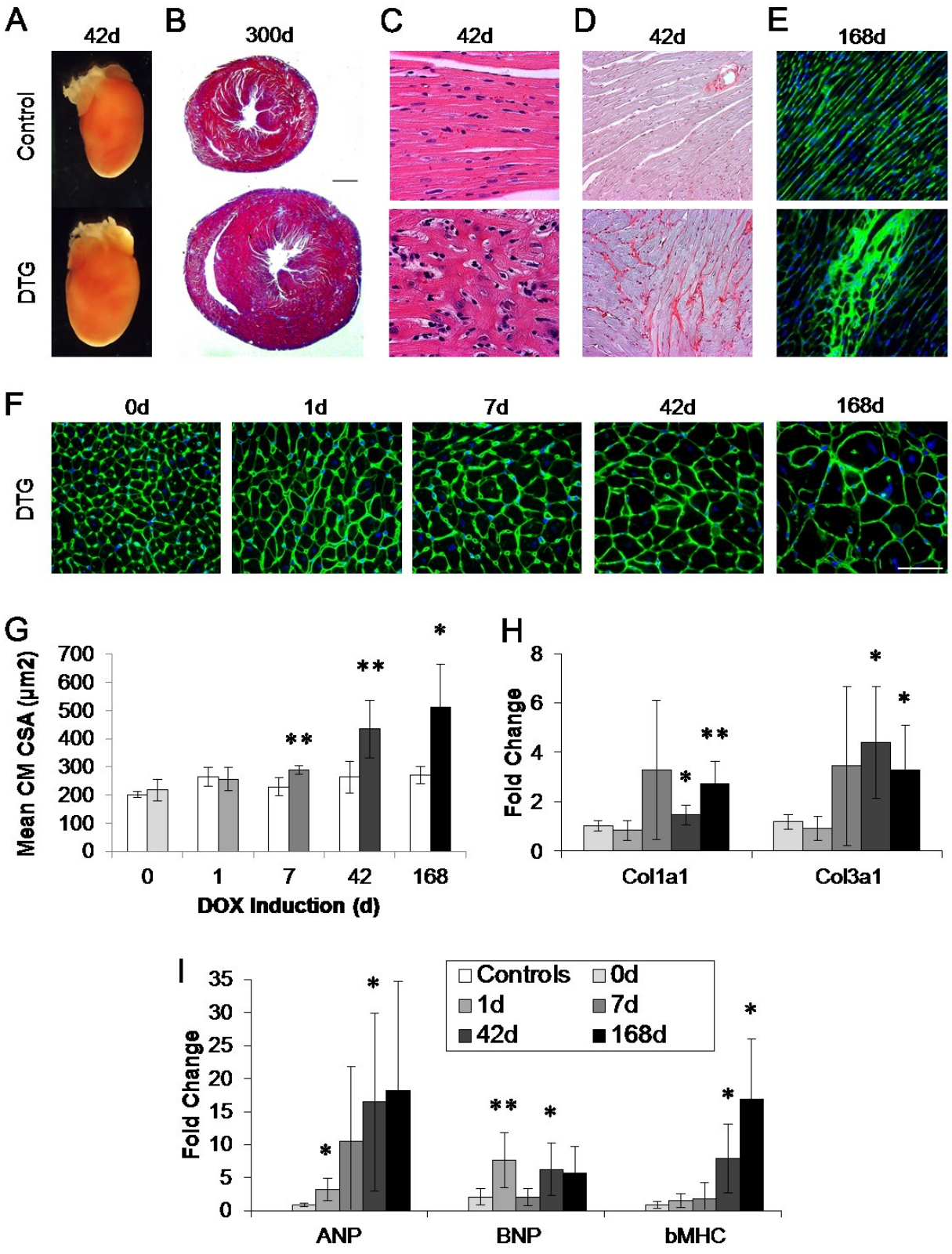
A
42d
Control
DTG
B
300d
C
42d
D
42d
E
168d
F
0d
1d
7d
42d
168d
DTG
G
Mean CM CSA (µm2)
700
600
500
400
300
200
100
0
0
1
7
42
168
DOX Induction (d)
H
Fold Change
8
6
4
2
0
Col1a1
Col3a1
I
Controls
0d
1d
7d
42d
168d
Fold Change
35
30
25
20
15
10
5
0
ANP
BNP
bMHC

Figure 3.5 Chronic induction of caFGFR1 results in a pathologic state with molecular and histologic characteristics of hypertrophic cardiomyopathy. (A) Induction of caFGFR1 for 42 days results in grossly enlarged hearts in double transgenic (DTG) compared to littermate control mice. (B) Following 300 days of transgene induction, massive DTG hearts show concentric hypertrophy with no evidence of progression to dilatation (scale bar = 1mm). (C-D) Histological examination of DTG hearts induced with DOX for 42 days reveals patchy areas of myocyte disarray (H&E, 20x magnification, C) and fibrosis (picrosirius red, 20x magnification, D). (E) Six months (168d) of transgene induction results in patchy areas of increased interstitial cells illustrated by FITC-tagged wheat germ agglutinin staining (WGA, 40x magnification). (F) FITC-WGA staining illustrates the progressive enlargement of cardiomyocytes in DTG mice following chronic induction with DOX chow (scale bar = 20μm). (G) Quantitation of mean cardiomyocyte cross-sectional area (CM CSA) demonstrates that cardiomyocytes are significantly larger by one week of transgene induction, with continued growth through six months of induction. (H-I) Quantitative RT-PCR for pathologic markers of LV remodeling reveals significant upregulation of the fibrotic markers collagens 1 and 3 (*col1a1, col3a1*, H) by 42 days of transgene induction, with significant upregulation of heart failure markers atrial natriutetic and b-type natriuretic peptides (*anp*, *bnp*) within one day of caFGFR1 expression and the hypertrophy marker β-myosin heavy chain (*bmhc*) by 42 days of induction with DOX (I) Fold change is versus corresponding time-matched littermate controls (not shown). DTG: n_{0d}=4, n_{1d}=7, n_{7d}=5, n_{42d}=4, n_{168d}=4; controls: n_{0d}=4, n_{1d}=6, n_{7d}=4, n_{42d}=5, n_{168d}=4. Error bars = standard deviation. *p<0.05, **p<0.01.

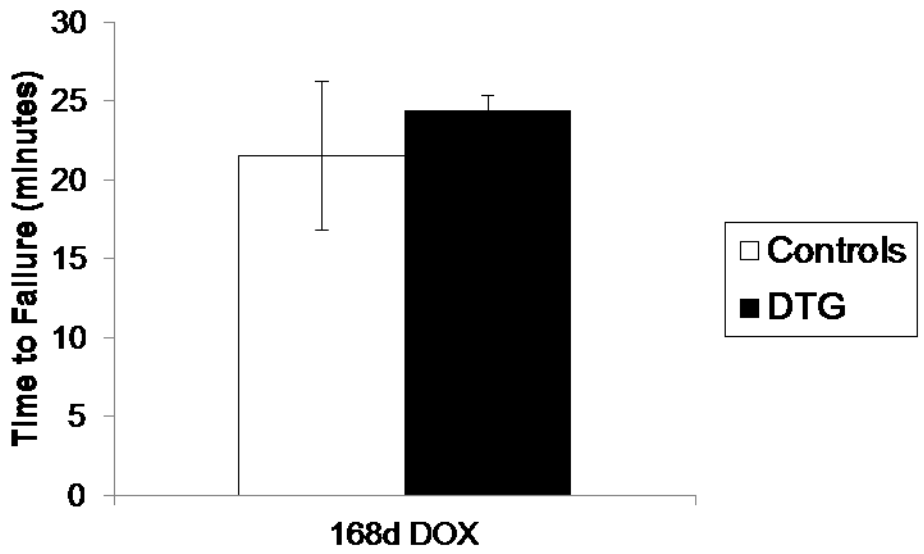

Figure 3.6 Chronic induction of caFGFR1 and significant concentric hypertrophy does not cause exercise intolerance in double transgenic mice. Twelve- to 14-week-old mice were fed DOX chow to induce caFGFR1 expression for 168 days (six months), and then subjected to an acute treadmill stress test to determine if the presence of severe hypertrophy resulted in exercise intolerance. Double transgenic mice (DTG) were capable of running for the same amount of time as their single transgenic littermate controls (n_{DTG}=3, $n_{control}$=4). Error bars = standard deviation.

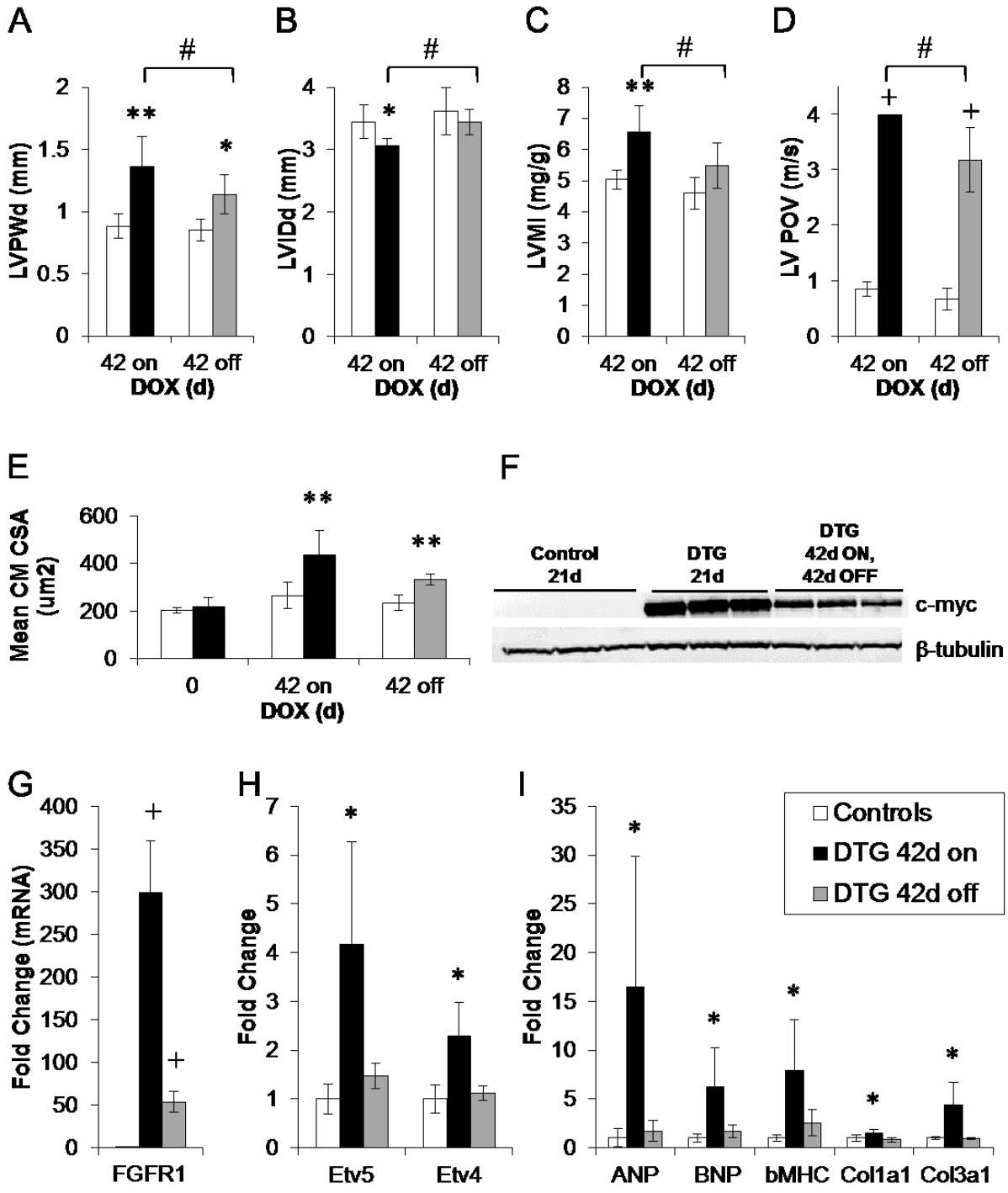

Figure 3.7 Transgene induction for 42 days, followed by DOX removal for 42 days leads to partial phenotype reversal. Twelve- to 14-week-old mice were fed DOX chow for 42 days to induce the HCM phenotype and then DOX was removed and mice were allowed to recover for 42 days. (A-E) Mice were monitored using serial screening echocardiograms. (A) LV diastolic posterior wall thickness (LVPWd)

was significantly increased in double transgenic mice (DTG, n=6) compared to littermate controls (n=4) following both DOX induction and DOX removal. While wall thickness did decrease slightly after removal of DOX, this difference was not significant. (B) LV internal diastolic diameter (LVIDd) was significantly decreased compared to controls following 42 days of DOX exposure. Unlike LVPWd, LVIDd returned to near control levels after removal of DOX for 42 days. (C) LV mass index (LVMI) was also significantly increased in DTG mice compared to littermate controls following 42 days of caFGFR1 induction. LVMI decreased significantly and approached control values following DOX removal. (D) Despite decreasing significantly following removal of DOX, peak outflow velocity (LV POV) from the proximal ventricle was still elevated compared to littermate controls. (E) WGA staining was performed to assess mean cardiomyocyte cross-sectional area (CM CSA) at the endpoint of this study. While myocyte size was smaller than that seen following six weeks of caFGFR1 induction, cells were still significantly larger than littermate controls. (F) Western blot analysis showing the significant decrease of transgene expression following removal of DOX (DTG 42d ON 42d OFF), compared to transgene expression after three weeks of induction (DTG 21d; protein samples from six weeks of induction were unavailable). No transgene expression is visible in TRE-caFGFR1-myc single transgenic controls (Control 21d). β-tubulin expression was used as a loading control. (G-I) Quantitative RT-PCR analysis demonstrates continued overexpression of *Fgfr1* in double transgenic hearts following 42 days off DOX (gray bar), despite a large reduction from the level of expression observed following 42 days on DOX (black bar, G). Expression of downstream mediators of FGF signaling (*Etv5, Etv4,* H) and markers of pathologic LV remodeling (I) are decreased to control levels 42 days following DOX removal. Error bars = standard deviation. *$p<0.05$, **$p<0.01$, +$p<0.001$ compared to littermate controls. #$p<0.05$ compared to double transgenic mice 42 days on DOX.

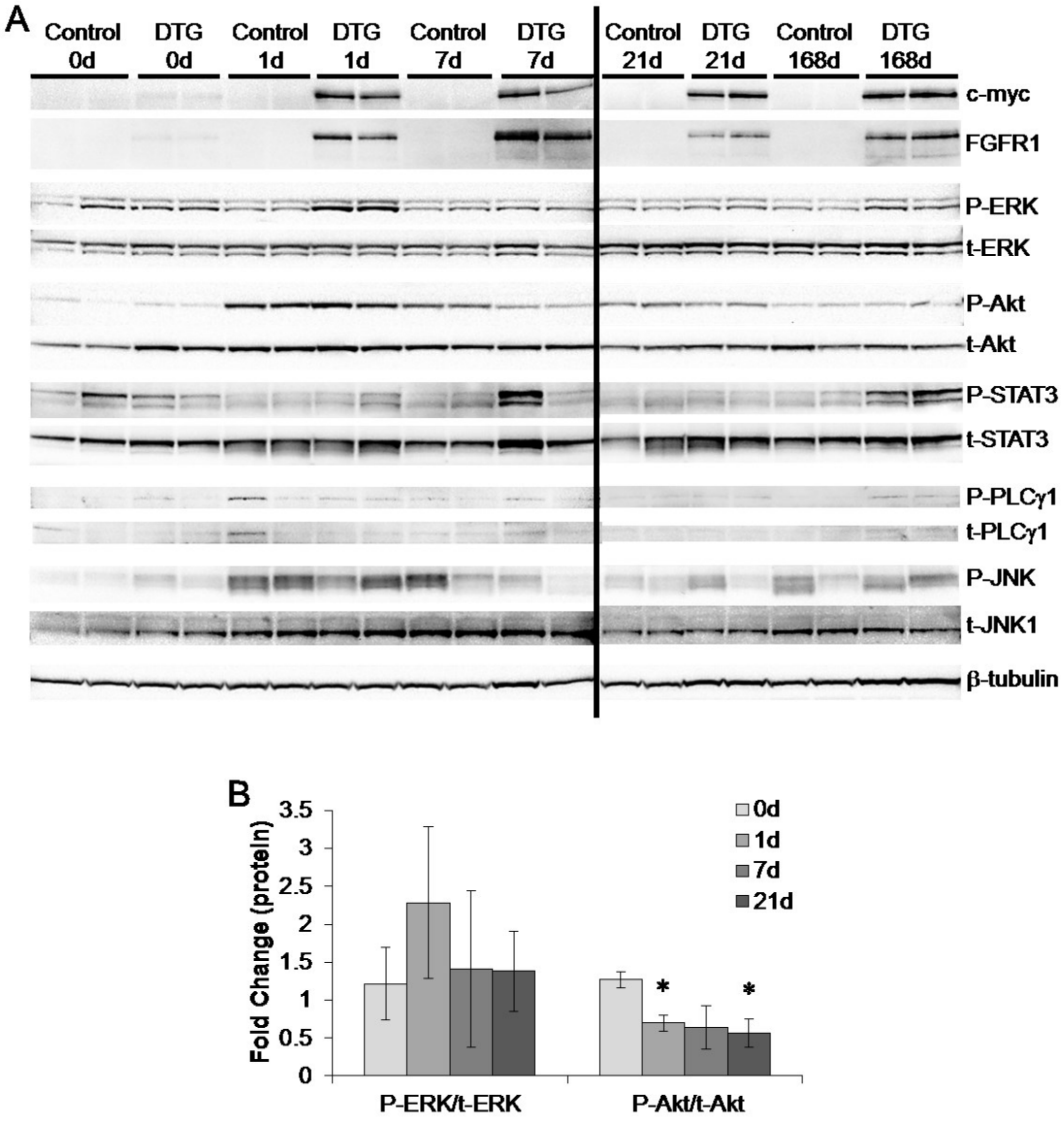

Figure 3.8 Induction of caFGFR1 results in transient ERK1/2 activation and sustained downregulation of Akt activation. (A) Representative Western blots examining signaling pathways downstream of the FGF receptor. Note that most pathways examined, as well as p38 and Stat5 (not shown), showed considerable variability. (B) Densitometric analysis of multiple independent Western blots demonstrated a transient, but insignificant, 2-fold increase in ERK1/2 activation, and a sustained decrease in Akt activation. DTG (shown): $n_{0d}=5$, $n_{1d}=3$, $n_{7d}=8$, $n_{21d}=6$; controls (not shown): $n_{0d}=2$, $n_{1d}=2$, $n_{7d}=4$, $n_{21d}=3$. Error bars = standard deviation. *$p<0.05$.

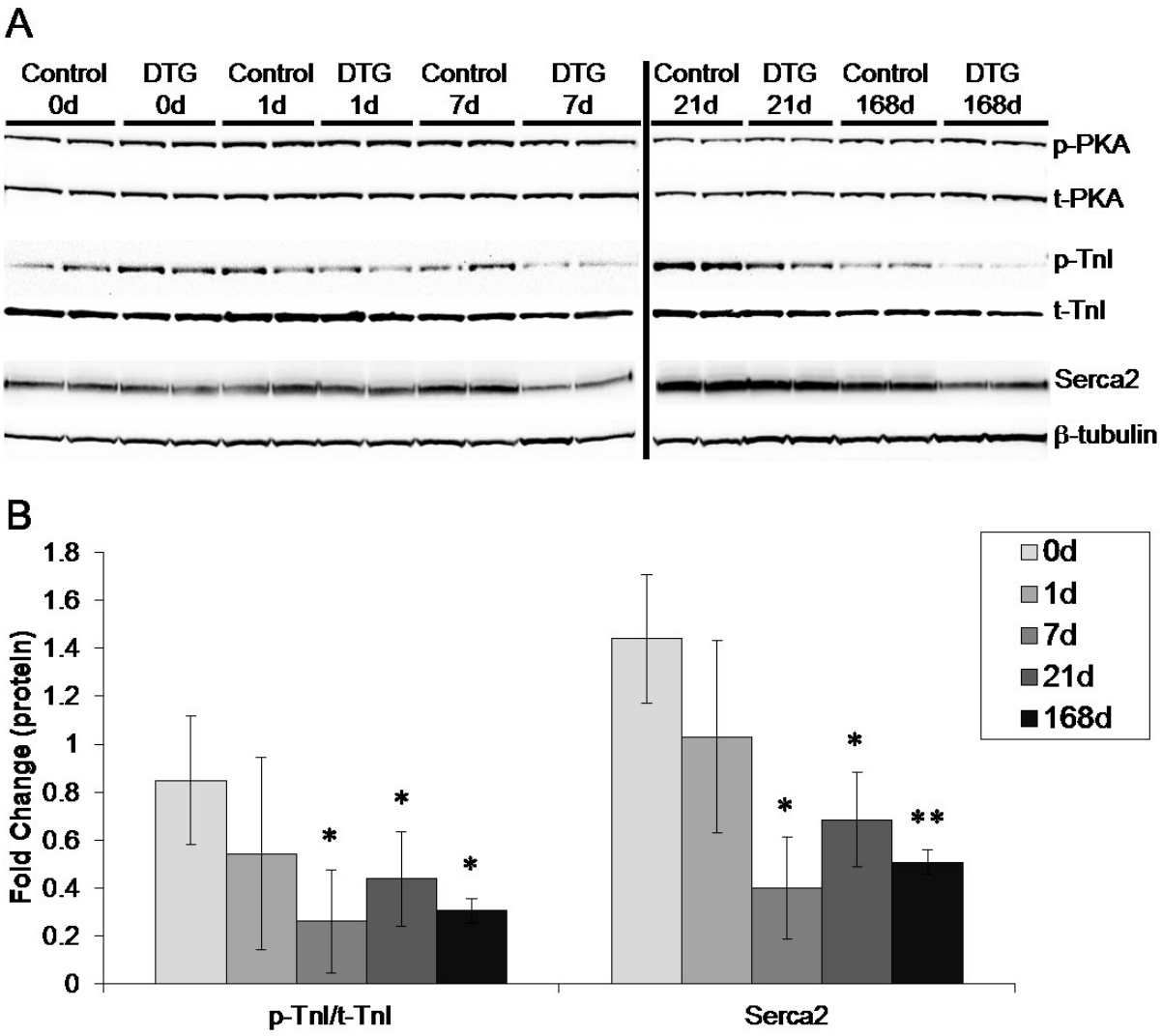

Figure 3.9 Double transgenic mice have significantly decreased troponin I phosphorylation and Serca2 expression. (A) Representative Western blots depicting no changes in the expression of phosphorylated protein kinase A (P-PKA) and decreased expression of phosphorylated troponin I (P-TnI) and Serca2a2. β-tubulin was used as a loading control. (B) Densitometric quantitation of p-TnI/t-TnI and Serca2a2, demonstrating a significant decrease in both by seven days of caFGFR1 induction. Fold change is versus corresponding time-matched littermate controls (not shown). DTG (shown): n_{0d}=5, n_{1d}=8, n_{7d}=8, n_{21d}=6, n_{168d}=2; controls (not shown): n_{0d}=2, n_{1d}=5, n_{7d}=4, n_{21d}=3, n_{168d}=2. Error bars = standard deviation. *p<0.05, **p<0.01.

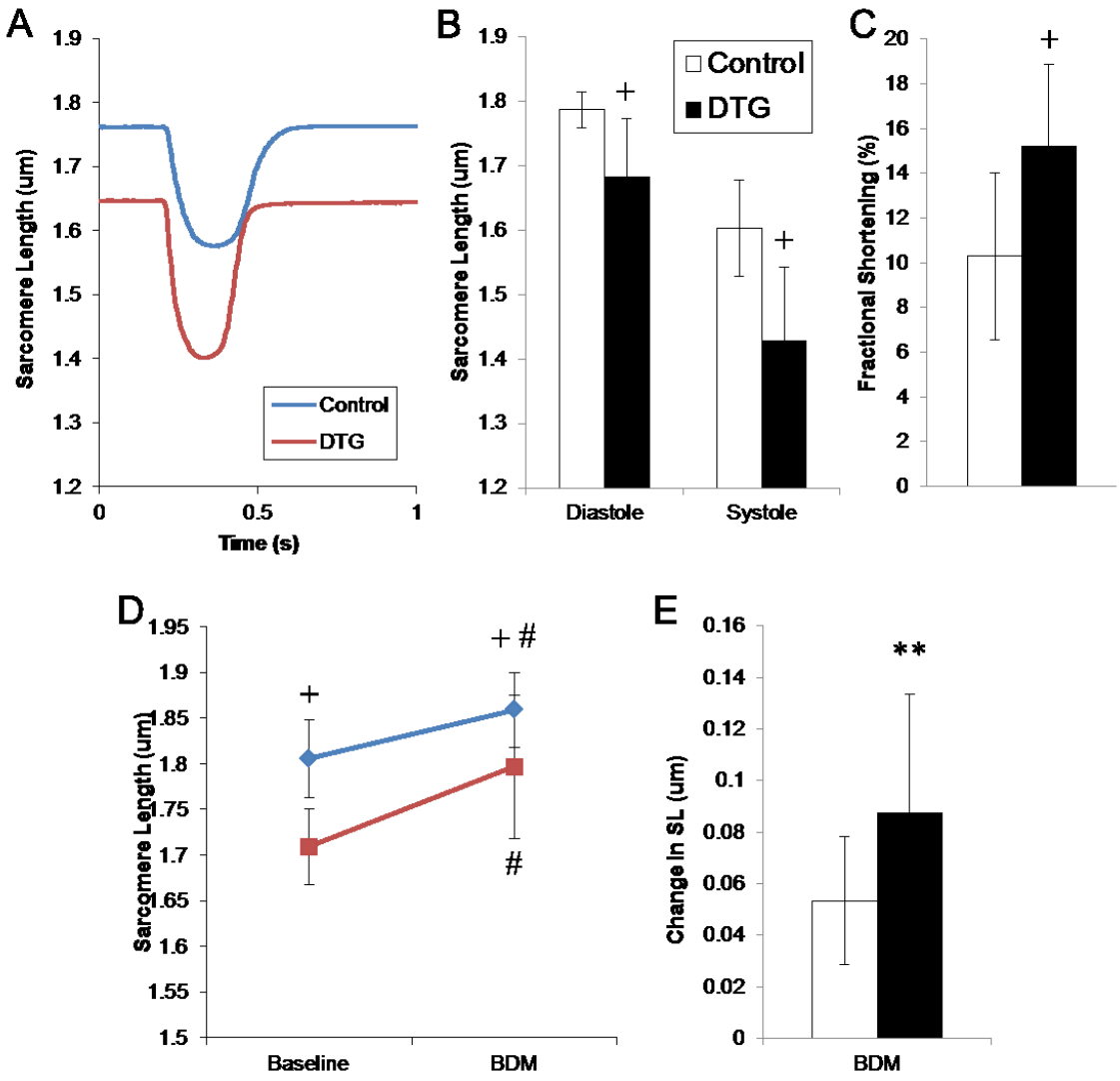

Figure 3.10 Ventricular myocytes from double transgenic mice have impaired relaxation and enhanced contraction. Double transgenic (DTG) and littermate controls were induced for 24-48 hours with DOX chow, and then unloaded cell shortening was assessed in freshly isolated ventricular myocytes. (A) Representative tracings illustrating the contractile differences between cardiomyocytes from DTG and control hearts. (B) DTG myocytes were significantly shorter at both systole and diastole, (C) with an overall increase in fractional shortening (n=4 mice, 17 myocytes total for both control and DTG). (D) Addition of BDM, an inhibitor of actin-myosin interactions, caused significant relaxation of both DTG and control myocytes, (E) and resulted in a greater change in sarcomere length in DTG myocytes (n=3 mice each, 19 control myocytes, 23 DTG myocytes). . Error bars=standard deviation. **p<0.01, +p<0.001 DTG vs. littermate controls; # p<0.05 vs. respective baseline measurements.

Parameter	αMHC-rtTA	αMHC-rtTA, TRE-caFGFR1	T-test
Number of mice	4	4	*P value*
Heart rate (bpm)	366 ± 104	332 ± 69	NS
MAP	64.9 ± 3.1	61.6 ± 1.6	NS
ESP (mmHg)	85.7 ± 7.0	79.4 ± 4.1	NS
EDP (mmHg)	5.8 ± 2.4	6.4 ± 1.9	NS
ESV (µL)	31.7 ± 9.0	18.2 ± 6.5	0.05
EDV (µL)	51.2 ± 9.0	31.8 ± 5.7	0.01
EF (%)	38.8 ± 8.2	43.8 ± 16.2	NS
dP/dt-max (mmHg/s)	4701 ± 739	4436 ± 1593	NS
dP/dt-min (mmHg/s)	-4307 ± 791	-3503 ± 952	NS
tau Glantz	16.7 ± 2.8	19.5 ± 6.3	NS

Table 3.1 Hemodynamic analysis of double transgenic and littermate control mice following 24 hours on DOX. Note absence of differences in all parameters except end systolic and end diastolic volumes (ESV, EDV). bpm, beats per minute; MAP, mean arterial pressue; ESP, end systolic pressure; EDP, end diastolic pressure; EF, ejection fraction; dP/dt, change in pressure over change in time.

Parameter	αMHC-rtTA	αMHC-rtTA, TRE-caFGFR1	T-test
Number of mice	2	3	***P value***
Heart rate (bpm)	307 ± 3	278 ± 48	NS
ESP (mmHg)	105.8 ± 2.7	191.6 ± 21.2	0.01
EDP (mmHg)	3.7 ± 4.9	8.6 ± 5.1	NS
ESV (µL)	16.0 ± 13.6	15.8 ± 9.0	NS
EDV (µL)	37.6 ± 5.0	34.8 ± 7.7	NS
EF (%)	59.3 ± 30.8	56.7 ± 14.8	NS
dP/dt-max (mmHg/s)	5841 ± 229	6046 ± 1177	NS
dP/dt-min (mmHg/s)	-4764 ± 159	-5134 ± 1491	NS
tau Glantz	16.4 ± 1.9	28.0 ± 2.2	0.009

Table 3.2 Hemodynamic analysis of double transgenic and littermate control ice following 42 days on DOX. Note the significant increases in end systolic pressure (ESP) and *tau* (Glantz). bpm, beats per minute; EDP, end diastolic pressure; ESV, end systolic volume; EDV, end diastolic volume; EF, ejection fraction; dP/dt, change in pressure over change in time.

	Ctl 0d	DTG 0d	Ctl 7d	DTG 7d	Ctl PD17	DTG PD17	Ctl U0126	DTG U0126	DTG Wort	DTG CsA
HR (bpm)	629 ± 86	611 ± 65	655 ± 43	611 ± 66	667 ± 23	642 ± 43	657 ± 44	619 ± 82	673 ± 47	651 ± 59
FS	0.49 ± 0.06	0.52 ± 0.06	0.50 ± 0.07	0.54 ± 0.05	0.48 ± 0.00	0.51 ± 0.06	0.50 ± 0.05	0.56 ± 0.07	0.55 ± 0.03	0.47 ± 0.06 *
LVMI (mg/g)	3.98 ± 0.56	4.02 ± 0.39	4.19 ± 0.50	5.28 ± 1.01 #	4.24 ± 0.27	3.83 ± 0.35 *	4.53 ± 0.66	4.52 ± 0.73 #	5.47 ± 1.18	5.05 ± 0.77
LVPWd (mm)	0.87 ± 0.11	0.85 ± 0.09	0.83 ± 0.06	1.14 ± 0.27 #	0.86 ± 0.09	0.97 ± 0.06 #	0.83 ± 0.06	1.03 ± 0.20	1.10 ± 0.24	1.13 ± 0.09
LVIDd (mm)	3.31 ± 0.32	3.31 ± 0.34	3.47 ± 0.21	3.03 ± 0.26 #	3.71 ± 0.22	3.08 ± 0.39 θ	3.62 ± 0.25	3.13 ± 0.14 θ	3.16 ± 0.09 #	2.91 ± 0.24
LV POV (m/s)	0.55 ± 0.18	0.86 ± 0.41 θ	0.69 ± 0.16	4.11 ± 0.76 #	0.60 ± 0.08	4.53 ± 0.56 #θ	0.62 ± 0.15	4.27 ± 0.94 #θ	5.12 ± 0.98 #	4.01 ± 0.66 #
HW/BW (mg/g)	6.06 ± 0.83	6.59 ± 0.59	4.65 ± 0.47	5.54 ± 0.72 θ	4.73 ± 0.14	5.00 ± 0.26	4.79 ± 0.71	5.43 ± 0.94	5.93 ± 0.16	5.90 ± 0.79
N	23 (echo), 5 (other)	51 (echo), 5 (other)	7	14	3	6	3	6	3	3

Table 3.3 Blockade of FGFR tyrosine kinase partially ameliorates LV hypertrophy development in caFGFR1-expressing mice. Mice were injected with PD173074 (FGFR tyrosine kinase inhibitor), U0126 (MEK1/2 inhibitor), Wortmannin (PI3K inhibitor), or Cyclosporine A (calcineurin inhibitor) for one week prior to addition of DOX chow. Drugs were continued throughout one week of transgene induction. DTG mice injected with the FGFR tyrosine kinase inhibitor, PD173074 (DTG PD17) had significantly lower LV mass index compared to DTG mice without drug. However, PD173074 did not reduce the peak outflow velocity (LV POV). Inhibition of other pathways downstream of the FGF receptor had little effect on phenotype development. PD17=PD173074, an FGFR tyrosine kinase inhibitor; U0126=MEK1/2 inhibitor; Wort=Wortmannin, a PI3K inhibitor; CsA=Cyclosporine A, a calcineurin inhibitor; DTG=double transgenic, Ctl=single transgenic control. * $p<0.05$ compared to DTG 7d; # $p<0.05$ compared to baseline; θ $p<0.05$ compared to respective single transgenic controls (ctl).

	Ctl 0d	DTG 0d	Ctl 7d	DTG 7d	Ctl Pro	DTG Pro	Ctl Los	DTG Los
HR (bpm)	629 ± 86	611 ± 65	655 ± 43	611 ± 66	649 ± 45	551 ± 72 θ	677 ± 24	639 ± 68
FS	0.49 ± 0.06	0.52 ± 0.06	0.50 ± 0.07	0.54 ± 0.05	0.39 ± 0.05	0.58 ± 0.01 *θ	0.44 ± 0.05	0.57 ± 0.04 θ
LVMI (mg/g)	3.98 ± 0.56	4.02 ± 0.39	4.19 ± 0.50	5.28 ± 1.01 #	3.91 ± 0.38	4.04 ± 0.72 *	3.42 ± 0.21 #	4.33 ± 0.61 *θ
LVPWd (mm)	0.87 ± 0.11	0.85 ± 0.09	0.829 ± 0.06	1.14 ± 0.27 #	0.80 ± 0.12	0.95 ± 0.16	0.70 ± 0.10	0.97 ± 0.06
LVIDd (mm)	3.31 ± 0.32	3.31 ± 0.34	3.47 ± 0.21	3.03 ± 0.26 #	3.40 ± 0.09	3.16 ± 0.26	3.41 ± 0.06	3.00 ± 0.19 θ
LV POV (m/s)	0.55 ± 0.18	0.86 ± 0.41 θ	0.69 ± 0.16	4.11 ± 0.76 #	0.48 ± 0.12	2.27 ± 1.23 *#θ	0.71 ± 0.13	3.90 ± 0.92 #θ
HW/BW (mg/g)	6.06 ± 0.83	6.59 ± 0.59	4.65 ± 0.47	5.54 ± 0.72 θ	4.59 ± 0.46	5.08 ± 0.32	4.39 ± 0.12	4.80 ± 0.24 *θ
N	23 (echo), 5 (other)	51 (echo), 5 (other)	7	14	3	5	3	6

Table 3.4 Blockade of beta-adrenergic and angiotensin receptors lessens phenotype development in caFGFR1-expressing mice. Mice were given propranolol or losartan in their drinking water one week before the start of DOX chow. Drugs were continued throughout one week transgene induction. Double transgenic mice given propranolol (DTG Pro) or losartan (DTG Los) had significantly lower LV mass index (LVMI) compared to one-week induced double transgenic mice without drug (DTG 7d). Additionally, propranolol (but not losartan) was able to significantly decrease the LV peak outflow velocity (LV POV) in DOX-induced double transgenic mice, although outflow velocity remained significantly elevated compared to baseline. Pro=propranolol, Los=losartan, DTG=double transgenic, Ctl=single transgenic control. *p<0.05 compared to DTG 7d; # p<0.05 compared to baseline; θ p<0.05 compared to respective single transgenic controls (ctl).

Chapter 4

Conclusions and Future Directions

Cardiovascular disease is a major public health problem that costs billions of dollars every year. Current strategies in heart failure treatment are directed at removing the causative factor (as in hypertension) or managing symptoms when this is not possible (as in myocardial infarction or genetic cardiomyopathies). One of the common components and key determinants of outcome in cardiovascular disease is myocardial remodeling, which results in changes in cardiac energetics and myocardial perfusion, in addition to the diastolic and systolic capacity of the heart [191]. This is an incredibly complex process that involves the interplay between different cellular populations in the hearts (endothelial, fibroblast, myocyte, inflammatory, vascular smooth muscle, *etc*.) as well as a variety of different signaling pathways. Additionally, the heart possesses the capacity for more beneficial remodeling to occur, as this is required during normal postnatal growth, as well as to accommodate the increased cardiovascular demands during pregnancy and exercise training. The balance between physiological remodeling and pathological remodeling is poorly understood, but clearly, it would be beneficial to inhibit maladaptive and promote favorable pathways. To do so, however, requires a much greater understanding of the signaling molecules and receptors that govern cardiac growth.

FGF2-knockout studies have demonstrated the clear necessity for this ligand in ventricular remodeling following injury or pressure overload, while other studies have shown FGF1 and FGF9 may also be beneficial to the remodeling process [31, 77, 85, 87-93, 97, 100, 107]. However, other FGF ligands that are involved in cardiovascular development are also expressed in the adult heart, and little is known regarding the roles they play during postnatal cardiac homeostasis, in addition to myocardial remodeling. In addition, the cellular targets of FGF signaling have not been investigated. The main goal of my thesis was to better characterize FGF signaling in the adult heart, with regard to how FGF ligand and receptor gene expression change in response to different physiological and pathological stimuli, as well as to gain a better understanding of how FGF signaling is regulated in the adult heart. Several pathways activated downstream of the FGF receptor have been clearly implicated in different aspects of ventricular remodeling, with proteins like SOS1, SHP2, and RAS involved in the development of hypertrophic cardiomyopathy, ERK1/2 and PKC involved in secondary pathological hypertrophy, and PI3K/Akt associated with physiological hypertrophy. Therefore, the FGF signaling pathway represents a potentially important therapeutic target for modulating ventricular remodeling in the adult heart.

Using an inducible cardiac-specific FGF9-overexpressing mouse model, Kory Lavine, a previous graduate student in our lab, implicated FGF9 in the pathogenesis of fibrosis and progression to heart failure. Given the involvement of FGF2 in the myocardial remodeling process, I hypothesized that FGF9 expression, as well as the expression of other FGF ligands and receptors, may be elevated in different types of pathological remodeling. What I discovered was that expression of *Fgf16*, significantly more so than *Fgf9*, was very tightly and consistently regulated following different pathological and physiological stimuli. In all cases of pathological insults examined (aortic constriction, MI, AngII), *Fgf16* expression was significantly repressed, while it showed slight but significant upregulation in physiological hypertrophy models. This was in contrast to *Fgfr1* and *Fgf2* which were significantly upregulated following MI and significantly downregulated in exercise-induced hypertrophy (Table 2.1).

These findings suggest several possibilities for the regulation of FGF signaling (presented in Figure 2.10), which are the focus of ongoing studies in our lab. Recent evidence suggests that FGF16 can oppose the growth-promoting action of FGF2 [39], which provides a potential model to explain the mirrored expression pattern of *Fgf2* and *Fgf16* under pathological and physiological conditions. I hypothesize that FGF16 levels must decrease in order for FGF2 to mediate myocardial remodeling following injury. It is also possible that the balance between these two ligands is critical for physiological remodeling to occur. Thus, it will be important to examine the response to exercise-induced hypertrophy in FGF2-knockout and –overexpressing mice, as well as FGF16-knockout mice. Additionally, I believe the creation of an FGF16-transgenic or inducible FGF16 mouse line (similar to our TRE-FGF9 mouse line) will be useful for these future experiments. Further *in vitro* studies will also be helpful to determine a more precise mechanism through which FGF16 inhibits FGF2-mediated myocyte growth.

The gene expression studies also suggested that a means of regulating the responsiveness to FGF signals is through regulation of receptor expression. Following MI, both *Fgfr1* and *Fgfr2* are significantly upregulated in both the infarcted and noninfarcted myocardium, implicating them as key receptors for the FGF2-mediated remodeling process, and providing an explanation for a lack of spontaneous hypertrophy development in FGF2-overexpressing mouse models. Further support for this model of regulation comes from studies presented in Chapter 3, in which I observed little to no expression of FGFR1 protein in the uninjured adult heart (Figure 3.1B), despite the presence of moderate levels of

Fgfr1 cDNA seen in quantitative RT-PCR studies. I thus hypothesize that under homeostatic conditions, FGFR1 is rapidly degraded (perhaps downstream of FGF16-mediated signaling), but is stabilized in the membrane following pathological insult. Rapid receptor desensitization is one of the key methods by which G-protein coupled receptor signaling is regulated [192], so it is possible that a similar mechanism can be extended to receptor tyrosine kinases.

Another model that would explain the lack of a baseline hypertrophy phenotype in FGF2-overexpressing hearts is that FGF receptors are uncoupled from their downstream signaling pathways under homeostatic conditions. To test this hypothesis, Kory Lavine created a cardiomyocyte-specific, doxycycline-inducible constitutively-active FGFR1 mouse line, and I anticipated that induction of this receptor would not result in cardiomyocyte hypertrophy unless the heart were injured. However, I observed a remarkable increase in cardiac contractility with low baseline levels of caFGFR1 expression, with the rapid development of hypertrophic cardiomyopathy within one week of transgene induction. This phenotype was present in 100% of mice expressing caFGFR1. Despite the continual progression of hypertrophy, caFGFR1-expressing hearts maintained their systolic function and none of the mice experienced heart failure or sudden cardiac death, even in response to forced exercise. Intriguingly, upon mechanistic evaluation, I did not observe activation of any of the classical FGF-activated pathways, including ERK1/2, Akt, Stat3, Stat5, p38, JNK, or PLCγ, which was consistent with finding from a Ras-induced HCM model [178]. Meanwhile, I noted a significant decrease in troponin I phosphorylation and expression of Serca2, suggesting the possibility that myofilament calcium sensitivity or intracellular calcium handling were altered. *In vitro* experiments utilizing freshly isolated ventricular myocytes from acutely-induced mice (24-48 hours on DOX chow) demonstrated impaired sarcomere relaxation in addition to enhanced fractional shortening. Partial rescue of the phenotype was achieved by inhibiting myosin-actin cross bridge formation, but not through chelation of intracellular calcium. These findings strongly suggested that caFGFR1 is capable of rapidly altering myocyte contractile properties, at least partly through direct effects on myofilament physiology, and not via the increased availability of cytosolic calcium. These studies have suggested the possibility of a novel downstream pathway capable of altering sarcomere biomechanics, but how or why this particular pathway is activated in caFGFR1-expressing myocytes is currently unclear and warrants further investigation. Future studies examining

skinned myofilaments are necessary to investigate mechanical properties more closely, in addition to calcium imaging studies in isolated myocytes to confirm the absence of calcium handling defects. Furthermore, expression and activation of protein phosphatases 1 and 2a should be examined, as these enzymes could provide a link between the FGF receptor and altered myocardial contractility.

It is most likely that FGF signaling is regulated by a combination of all of these mechanisms, which allow the signals, the cellular targets, and the responses to be fine-tuned to the particular stimulus. It is clear that we have only begun to scratch the surface of cardiac FGF signaling, as many significant questions remain. In what cells are the various ligands and receptors expressed and in what cells are they necessary and/or sufficient to induce remodeling in the adult heart? In order to appropriately target treatments and understand which remodeling effects are cell autonomous or non-autonomous, receptor loss-of-function studies must be performed. Other than cardiomyocyte-specific double conditional receptor knockout discussed in Chapter 2, I established several other DCKO lines to ablate *Fgfr1/2* expression from endothelial and epicardial cells that are currently being used in our lab to assess the relative contribution(s) of FGF signaling to the different cell types during periods of normal physiological cardiac growth, physiological hypertrophy, and following MI.

When does the cardiomyocyte response to FGF signaling switch from proliferation to hypercontractility and hypertrophy, and what FGF ligands are capable of reproducing the hypercontractility observed in caFGFR1-expressing mice? The doxycycline-inducible FGF9 and caFGFR1 mouse lines can be utilized to investigate myocardial responsiveness to FGF signals at different postnatal time points. In addition, I created a new doxycycline-inducible FGF2 mouse line that can be used to assess the effects of acutely increasing FGF2 expression at different time points and in in different cells.

Finally, what factors determine which downstream signaling pathway(s) gets activated? How can we direct FGF signaling towards the more beneficial PI3K-Akt pathway and away from the maladaptive ERK1/2 or PKC pathways? Is there a way to translate the caFGFR1-mediated hypercontractility into a viable treatment alternative for patients with systolic dysfunction? Answering all of these questions will be essential in order to harness the full potential of the FGF signaling pathway and implement it in such a

way to therapeutically guide the tissue response to injury towards physiological, rather than the pathological remodeling.

Chapter 5

Materials and Methods

Mouse models. TRE-caFGFR1 mice were generated by Kory Lavine by subcloning a cDNA fragment encoding *FGFR31C(R248C)-cmyc* into pTRE2 (Invitrogen). The resultant *pTRE2-FGFR31C(R248C)* vector was linearized and injected into FVB blastocysts. 8 founder lines were obtained and 4 were screened by crossing the founder to αMHC-rtTA transgenic mice, feeding double transgenic offspring doxycycline chow (Research Diets), and assaying for transgene expression by western blot. Western blotting was performed using antibodies against the c-myc epitope and β-tubulin (see more detailed description of WB below). All mice were maintained on a mixed background, primarily C57/Bl6/129.

αMHC-rtTA, TRE-FGF9 mice were fed doxycycline-containing chow (DOX, Research Diets) for 20 days to induce transgene expression. Mice were then analyzed utilized echocardiography, and postmortem analysis described below. αMHC-rtTA, TRE-caFGFR1 mice were fed DOX chow for varying lengths of time (from 24 hours up to ten months) and analyzed using techniques described below.

To inactivate FGF receptor signaling in cardiomyocytes, αMHC-CreER, $FGFR1^{f/f}$, $FGFR2^{f/f}$ DCKO mice were injected with 40mg/kg tamoxifen (Sigma). Briefly, 40 mg of tamoxifen was added to 400 μL of 100% ethanol and sonicated until dissolved. 3.6 mL of sunflower seed oil (Sigma) was then added and the solution was sonicated again until it was homogenous, for a final tamoxifen concentration of 10mg/mL. For an average mouse of 25g, 100 μL was injected intraperitoneally using a 25-gauge needle.

TRE-FGF2 mice were generated by subcloning a cDNA fragment encoding human *Fgf2* into the pTRE2-FGF9/EGFP plasmid (Figure 5.1). *Fgf9* was excised from the plasmid utilizing SacII and EcoRI restriction enzymes, according to the protocol from New England Biolabs (NEB, "Optimizing Restriction Endonuclear Reactions": 500 ng plasmid, 0.5 μL of each restriction enzyme, 2.5 μL 10x buffer, 0.25 μL 100x BSA, and water up to 25 μL; 37C water bath for 1 hour). The digest was separated on a 0.7% agarose gel, and the ~4 kb fragment was excised and purified utilizing the Qiagen gel extraction kit. A linker segment was created to add an additional EcoRI restriction site into the plasmid. 5'-AATTCCGTCGACTTGC-3' and 5'-AAGTCGACGG-3' oligomers were purchased from Integrated DNA Technologies and reconstituted as directed. To anneal the oligomers into the linker segment, 100 μL of each oligomer were mixed together and heated to 94C, then cooled to room temperature. The linker was ligated into the pTRE2 plasmid utilizing the standard NEB protocol for "DNA ligation with T4 DNA Ligase,"

and then transformed into DH5α bacteria. Briefly, 5 μL of the ligation mix was added to 100 μL bacteria, placed on ice for 30 minutes, then at 42C for 90 seconds, then back on ice for 2 minutes. 300 μL of LB was added and samples were placed in the 37C shaker for 1 hour, after which they were plated in agar dishes containing ampicillin overnight in the 37C shaker. Several colonies were selected the following morning using sterile loops and placed in 15-mL round bottom tubes with 6 mL of LB and 6 μL of ampicillin. Minipreps were incubated in the 37C shaker overnight, and plasmids were isolated the following day utilizing the Qiagen Miniprep kit.

A human FGF2 plasmid was generously provided by Marja Hurle; FGF2 was excised utilizing an EcoRI digest and 960 bp segment was purified as described for the pTRE2 plasmid. The pTRE2-linker plasmid was opened using EcoRI and gel purified. Ligation of the p-TRE2-linker and FGF2 fragments was achieved utilizing a 1:10 vector:insert ratio. Transformation and purification of plasmids were performed as described above. Plasmids were digested with SalI (which was introduced in the linker and would make only one cut) and then screened for proper size (5.12 kb). Appropriately-sized bands were excised, re-ligated and maxi-prepped utilizing a Qiagen Maxiprep kit. FGF2 transgene (3.4 kb) was excised for injection into FVB blastocysts utilizing AatII and DrdI. Nine founder lines were obtained and are currently being screened by Southern blot for GFP to determine the most stable line.

Echocardiography. Non-invasive ultrasound examination of the cardiovascular system was performed using a Vevo 2100 Ultrasound System (VisualSonics Inc, Toronto, Ontario, Canada) according to the following procedures. First, mice were lightly anesthetized with an intraperitoneal injection of 2% Avertin (tribromoethanol, 0.005 ml/g). One fifth of the initial dose was given as a maintenance dose at regular intervals depending on the level of anesthesia. Low-dose Avertin was used because it does not have significant negative inotropic or chronotropic effect. Hair was removed from the anterior chest with a combination of shaving and chemical hair remover, and the animals were placed on a warming pad in a left lateral decubitus position. Ultrasound coupling gel was applied to the chest. Examination of cardiac structure and function under these near-physiologic condition was obtained with hand-held manipulation of the ultrasound transducer. Care was taken to maintain adequate contact while avoiding excessive pressure on the chest. Complete two-dimensional, M-mode, and Doppler ultrasound examination was performed from multiple views. After completion of the imaging studies, mice were kept warm and allowed

to recover until returned to their cage. Digitally acquired images were analyzed off-line on a computer workstation running Vevo 2100 analysis software. [Methods and echocardiography performed by Dr. Attila Kovacs in the Washington University Mouse Cardiovascular Phenotyping Core. Analysis performed by Sarah Cilvik.]

Cardiac Surgery. Eight- to 12-week-old mice were subjected to LAD ligation (MI) or ascending aortic banding, as previously described [154, 193, 194]. Surgeries were performed by Carla Weinheimer in the Washington University Mouse Cardiovascular Phenotyping Core.

Hemodynamic Analysis. Adult mice were anesthetized with thiopental sodium 60 mg/kg administered i.p. This anesthesia produces a near physiologic heart rate of 500 beats/min while still allowing for a surgical plane of anesthesia. The mice were intubated and ventilated with a Harvard ventilator set at 200-400 µl. The bilateral carotid arteries were identified in the region of the trachea and the right carotid was cannulated with a 1.4 french high fidelity micromonometer pressure-volume catheter (SciSense Advantage System, London, Ontario, Canada). The catheter was advanced retrogradely through the aortic valve into the left ventricle to assess pressure volume loops. Continuous aortic pressures, LV systolic and diastolic pressures, the derivative of LV pressure (dP/dT), and tau was recorded and analyzed with Scisense analysis software. Pressure-volume loops were analyzed. before, during, and after an occlusion of the IVC to assess load-independent measurements of myocardial contractility. [Written by Attila Kovacs and performed by Carla Weinheimer and Carrie Giersach in the Washington University Mouse Cardiovascular Phenotyping Core.]

Exercise tolerance. To determine if chronic induction of caFGFR1 and the resulting concentric hypertrophy would result in impair performance during forced exercise, adult mice were fed DOX chow for six months and then subjected to an acute treadmill stress test, where their exercise tolerance was measured by the length of time they were able to run unassisted (time to failure). Exercise tests were carried out using a state-of-the-art Exer4-OxyMax motorized treadmill (Columbus Instruments, Columbus, Ohio). Electrified bars delivered a very mild stimulus when a mouse failed to keep pace with the belt. For this experiment, mice began running at 10 meters/min, and the speed was increased by 3 meters/min every 3 minutes. Time to failure was reached when a mouse remained on the electrified bar for >5

seconds. [Protocol adapted from Carla Weinheimer and run in collaboration with Carrie Giersach in Washington University Mouse Cardiovascular Phenotyping Core.]

Inhibitor studies. Eight- to 12-week-old MHC-rtTA, TRE-caFGFR1 mice were treated with one of the following drugs, starting one week prior to addition of DOX chow and continuing throughout the one week of transgene induction: Losartan (600mg/L in drinking water, Sigma #61188), propranolol (500mg/L in drinking water, Sigma #P0884), diltiazem (450mg/L in drinking water, Sigma #D2521), Cyclosporine A (15mg/kg twice daily subcutaneous injections, Sigma #30024), Wortmannin (1mg/kg/d IP, Sigma #W1628), U0126 (1mg/kg IP every 3 days, Calbiochem #662005), or PD173074 (1mg/kg/d IP, Pfizer), according to published studies [177, 190, 195-198].

Myocyte Isolation, cell contractility, and sarcomere length measurements. Ventricular myocytes from acutely-induced (24-48 hours following doxycycline treatment) control or double transgenic (caFGFR1-expressing) mice were isolated using a method described previously [199]. Following isolation, the ventricular myocyte suspension was washed 3 times in Wittenberg Isolation medium containing 50mg/ml BSA, 12.5mg/ml Taurine with increasing concentrations of CaCl2 (150uM, 400uM, and 900uM). The cells were then washed with Tyrode's solution containing (in mM) NaCl, 137; KCl, 5.4; NaH_2PO_4, 0.16; glucose, 10; $CaCl_2$, 1.0; $MgCl_2$, 0.5; HEPES, 5.0; $NaHCO_3$, 3.0; pH 7.3–7.4. Freshly isolated myocytes were transferred to a recording chamber mounted on the stage of a Nikon Diaphot inverted microscope and perfused at 60ml/hour with normal Tyrode's solution. The cells were allowed to settle for 5 minutes and were subsequently paced at 5-10V at 0.5 Hz for 5 minutes before recording. All experiments were performed at room temperature. Video images of individual myocyte contractions were acquired and analyzed using a Myocam camera (IonOptix). To assess the relaxation of diastolic sarcomere length, cells were loaded with 100uM BAPTA-AM (Sigma) for 1 hour prior to recording or treated with Tyrode's solution containing 40mM 2, 3-butanedione monoxime (BDM) (Sigma). [Methods written and performed by Keita Uchida in the lab of Colin Nichols.]

Gross pathology and histological analysis. At study endpoints, mice were fully anesthetized with an intraperitonieal injection of 2.5% Avertin (0.015 mL/g) and total body weight was measured. Hearts were removed, rinsed briefly in PBS, and then placed into a solution of PBS saturated with potassium chloride to arrest hearts in diastole. Both outflow tract and atria were carefully dissected away,

and biventricular weight was measured. Normalized heart size was determined by calculating the ratio of biventricular weight (mg) to overall mouse weight (g; heart weight: body weight ratio). The apical third of the heart was removed and flash frozen in liquid nitrogen for protein or RNA analysis, while the remaining heart tissue was fixed in 10% neutral buffered formalin for 24-48 hours at room temperature. Samples were then dehydrated in 70% ethanol, embedded in paraffin, cut in 5 μm sections, and stained with H&E. Fibrosis was detected on sections using a Picrosirius red stain kit (24901, Polysciences, Inc., Warrington, PA) with Weigert's iron hematolxylin counterstaining (HT1079, Sigma-Aldrich, St. Louis, MO).

Fluorescein-tagged wheat germ agglutinin (FITC-WGA, L4895, Sigma-Aldrich, St. Louis, MO) was used to label all cell membranes, thus illuminating areas of increased interstitial cells and also making quantitation of cardiomyocyte cross-sectional area possible. Sections were dewaxed using xylenes, rehydrated through an ethanol series to water, rinsed in PBS, and then stained with WGA-FITC (1:100) for one hour at room temperature. Finally, sections were rinsed and mounted in Vectashield Hard Set with DAPI (H-1500, Vector Laboratories, Burlingame, CA), and imaged using a Zeiss Apotome Microscopy system. Five to ten images showing cardiomyocytes in cross section were taken from different regions of the ventricular wall in each sample, and mean cardiomyocyte cross sectional area was determined by tracing (using ImageJ software) the membrane of at least 300 cardiomyocytes per sample.

For analysis of Cre activation in MHC-CreER DCKO R26R hearts, staining for β-galatctosidase was performed. Hearts were placed in Mirsky's fixative (National Diagnostics, HS-102) overnight at room temperature, and then rinsed the following day with PBS and placed in 30% sucrose (in PBS) overnight at 4C. Hearts were then mounted in OCT and frozen at -80C. Twelve-μm sections were cut using a cryostat. Slides were allowed to warm to room temperature for 30 minutes and then placed in a humidity chamber and stained with LacZ stain: 950 μL LacZ wash buffer (498 mL 1x PBS, 1 mL 1M $MgCl_2$, 1mL 10% NP40), 0.25mM potassium ferrous cyanide, 0.25mM potassium ferric cyanide, and 50 μL of 2% X-gal stock (in DMF). Slides were protected from light and placed at 37C for 1-2 hours, room temperature for 8-10 hours, or 4C overnight, and checked periodically for development of stain. Once complete staining was achieved, slides were rinsed in PBS (5 minutes x 3), followed by tap water (5 minutes), and then counterstained with nuclear fast red for 2-5 minutes. Finally, slides were rinsed in tap water (5

minutes x 2), followed by 100% ethanol (2 minutes x 2), followed by xylenes (5 minutes x 2), and then mounted with cytoseal.

Protein extraction and Western blotting. Protein was extracted from flash frozen apical pieces of the heart using RIPA buffer (50mM Tris pH7.4, 150mM NaCl, 1mM EDTA, 1% NP-40, 0.1% SDS, 1% sodium deoxycholate, 1% Triton x-100) with freshly added 2% Protease Inhibitor Cocktail (P8340, Sigma-Aldrich) and Phosphatase Inhibitor Cocktail I and II (P2850 and P5726, Sigma-Aldrich). Protein concentration was determined utilizing a Pierce BCA assay kit (23225, Thermo Scientific, Rockford, IL). Total protein (60 µg) was separated on NuPAGE Novex 4-12% Bis-Tris Midi gels (WG1401, Invitrogen, Grand Island, NY) and transferred to PVDF membranes (iBlot Gel Transfer Stacks PVDF Regular, IB4010, Invitrogen). Membranes were blocked for one hour at room temperature with gentle shaking in TBST (50mM Tris, pH7.4, 150mM NaCl, 0.1% Tween20) containing 5% nonfat milk, and then probed with the antibodies listed in Table 5.1 overnight at 4ºC. After three rinses in TBST, membranes were incubated for one hour at room temperature in horseradish peroxidase-linked secondary antibodies, as described in Table 5.1, in TBST with 5% nonfat milk, rinsed again in TBST, and developed using SuperSignal West Femto Maximum Sensitivity Substrate (34096, Thermo Scientific).

The membrane was then stripped utilizing multiple washes of boiled 100 mM glycine and TBST wash buffer at room temperature (glycine reprobing protocol using the iBlot dry blotting system, Invitrogen) and sequentially reprobed with additional antibodies. Protein bands were quantified by densitometry, and protein loading normalized to β-tubulin. Phospho-ERK1/2 and phospho-Akt were normalized to total-ERK1/2 and total-Akt protein levels, and then scaled relative to controls, where control samples were set at a value of 1.

RNA isolation, cDNA synthesis, and quantitative RT-PCR. RNA was extracted from flash frozen apical pieces of the heart using a Qiagen RNeasy Mini kit (protocol from Appedix C in 3rd edition RNeasy Mini Handbook, 74104, Qiagen, Valencia, CA), with on-column DNA digest. RNA concentration was determined utilizing a Nanodrop spectrophotometer. cDNA was made using the BioRad iScript Reverse Transcription Supermix for RT-qPCR kit (170-8841, BioRad, Hercules, CA). Quantitative RT-PCR was performed on an Applied Biosystems (ABI) 7500 machine using ABI Taqman® Fast Advaned

Master Mix (ABI #4444557) and Taqman® gene expression assays listed in Table 5.2 (ABI). All samples were normalized to *Hprt* and then scaled relative to controls using the standard ddCt method.

Statistical analysis. In all figures, error bars represent standard deviation, unless otherwise noted. Statistical analysis was carried out using a standard student T-test, with a $p<0.05$ considered significant. Individual outliers were determined using Grubbs' test.

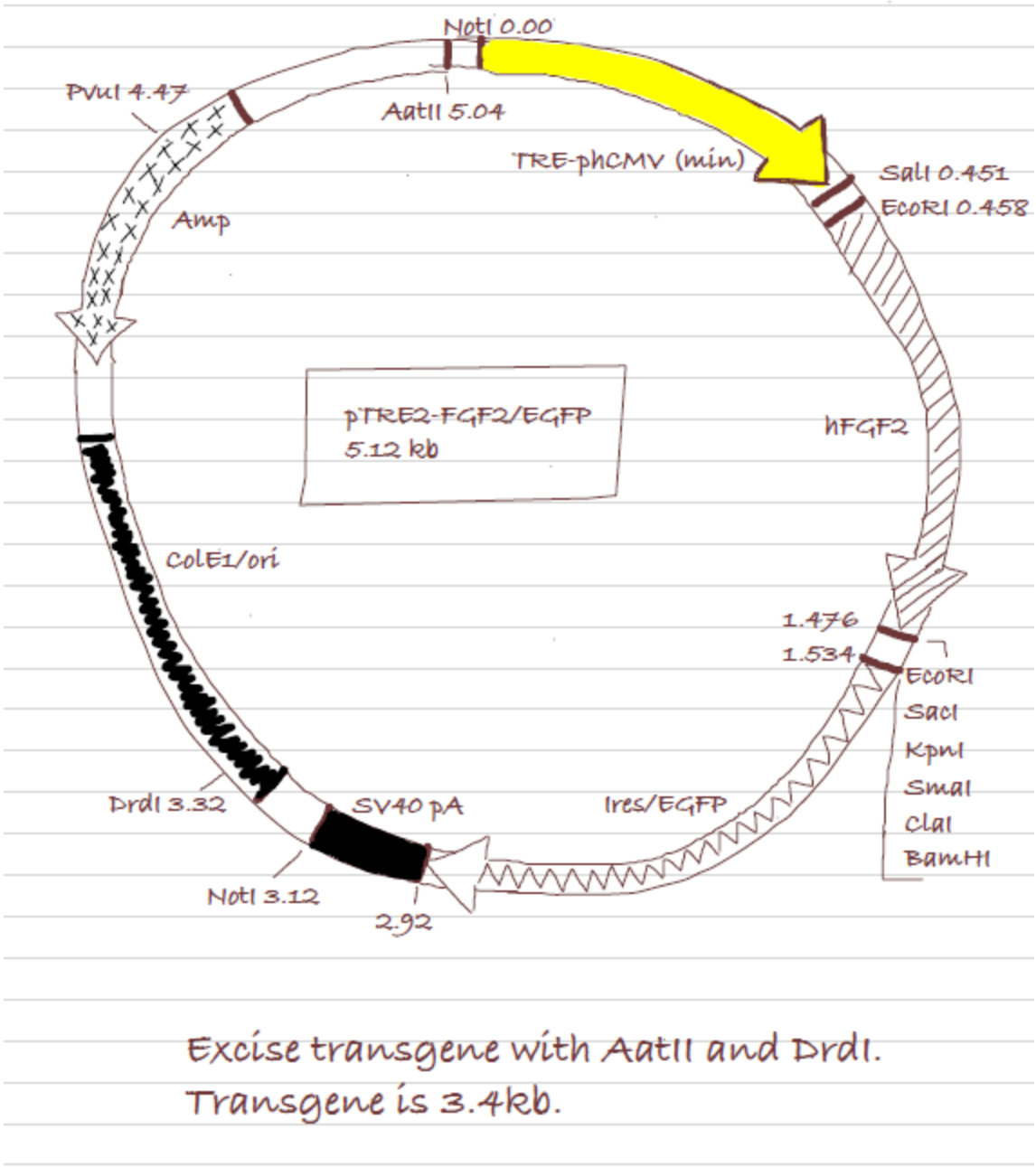

Figure 5.1 pTRE2-FGF2/EGFP plasmid.

Antibody	Catalog #	Conc.	Secondary	Catalog #	Conc.
Mouse anti-Serca2	Thermo Scientific #2A7-A1	1:2000	Goat anti-mouse IgG HRP	Santa Cruz sc-2055	1:10,000
Mouse anti-human c-myc	DSHB 9E10	1:2000	Goat anti-mouse IgG HRP	Santa Cruz sc-2055	1:5000
Rabbit anti-mouse phospho-ERK1/2$^{T202/Y204}$	Cell Signaling #4376S	1:1000	Goat anti-rabbit IgG HRP	Santa Cruz sc-2301	1:10,000
Rabbit anti-mouse ERK1/2	Cell Signaling #9102S	1:1000	Goat anti-rabbit IgG HRP	Santa Cruz sc-2301	1:10,000
Rabbit anti-mouse phospho-Akt^{S473}	Cell Signaling #4058S	1:1000	Goat anti-rabbit IgG HRP	Santa Cruz sc-2301	1:10,000
Rabbit anti-mouse Akt	Cell Signaling #9272S	1:1000	Goat anti-rabbit IgG HRP	Santa Cruz sc-2301	1:10,000
Rabbit anti-PLCg1 [pY^{783}]	Invitrogen #44-696G	1:500	Goat anti-rabbit IgG HRP	Santa Cruz sc-2301	1:2000
Rabbit anti-PLCg1 (D9H10) XP	Cell Signaling #5690	1:500	Goat anti-rabbit IgG HRP	Santa Cruz sc-2301	1:5000
Rabbit anti-FGF receptor 1 XP	Cell Signaling #9740	1:1000	Goat anti-rabbit IgG HRP	Santa Cruz sc-2301	1:2000
Rabbit anti-phospho-Stat3 (Tyr705) XP	Cell Signaling #9145	1:2000	Goat anti-rabbit IgG HRP	Santa Cruz sc-2301	1:2000
Mouse anti-Stat3 (124H6)	Cell Signaling #9139	1:2000	Goat anti-mouse IgG HRP	Santa Cruz sc-2055	1:5000
Rabbit anti-Stat5 (Tyr694) (C71E5)	Cell Signaling #9314	1:2000	Goat anti-rabbit IgG HRP	Santa Cruz sc-2301	1:2000
Rabbit anti-phospho Troponin I (Ser23/24)	Cell Signaling #4004	1:2000	Goat anti-rabbit IgG HRP	Santa Cruz sc-2301	1:10,000
Mouse anti-Troponin I	DSHB TI-1	1:2000	Goat anti-mouse IgG HRP	Santa Cruz sc-2055	1:10000
Rabbit anti-phospho-p38 (Thr180/Tyr182) (D3F9) Xp	Cell Signaling #4511	1:2000	Goat anti-rabbit IgG HRP	Santa Cruz sc-2301	1:5000
Rabbit anti-p38	Cell Signaling #9212	1:2000	Goat anti-rabbit IgG HRP	Santa Cruz sc-2301	1:5000
Mouse anti-phospho-SAPK/JNK (Thr183/Tyr185)	Cell Signaling #9255	1:2000	Goat anti-mouse IgG HRP	Santa Cruz sc-2055	1:10,000
Goat anti-JNK1/2	Santa Cruz sc-474	1:1500	Donkey anti-goat IgG HRP	Santa Cruz sc-2304	1:2000
Rabbit anti-phospho-PKA	Cell Signaling #5661	1:1000	Goat anti-rabbit IgG HRP	Santa Cruz sc-2301	1:10,000
Rabbit anti-PKA	Cell Signaling #5842	1:1000	Goat anti-rabbit IgG HRP	Santa Cruz sc-2301	1:10,000
Rabbit anti-phospho-phospholamban	Cell Signaling #8496	1:2000	Goat anti-rabbit IgG HRP	Santa Cruz sc-2301	1:20,000
Rabbit anti-phospholamban	Cell Signaling #8495	1:2000	Goat anti-rabbit IgG HRP	Santa Cruz sc-2301	1:20,000
Rabbit anti-b-tubulin	Abcam #ab6046	1:50,000	Goat anti-rabbit IgG HRP	Santa Cruz sc-2301	1:50,000

Table 5.1 Primary and secondary antibodies utilized for Western blotting.

Gene	Applied Biosystems (ABI) Taqman ® Gene Expression Assay
Fgfr1	Mm00438923_m1
Fgfr1 (tyrosine kinase domain)	Mm0125485_g1
Fgfr2	Mm00438941_m1
Fgfr3	Mm00433294_m1
Fgfr4	Mm00433314_m1
Fgf2	Mm00433287_m1
Fgf7	Mm00433291_m1
Fgf9	Mm00442795_m1
Fgf10	Mm00433275_m1
Fgf16	Mm00651404_m1
Fgf20	Mm00748347_m1
VegfA	Mm00437304_m1
PdgfA	Mm01205760_m1
PdgfB	Mm01298579_m1
PdgfC	Mm00480205_m1
TGFb1	Mm03024053_m1
TGFb2	Mm03024009_m1
TGFb3	Mm00436960_m1
Anp (Nppa)	Mm01255748_g1
Bnp (Nppb)	Mm00435304_g1
bMHC (Myh7)	Mm00600555_m1
Col1a1	Mm00801666_g1
Col3a1	Mm01254476_m1
Etv4 (pea3)	Mm00476696_m1
Etv5 (erm)	Mm00465816_m1
Serca2 (Atp2a2)	Mm01201431_m1
Hprt	Mm01545399_m1

Table 5.2 ABI Taqman® Gene Expression Assays for quantitative RT-PCR analysis.

Chapter 6

References

1. Roger, V.L., et al., *Heart disease and stroke statistics--2012 update: a report from the American Heart Association.* Circulation, 2012. **125**(1): p. e2-e220.
2. Heineke, J. and J.D. Molkentin, *Regulation of cardiac hypertrophy by intracellular signalling pathways.* Nat Rev Mol Cell Biol, 2006. **7**(8): p. 589-600.
3. Barry, S.P., S.M. Davidson, and P.A. Townsend, *Molecular regulation of cardiac hypertrophy.* Int J Biochem Cell Biol, 2008. **40**(10): p. 2023-39.
4. Chatterjee, K. and B. Massie, *Systolic and diastolic heart failure: differences and similarities.* J Card Fail, 2007. **13**(7): p. 569-76.
5. Tsoutsman, T., L. Lam, and C. Semsarian, *Genes, calcium and modifying factors in hypertrophic cardiomyopathy.* Clin Exp Pharmacol Physiol, 2006. **33**(1-2): p. 139-45.
6. Ho, C.Y., *Hypertrophic cardiomyopathy.* Heart Fail Clin, 2010. **6**(2): p. 141-59.
7. McMullen, J.R. and G.L. Jennings, *Differences between pathological and physiological cardiac hypertrophy: novel therapeutic strategies to treat heart failure.* Clin Exp Pharmacol Physiol, 2007. **34**(4): p. 255-62.
8. Ellison, G.M., et al., *Physiological cardiac remodelling in response to endurance exercise training: cellular and molecular mechanisms.* Heart, 2012. **98**(1): p. 5-10.
9. Rajabi, M., et al., *Return to the fetal gene program protects the stressed heart: a strong hypothesis.* Heart Fail Rev, 2007. **12**(3-4): p. 331-43.
10. Izumo, S., B. Nadal-Ginard, and V. Mahdavi, *Protooncogene induction and reprogramming of cardiac gene expression produced by pressure overload.* Proc Natl Acad Sci U S A, 1988. **85**(2): p. 339-43.
11. van den Bosch, B.J., et al., *Early and transient gene expression changes in pressure overload-induced cardiac hypertrophy in mice.* Genomics, 2006. **88**(4): p. 480-8.
12. Itoh, N. and D.M. Ornitz, *Evolution of the Fgf and Fgfr gene families.* Trends Genet, 2004. **20**(11): p. 563-9.
13. Ornitz, D.M. and N. Itoh, *Fibroblast growth factors.* Genome Biol, 2001. **2**(3): p. REVIEWS3005.
14. Itoh, N. and D.M. Ornitz, *Functional evolutionary history of the mouse Fgf gene family.* Dev Dyn, 2008. **237**(1): p. 18-27.
15. Bottcher, R.T. and C. Niehrs, *Fibroblast growth factor signaling during early vertebrate development.* Endocr Rev, 2005. **26**(1): p. 63-77.
16. Eswarakumar, V.P., I. Lax, and J. Schlessinger, *Cellular signaling by fibroblast growth factor receptors.* Cytokine Growth Factor Rev, 2005. **16**(2): p. 139-49.
17. Chellaiah, A.T., et al., *Fibroblast growth factor receptor (FGFR) 3. Alternative splicing in immunoglobulin-like domain III creates a receptor highly specific for acidic FGF/FGF-1.* J Biol Chem, 1994. **269**(15): p. 11620-7.
18. Miki, T., et al., *Determination of ligand-binding specificity by alternative splicing: two distinct growth factor receptors encoded by a single gene.* Proc Natl Acad Sci U S A, 1992. **89**(1): p. 246-50.
19. Naski, M.C. and D.M. Ornitz, *FGF signaling in skeletal development.* Front Biosci, 1998. **3**: p. d781-94.
20. Orr-Urtreger, A., et al., *Developmental localization of the splicing alternatives of fibroblast growth factor receptor-2 (FGFR2).* Dev Biol, 1993. **158**(2): p. 475-86.
21. Turner, N. and R. Grose, *Fibroblast growth factor signalling: from development to cancer.* Nat Rev Cancer, 2010. **10**(2): p. 116-29.
22. Dailey, L., et al., *Mechanisms underlying differential responses to FGF signaling.* Cytokine Growth Factor Rev, 2005. **16**(2): p. 233-47.
23. Miller, D.L., et al., *Compensation by fibroblast growth factor 1 (FGF1) does not account for the mild phenotypic defects observed in FGF2 null mice.* Mol Cell Biol, 2000. **20**(6): p. 2260-8.
24. Cummins, P., *Fibroblast and transforming growth factor expression in the cardiac myocyte.* Cardiovasc Res, 1993. **27**(7): p. 1150-4.
25. Kardami, E., et al., *Regulation of basic fibroblast growth factor (bFGF) and FGF receptors in the heart.* Ann N Y Acad Sci, 1995. **752**: p. 353-69.
26. Speir, E., et al., *Acidic and basic fibroblast growth factors in adult rat heart myocytes. Localization, regulation in culture, and effects on DNA synthesis.* Circ Res, 1992. **71**(2): p. 251-9.

27. Weiner, H.L. and J.L. Swain, *Acidic fibroblast growth factor mRNA is expressed by cardiac myocytes in culture and the protein is localized to the extracellular matrix.* Proc Natl Acad Sci U S A, 1989. **86**(8): p. 2683-7.
28. Schreiber, A.B., et al., *A unique family of endothelial cell polypeptide mitogens: the antigenic and receptor cross-reactivity of bovine endothelial cell growth factor, brain-derived acidic fibroblast growth factor, and eye-derived growth factor-II.* J Cell Biol, 1985. **101**(4): p. 1623-6.
29. Sheikh, F., et al., *Expression of fibroblast growth factor receptor-1 in rat heart H9c2 myoblasts increases cell proliferation.* Mol Cell Biochem, 1997. **176**(1-2): p. 89-97.
30. Armstrong, M.T., D.Y. Lee, and P.B. Armstrong, *Regulation of proliferation of the fetal myocardium.* Dev Dyn, 2000. **219**(2): p. 226-36.
31. Schultz, J.E., et al., *Fibroblast growth factor-2 mediates pressure-induced hypertrophic response.* J Clin Invest, 1999. **104**(6): p. 709-19.
32. Zhou, M., et al., *Fibroblast growth factor 2 control of vascular tone.* Nat Med, 1998. **4**(2): p. 201-7.
33. Colvin, J.S., et al., *Genomic organization and embryonic expression of the mouse fibroblast growth factor 9 gene.* Dev Dyn, 1999. **216**(1): p. 72-88.
34. Hajihosseini, M.K. and J.K. Heath, *Expression patterns of fibroblast growth factors-18 and -20 in mouse embryos is suggestive of novel roles in calvarial and limb development.* Mech Dev, 2002. **113**(1): p. 79-83.
35. Kok, L.D., et al., *Cloning and characterization of a cDNA encoding a novel fibroblast growth factor preferentially expressed in human heart.* Biochem Biophys Res Commun, 1999. **255**(3): p. 717-21.
36. Lavine, K.J., et al., *Endocardial and epicardial derived FGF signals regulate myocardial proliferation and differentiation in vivo.* Dev Cell, 2005. **8**(1): p. 85-95.
37. Hotta, Y., et al., *Fgf16 is required for cardiomyocyte proliferation in the mouse embryonic heart.* Dev Dyn, 2008. **237**(10): p. 2947-54.
38. Lu, S.Y., et al., *FGF-16 is required for embryonic heart development.* Biochem Biophys Res Commun, 2008. **373**(2): p. 270-4.
39. Lu, S.Y., et al., *FGF-16 is released from neonatal cardiac myocytes and alters growth-related signaling: a possible role in postnatal development.* Am J Physiol Cell Physiol, 2008. **294**(5): p. C1242-9.
40. Zaffran, S. and R.G. Kelly, *New developments in the second heart field.* Differentiation, 2012. **84**(1): p. 17-24.
41. Park, E.J., et al., *Required, tissue-specific roles for Fgf8 in outflow tract formation and remodeling.* Development, 2006. **133**(12): p. 2419-33.
42. Sato, A., et al., *FGF8 signaling is chemotactic for cardiac neural crest cells.* Dev Biol, 2011. **354**(1): p. 18-30.
43. Meyers, E.N. and G.R. Martin, *Differences in left-right axis pathways in mouse and chick: functions of FGF8 and SHH.* Science, 1999. **285**(5426): p. 403-6.
44. Brown, C.B., et al., *Cre-mediated excision of Fgf8 in the Tbx1 expression domain reveals a critical role for Fgf8 in cardiovascular development in the mouse.* Dev Biol, 2004. **267**(1): p. 190-202.
45. Ilagan, R., et al., *Fgf8 is required for anterior heart field development.* Development, 2006. **133**(12): p. 2435-45.
46. Abu-Issa, R., et al., *Fgf8 is required for pharyngeal arch and cardiovascular development in the mouse.* Development, 2002. **129**(19): p. 4613-25.
47. Meyers, E.N., M. Lewandoski, and G.R. Martin, *An Fgf8 mutant allelic series generated by Cre- and Flp-mediated recombination.* Nat Genet, 1998. **18**(2): p. 136-41.
48. Watanabe, Y., et al., *Role of mesodermal FGF8 and FGF10 overlaps in the development of the arterial pole of the heart and pharyngeal arch arteries.* Circ Res, 2010. **106**(3): p. 495-503.
49. Marguerie, A., et al., *Congenital heart defects in Fgfr2-IIIb and Fgf10 mutant mice.* Cardiovasc Res, 2006. **71**(1): p. 50-60.
50. Beer, H.D., et al., *Mouse fibroblast growth factor 10: cDNA cloning, protein characterization, and regulation of mRNA expression.* Oncogene, 1997. **15**(18): p. 2211-8.
51. Kelly, R.G., N.A. Brown, and M.E. Buckingham, *The arterial pole of the mouse heart forms from Fgf10-expressing cells in pharyngeal mesoderm.* Dev Cell, 2001. **1**(3): p. 435-40.

52. Vega-Hernandez, M., et al., *FGF10/FGFR2b signaling is essential for cardiac fibroblast development and growth of the myocardium.* Development, 2011. **138**(15): p. 3331-40.
53. Urness, L.D., et al., *Redundant and dosage sensitive requirements for Fgf3 and Fgf10 in cardiovascular development.* Dev Biol, 2011. **356**(2): p. 383-97.
54. Vincentz, J.W., et al., *Fgf15 is required for proper morphogenesis of the mouse cardiac outflow tract.* Genesis, 2005. **41**(4): p. 192-201.
55. Saitsu, H., K. Shiota, and M. Ishibashi, *Analysis of Fibroblast growth factor 15 cis-elements reveals two conserved enhancers which are closely related to cardiac outflow tract development.* Mech Dev, 2006. **123**(9): p. 665-73.
56. de Lapeyriere, O., et al., *Structure, chromosome mapping and expression of the murine Fgf-6 gene.* Oncogene, 1990. **5**(6): p. 823-31.
57. Finch, P.W., et al., *Pattern of keratinocyte growth factor and keratinocyte growth factor receptor expression during mouse fetal development suggests a role in mediating morphogenetic mesenchymal-epithelial interactions.* Dev Dyn, 1995. **203**(2): p. 223-40.
58. Fiore, F., et al., *Apparent normal phenotype of Fgf6-/- mice.* Int J Dev Biol, 1997. **41**(4): p. 639-42.
59. Mason, I.J., et al., *FGF-7 (keratinocyte growth factor) expression during mouse development suggests roles in myogenesis, forebrain regionalisation and epithelial-mesenchymal interactions.* Mech Dev, 1994. **45**(1): p. 15-30.
60. Morabito, C.J., et al., *Positive and negative regulation of epicardial-mesenchymal transformation during avian heart development.* Dev Biol, 2001. **234**(1): p. 204-15.
61. Antoine, M., et al., *Fibroblast growth factor 16 and 18 are expressed in human cardiovascular tissues and induce on endothelial cells migration but not proliferation.* Biochem Biophys Res Commun, 2006. **346**(1): p. 224-33.
62. Zhang, Y., et al., *Foxp1 coordinates cardiomyocyte proliferation through both cell-autonomous and nonautonomous mechanisms.* Genes Dev, 2010. **24**(16): p. 1746-57.
63. Orr-Urtreger, A., et al., *Developmental expression of two murine fibroblast growth factor receptors, flg and bek.* Development, 1991. **113**(4): p. 1419-34.
64. Peters, K.G., et al., *Two FGF receptor genes are differentially expressed in epithelial and mesenchymal tissues during limb formation and organogenesis in the mouse.* Development, 1992. **114**(1): p. 233-43.
65. Sugi, Y., et al., *Developmental expression of fibroblast growth factor receptor-1 (cek-1; flg) during heart development.* Dev Dyn, 1995. **202**(2): p. 115-25.
66. Jin, Y., et al., *Cloning and expression of fibroblast growth factor receptor-1 isoforms in the mouse heart: evidence for isoform switching during heart development.* J Mol Cell Cardiol, 1994. **26**(11): p. 1449-59.
67. Pasumarthi, K.B., et al., *Characterization of fibroblast growth factor receptor 1 RNA expression in the embryonic mouse heart.* Ann N Y Acad Sci, 1995. **752**: p. 406-16.
68. Arman, E., et al., *Targeted disruption of fibroblast growth factor (FGF) receptor 2 suggests a role for FGF signaling in pregastrulation mammalian development.* Proc Natl Acad Sci U S A, 1998. **95**(9): p. 5082-7.
69. Deng, C.X., et al., *Murine FGFR-1 is required for early postimplantation growth and axial organization.* Genes Dev, 1994. **8**(24): p. 3045-57.
70. Yamaguchi, T.P., et al., *fgfr-1 is required for embryonic growth and mesodermal patterning during mouse gastrulation.* Genes Dev, 1994. **8**(24): p. 3032-44.
71. Deng, C., et al., *Fibroblast growth factor receptor 3 is a negative regulator of bone growth.* Cell, 1996. **84**(6): p. 911-21.
72. Weinstein, M., et al., *FGFR-3 and FGFR-4 function cooperatively to direct alveogenesis in the murine lung.* Development, 1998. **125**(18): p. 3615-23.
73. Ciruna, B.G., et al., *Chimeric analysis of fibroblast growth factor receptor-1 (Fgfr1) function: a role for FGFR1 in morphogenetic movement through the primitive streak.* Development, 1997. **124**(14): p. 2829-41.
74. Dell'Era, P., et al., *Fibroblast growth factor receptor-1 is essential for in vitro cardiomyocyte development.* Circ Res, 2003. **93**(5): p. 414-20.
75. Park, E.J., et al., *An FGF autocrine loop initiated in second heart field mesoderm regulates morphogenesis at the arterial pole of the heart.* Development, 2008. **135**(21): p. 3599-610.

76. Revest, J.M., et al., *Fibroblast growth factor receptor 2-IIIb acts upstream of Shh and Fgf4 and is required for limb bud maintenance but not for the induction of Fgf8, Fgf10, Msx1, or Bmp4.* Dev Biol, 2001. **231**(1): p. 47-62.
77. House, S.L., et al., *Cardiac-specific overexpression of fibroblast growth factor-2 protects against myocardial dysfunction and infarction in a murine model of low-flow ischemia.* Circulation, 2003. **108**(25): p. 3140-8.
78. Fernandez, B., et al., *Transgenic myocardial overexpression of fibroblast growth factor-1 increases coronary artery density and branching.* Circ Res, 2000. **87**(3): p. 207-13.
79. Izumo, S., et al., *Myosin heavy chain messenger RNA and protein isoform transitions during cardiac hypertrophy. Interaction between hemodynamic and thyroid hormone-induced signals.* J Clin Invest, 1987. **79**(3): p. 970-7.
80. Lompre, A.M., J.J. Mercadier, and K. Schwartz, *Changes in gene expression during cardiac growth.* Int Rev Cytol, 1991. **124**: p. 137-86.
81. Schoenfeld, J.R., et al., *Distinct molecular phenotypes in murine cardiac muscle development, growth, and hypertrophy.* J Mol Cell Cardiol, 1998. **30**(11): p. 2269-80.
82. Schwartz, K., et al., *Alpha-skeletal muscle actin mRNA's accumulate in hypertrophied adult rat hearts.* Circ Res, 1986. **59**(5): p. 551-5.
83. Kaye, D., et al., *Role of transiently altered sarcolemmal membrane permeability and basic fibroblast growth factor release in the hypertrophic response of adult rat ventricular myocytes to increased mechanical activity in vitro.* J Clin Invest, 1996. **97**(2): p. 281-91.
84. Scheinowitz, M., et al., *Basic fibroblast growth factor induces myocardial hypertrophy following acute infarction in rats.* Exp Physiol, 1998. **83**(5): p. 585-93.
85. House, S.L., et al., *Fibroblast Growth Factor 2 Mediates Isoproterenol-induced Cardiac Hypertrophy through Activation of the Extracellular Regulated Kinase.* Mol Cell Pharmacol, 2010. **2**(4): p. 143-154.
86. Pellieux, C., et al., *Dilated cardiomyopathy and impaired cardiac hypertrophic response to angiotensin II in mice lacking FGF-2.* J Clin Invest, 2001. **108**(12): p. 1843-51.
87. Lopez, J.J., et al., *Angiogenic potential of perivascularly delivered aFGF in a porcine model of chronic myocardial ischemia.* Am J Physiol, 1998. **274**(3 Pt 2): p. H930-6.
88. Banai, S., et al., *Effects of acidic fibroblast growth factor on normal and ischemic myocardium.* Circ Res, 1991. **69**(1): p. 76-85.
89. Buehler, A., et al., *Angiogenesis-independent cardioprotection in FGF-1 transgenic mice.* Cardiovasc Res, 2002. **55**(4): p. 768-77.
90. Palmen, M., et al., *Fibroblast growth factor-1 improves cardiac functional recovery and enhances cell survival after ischemia and reperfusion: a fibroblast growth factor receptor, protein kinase C, and tyrosine kinase-dependent mechanism.* J Am Coll Cardiol, 2004. **44**(5): p. 1113-23.
91. Cuevas, P., et al., *Protection of rat myocardium by mitogenic and non-mitogenic fibroblast growth factor during post-ischemic reperfusion.* Growth Factors, 1997. **15**(1): p. 29-40.
92. Cuevas, P., et al., *Cardioprotection from ischemia by fibroblast growth factor: role of inducible nitric oxide synthase.* Eur J Med Res, 1999. **4**(12): p. 517-24.
93. Cuevas, P., et al., *Fibroblast growth factor-1 prevents myocardial apoptosis triggered by ischemia reperfusion injury.* Eur J Med Res, 1997. **2**(11): p. 465-8.
94. Landau, C., A.K. Jacobs, and C.C. Haudenschild, *Intrapericardial basic fibroblast growth factor induces myocardial angiogenesis in a rabbit model of chronic ischemia.* Am Heart J, 1995. **129**(5): p. 924-31.
95. Lazarous, D.F., et al., *Effects of chronic systemic administration of basic fibroblast growth factor on collateral development in the canine heart.* Circulation, 1995. **91**(1): p. 145-53.
96. Unger, E.F., et al., *Basic fibroblast growth factor enhances myocardial collateral flow in a canine model.* Am J Physiol, 1994. **266**(4 Pt 2): p. H1588-95.
97. Virag, J.A., et al., *Fibroblast growth factor-2 regulates myocardial infarct repair: effects on cell proliferation, scar contraction, and ventricular function.* Am J Pathol, 2007. **171**(5): p. 1431-40.
98. Miyamoto, M., et al., *Molecular cloning of a novel cytokine cDNA encoding the ninth member of the fibroblast growth factor family, which has a unique secretion property.* Mol Cell Biol, 1993. **13**(7): p. 4251-9.

99. Hall, J.L., et al., *Genomic profiling of the human heart before and after mechanical support with a ventricular assist device reveals alterations in vascular signaling networks.* Physiol Genomics, 2004. **17**(3): p. 283-91.
100. Korf-Klingebiel, M., et al., *Conditional transgenic expression of fibroblast growth factor 9 in the adult mouse heart reduces heart failure mortality after myocardial infarction.* Circulation, 2011. **123**(5): p. 504-14.
101. Faul, C., et al., *FGF23 induces left ventricular hypertrophy.* J Clin Invest, 2011. **121**(11): p. 4393-408.
102. Smallwood, P.M., et al., *Fibroblast growth factor (FGF) homologous factors: new members of the FGF family implicated in nervous system development.* Proc Natl Acad Sci U S A, 1996. **93**(18): p. 9850-7.
103. Fon Tacer, K., et al., *Research resource: Comprehensive expression atlas of the fibroblast growth factor system in adult mouse.* Mol Endocrinol, 2010. **24**(10): p. 2050-64.
104. Wang, C., et al., *Identification of novel interaction sites that determine specificity between fibroblast growth factor homologous factors and voltage-gated sodium channels.* J Biol Chem, 2011. **286**(27): p. 24253-63.
105. Wei, E.Q., et al., *Fibroblast growth factor homologous factors in the heart: a potential locus for cardiac arrhythmias.* Trends Cardiovasc Med, 2011. **21**(7): p. 199-203.
106. Hughes, S.E., *Differential expression of the fibroblast growth factor receptor (FGFR) multigene family in normal human adult tissues.* J Histochem Cytochem, 1997. **45**(7): p. 1005-19.
107. Zhao, T., et al., *Acidic and basic fibroblast growth factors involved in cardiac angiogenesis following infarction.* Int J Cardiol, 2011. **152**(3): p. 307-13.
108. Seyed, M. and J.X. Dimario, *Fibroblast growth factor receptor 1 gene expression is required for cardiomyocyte proliferation and is repressed by Sp3.* J Mol Cell Cardiol, 2008. **44**(3): p. 510-9.
109. Hellman, U., et al., *Parallel up-regulation of FGF-2 and hyaluronan during development of cardiac hypertrophy in rat.* Cell Tissue Res, 2008. **332**(1): p. 49-56.
110. Wang, X.H., et al., *Dynamic changes in the expression of growth factor receptors in the myocardium microvascular endothelium after murine myocardial infarction.* Chin Med J (Engl), 2007. **120**(6): p. 485-90.
111. Muinck, E.D., et al., *Protection against myocardial ischemia-reperfusion injury by the angiogenic Masterswitch protein PR 39 gene therapy: the roles of HIF1alpha stabilization and FGFR1 signaling.* Antioxid Redox Signal, 2007. **9**(4): p. 437-45.
112. Matsunaga, S., et al., *Endothelium-targeted overexpression of constitutively active FGF receptor induces cardioprotection in mice myocardial infarction.* J Mol Cell Cardiol, 2009. **46**(5): p. 663-73.
113. Hadari, Y.R., et al., *Binding of Shp2 tyrosine phosphatase to FRS2 is essential for fibroblast growth factor-induced PC12 cell differentiation.* Mol Cell Biol, 1998. **18**(7): p. 3966-73.
114. Sala, V., et al., *Signaling to Cardiac Hypertrophy: Insights from Human and Mouse RASopathies.* Mol Med, 2012. **18**(9): p. 938-47.
115. Gelb, B.D. and M. Tartaglia, *RAS signaling pathway mutations and hypertrophic cardiomyopathy: getting into and out of the thick of it.* J Clin Invest, 2011. **121**(3): p. 844-7.
116. Tidyman, W.E. and K.A. Rauen, *Noonan, Costello and cardio-facio-cutaneous syndromes: dysregulation of the Ras-MAPK pathway.* Expert Rev Mol Med, 2008. **10**: p. e37.
117. Tartaglia, M., et al., *Mutations in PTPN11, encoding the protein tyrosine phosphatase SHP-2, cause Noonan syndrome.* Nat Genet, 2001. **29**(4): p. 465-8.
118. Digilio, M.C., et al., *Grouping of multiple-lentigines/LEOPARD and Noonan syndromes on the PTPN11 gene.* Am J Hum Genet, 2002. **71**(2): p. 389-94.
119. Legius, E., et al., *PTPN11 mutations in LEOPARD syndrome.* J Med Genet, 2002. **39**(8): p. 571-4.
120. Hunter, J.J., et al., *Ventricular expression of a MLC-2v-ras fusion gene induces cardiac hypertrophy and selective diastolic dysfunction in transgenic mice.* J Biol Chem, 1995. **270**(39): p. 23173-8.
121. Gottshall, K.R., et al., *Ras-dependent pathways induce obstructive hypertrophy in echo-selected transgenic mice.* Proc Natl Acad Sci U S A, 1997. **94**(9): p. 4710-5.
122. Wu, X., et al., *MEK-ERK pathway modulation ameliorates disease phenotypes in a mouse model of Noonan syndrome associated with the Raf1(L613V) mutation.* J Clin Invest, 2011. **121**(3): p. 1009-25.

123. Chen, P.C., et al., *Activation of multiple signaling pathways causes developmental defects in mice with a Noonan syndrome-associated Sos1 mutation.* J Clin Invest, 2010. **120**(12): p. 4353-65.
124. Nakamura, T., et al., *Mediating ERK 1/2 signaling rescues congenital heart defects in a mouse model of Noonan syndrome.* J Clin Invest, 2007. **117**(8): p. 2123-32.
125. Bueno, O.F., et al., *The MEK1-ERK1/2 signaling pathway promotes compensated cardiac hypertrophy in transgenic mice.* EMBO J, 2000. **19**(23): p. 6341-50.
126. Kehat, I., et al., *Extracellular signal-regulated kinases 1 and 2 regulate the balance between eccentric and concentric cardiac growth.* Circ Res, 2011. **108**(2): p. 176-83.
127. Marin, T.M., et al., *Rapamycin reverses hypertrophic cardiomyopathy in a mouse model of LEOPARD syndrome-associated PTPN11 mutation.* J Clin Invest, 2011. **121**(3): p. 1026-43.
128. Schramm, C., et al., *The PTPN11 loss-of-function mutation Q510E-Shp2 causes hypertrophic cardiomyopathy by dysregulating mTOR signaling.* Am J Physiol Heart Circ Physiol, 2012. **302**(1): p. H231-43.
129. Ishida, H., et al., *LEOPARD-type SHP2 mutant Gln510Glu attenuates cardiomyocyte differentiation and promotes cardiac hypertrophy via dysregulation of Akt/GSK-3beta/beta-catenin signaling.* Am J Physiol Heart Circ Physiol, 2011. **301**(4): p. H1531-9.
130. Koziris, L.P., et al., *Serum levels of total and free IGF-I and IGFBP-3 are increased and maintained in long-term training.* J Appl Physiol, 1999. **86**(4): p. 1436-42.
131. McMullen, J.R., et al., *The insulin-like growth factor 1 receptor induces physiological heart growth via the phosphoinositide 3-kinase(p110alpha) pathway.* J Biol Chem, 2004. **279**(6): p. 4782-93.
132. McMullen, J.R., et al., *Phosphoinositide 3-kinase(p110alpha) plays a critical role for the induction of physiological, but not pathological, cardiac hypertrophy.* Proc Natl Acad Sci U S A, 2003. **100**(21): p. 12355-60.
133. Luo, J., et al., *Class IA phosphoinositide 3-kinase regulates heart size and physiological cardiac hypertrophy.* Mol Cell Biol, 2005. **25**(21): p. 9491-502.
134. Kim, J., et al., *Insulin-like growth factor I receptor signaling is required for exercise-induced cardiac hypertrophy.* Mol Endocrinol, 2008. **22**(11): p. 2531-43.
135. DeBosch, B., et al., *Akt1 is required for physiological cardiac growth.* Circulation, 2006. **113**(17): p. 2097-104.
136. Condorelli, G., et al., *Akt induces enhanced myocardial contractility and cell size in vivo in transgenic mice.* Proc Natl Acad Sci U S A, 2002. **99**(19): p. 12333-8.
137. Matsui, T., et al., *Phenotypic spectrum caused by transgenic overexpression of activated Akt in the heart.* J Biol Chem, 2002. **277**(25): p. 22896-901.
138. Shioi, T., et al., *Akt/protein kinase B promotes organ growth in transgenic mice.* Mol Cell Biol, 2002. **22**(8): p. 2799-809.
139. Shiojima, I., et al., *Disruption of coordinated cardiac hypertrophy and angiogenesis contributes to the transition to heart failure.* J Clin Invest, 2005. **115**(8): p. 2108-18.
140. Shiojima, I. and K. Walsh, *Regulation of cardiac growth and coronary angiogenesis by the Akt/PKB signaling pathway.* Genes Dev, 2006. **20**(24): p. 3347-65.
141. Kardami, E., et al., *Fibroblast growth factor 2 isoforms and cardiac hypertrophy.* Cardiovasc Res, 2004. **63**(3): p. 458-66.
142. Dorn, G.W., 2nd and T. Force, *Protein kinase cascades in the regulation of cardiac hypertrophy*. J Clin Invest, 2005. **115**(3): p. 527-37.
143. Dorey, K. and E. Amaya, *FGF signalling: diverse roles during early vertebrate embryogenesis.* Development, 2010. **137**(22): p. 3731-42.
144. Valencik, M.L. and J.A. McDonald, *Codon optimization markedly improves doxycycline regulated gene expression in the mouse heart.* Transgenic Res, 2001. **10**(3): p. 269-75.
145. White, A.C., et al., *FGF9 and SHH signaling coordinate lung growth and development through regulation of distinct mesenchymal domains.* Development, 2006. **133**(8): p. 1507-17.
146. Nagueh, S.F., et al., *Recommendations for the evaluation of left ventricular diastolic function by echocardiography.* J Am Soc Echocardiogr, 2009. **22**(2): p. 107-33.
147. Takeda, N. and I. Manabe, *Cellular Interplay between Cardiomyocytes and Nonmyocytes in Cardiac Remodeling.* Int J Inflam, 2011. **2011**: p. 535241.
148. Shioi, T., et al., *The conserved phosphoinositide 3-kinase pathway determines heart size in mice.* EMBO J, 2000. **19**(11): p. 2537-48.

149. Billet, S., et al., *Gain-of-function mutant of angiotensin II receptor, type 1A, causes hypertension and cardiovascular fibrosis in mice.* J Clin Invest, 2007. **117**(7): p. 1914-25.
150. Xu, J., et al., *Role of cardiac overexpression of ANG II in the regulation of cardiac function and remodeling postmyocardial infarction.* Am J Physiol Heart Circ Physiol, 2007. **293**(3): p. H1900-7.
151. Nakanishi, M., et al., *Genetic disruption of angiotensin II type 1a receptor improves long-term survival of mice with chronic severe aortic regurgitation.* Circ J, 2007. **71**(8): p. 1310-6.
152. Skaletz-Rorowski, A., et al., *Angiotensin AT1 receptor upregulates expression of basic fibroblast growth factor, basic fibroblast growth factor receptor and coreceptor in human coronary smooth muscle cells.* Basic Res Cardiol, 2004. **99**(4): p. 272-8.
153. Lavine, K.J., A. Kovacs, and D.M. Ornitz, *Hedgehog signaling is critical for maintenance of the adult coronary vasculature in mice.* J Clin Invest, 2008. **118**(7): p. 2404-14.
154. Degabriele, N.M., et al., *Critical appraisal of the mouse model of myocardial infarction.* Exp Physiol, 2004. **89**(4): p. 497-505.
155. Limana, F., et al., *Myocardial infarction induces embryonic reprogramming of epicardial c-kit(+) cells: Role of the pericardial fluid.* Journal of Molecular and Cellular Cardiology, 2009.
156. Limana, F., et al., *Identification of myocardial and vascular precursor cells in human and mouse epicardium.* Circ Res, 2007. **101**(12): p. 1255-65.
157. Hsieh, P.C., et al., *Evidence from a genetic fate-mapping study that stem cells refresh adult mammalian cardiomyocytes after injury.* Nat Med, 2007. **13**(8): p. 970-4.
158. Wills, A.A., et al., *Regulated addition of new myocardial and epicardial cells fosters homeostatic cardiac growth and maintenance in adult zebrafish.* Development, 2008. **135**(1): p. 183-92.
159. Nossuli, T.O., et al., *A chronic mouse model of myocardial ischemia-reperfusion: essential in cytokine studies.* Am J Physiol Heart Circ Physiol, 2000. **278**(4): p. H1049-55.
160. Itoh, N. and D.M. Ornitz, *Fibroblast growth factors: from molecular evolution to roles in development, metabolism and disease.* J Biochem, 2011. **149**(2): p. 121-30.
161. Sohal, D.S., et al., *Temporally regulated and tissue-specific gene manipulations in the adult and embryonic heart using a tamoxifen-inducible Cre protein.* Circ Res, 2001. **89**(1): p. 20-5.
162. Merki, E., et al., *Epicardial retinoid X receptor alpha is required for myocardial growth and coronary artery formation.* Proc Natl Acad Sci U S A, 2005. **102**(51): p. 18455-60.
163. Li, W.L., et al., *Endothelial cell-specific expression of Cre recombinase in transgenic mice.* Yi Chuan Xue Bao, 2005. **32**(9): p. 909-15.
164. Corda, S., et al., *Trophic effect of human pericardial fluid on adult cardiac myocytes. Differential role of fibroblast growth factor-2 and factors related to ventricular hypertrophy.* Circ Res, 1997. **81**(5): p. 679-87.
165. Keller, M., et al., *Active caspase-1 is a regulator of unconventional protein secretion.* Cell, 2008. **132**(5): p. 818-31.
166. Detillieux, K.A., et al., *Biological activities of fibroblast growth factor-2 in the adult myocardium.* Cardiovasc Res, 2003. **57**(1): p. 8-19.
167. Ho, C.Y., *Genetics and clinical destiny: improving care in hypertrophic cardiomyopathy.* Circulation, 2010. **122**(23): p. 2430-40; discussion 2440.
168. Naski, M.C., et al., *Graded activation of fibroblast growth factor receptor 3 by mutations causing achondroplasia and thanatophoric dysplasia.* Nat Genet, 1996. **13**(2): p. 233-7.
169. Zhang, Z., et al., *FGF-regulated Etv genes are essential for repressing Shh expression in mouse limb buds.* Dev Cell, 2009. **16**(4): p. 607-13.
170. Ho, C.Y., *Hypertrophic cardiomyopathy in 2012.* Circulation, 2012. **125**(11): p. 1432-8.
171. Saucerman, J.J. and A.D. McCulloch, *Cardiac beta-adrenergic signaling: from subcellular microdomains to heart failure.* Ann N Y Acad Sci, 2006. **1080**: p. 348-61.
172. Backx, P.H., et al., *Mechanism of force inhibition by 2,3-butanedione monoxime in rat cardiac muscle: roles of [Ca2+]i and cross-bridge kinetics.* J Physiol, 1994. **476**(3): p. 487-500.
173. Flagg, T.P., et al., *Ca2+-independent alterations in diastolic sarcomere length and relaxation kinetics in a mouse model of lipotoxic diabetic cardiomyopathy.* Circ Res, 2009. **104**(1): p. 95-103.
174. Koitabashi, N. and D.A. Kass, *Reverse remodeling in heart failure--mechanisms and therapeutic opportunities.* Nat Rev Cardiol, 2012. **9**(3): p. 147-57.
175. Fifer, M.A. and G.J. Vlahakes, *Management of symptoms in hypertrophic cardiomyopathy.* Circulation, 2008. **117**(3): p. 429-39.

176. Marian, A.J., *Contemporary treatment of hypertrophic cardiomyopathy.* Tex Heart Inst J, 2009. **36**(3): p. 194-204.
177. Teekakirikul, P., et al., *Cardiac fibrosis in mice with hypertrophic cardiomyopathy is mediated by non-myocyte proliferation and requires Tgf-beta.* J Clin Invest, 2010. **120**(10): p. 3520-9.
178. Zheng, M., et al., *Sarcoplasmic reticulum calcium defect in Ras-induced hypertrophic cardiomyopathy heart.* Am J Physiol Heart Circ Physiol, 2004. **286**(1): p. H424-33.
179. Winegrad, S., *Regulation of cardiac contractile proteins. Correlations between physiology and biochemistry.* Circ Res, 1984. **55**(5): p. 565-74.
180. Layland, J., R.J. Solaro, and A.M. Shah, *Regulation of cardiac contractile function by troponin I phosphorylation.* Cardiovasc Res, 2005. **66**(1): p. 12-21.
181. Jideama, N.M., et al., *Dephosphorylation specificities of protein phosphatase for cardiac troponin I, troponin T, and sites within troponin T.* Int J Biol Sci, 2006. **2**(1): p. 1-9.
182. Deshmukh, P.A., B.C. Blunt, and P.A. Hofmann, *Acute modulation of PP2a and troponin I phosphorylation in ventricular myocytes: studies with a novel PP2a peptide inhibitor.* Am J Physiol Heart Circ Physiol, 2007. **292**(2): p. H792-9.
183. Yang, F., D.L. Aiello, and W.G. Pyle, *Cardiac myofilament regulation by protein phosphatase type 1alpha and CapZ.* Biochem Cell Biol, 2008. **86**(1): p. 70-8.
184. Wijnker, P.J., et al., *Protein phosphatase 2A affects myofilament contractility in non-failing but not in failing human myocardium.* J Muscle Res Cell Motil, 2011. **32**(3): p. 221-33.
185. Kolupaeva, V., E. Laplantine, and C. Basilico, *PP2A-mediated dephosphorylation of p107 plays a critical role in chondrocyte cell cycle arrest by FGF.* PLoS One, 2008. **3**(10): p. e3447.
186. Dougherty, M.K., et al., *Regulation of Raf-1 by direct feedback phosphorylation.* Mol Cell, 2005. **17**(2): p. 215-24.
187. Lao, D.H., et al., *Direct binding of PP2A to Sprouty2 and phosphorylation changes are a prerequisite for ERK inhibition downstream of fibroblast growth factor receptor stimulation.* J Biol Chem, 2007. **282**(12): p. 9117-26.
188. Robinson, P., et al., *Dilated and hypertrophic cardiomyopathy mutations in troponin and alpha-tropomyosin have opposing effects on the calcium affinity of cardiac thin filaments.* Circ Res, 2007. **101**(12): p. 1266-73.
189. Wang, Y., et al., *Generation and functional characterization of knock-in mice harboring the cardiac troponin I-R21C mutation associated with hypertrophic cardiomyopathy.* J Biol Chem, 2012. **287**(3): p. 2156-67.
190. Semsarian, C., et al., *The L-type calcium channel inhibitor diltiazem prevents cardiomyopathy in a mouse model.* J Clin Invest, 2002. **109**(8): p. 1013-20.
191. Gonzalez, A., et al., *New targets to treat the structural remodeling of the myocardium.* J Am Coll Cardiol, 2011. **58**(18): p. 1833-43.
192. Penela, P., C. Ribas, and F. Mayor, Jr., *Mechanisms of regulation of the expression and function of G protein-coupled receptor kinases.* Cell Signal, 2003. **15**(11): p. 973-81.
193. Lau, J.M., et al., *The 14-3-3tau phosphoserine-binding protein is required for cardiomyocyte survival.* Mol Cell Biol, 2007. **27**(4): p. 1455-66.
194. Tarnavski, O., et al., *Mouse cardiac surgery: comprehensive techniques for the generation of mouse models of human diseases and their application for genomic studies.* Physiol Genomics, 2004. **16**(3): p. 349-60.
195. Li, H., et al., *Regulator of G protein signaling 5 protects against cardiac hypertrophy and fibrosis during biomechanical stress of pressure overload.* Proc Natl Acad Sci U S A, 2010. **107**(31): p. 13818-23.
196. Meguro, T., et al., *Cyclosporine attenuates pressure-overload hypertrophy in mice while enhancing susceptibility to decompensation and heart failure.* Circ Res, 1999. **84**(6): p. 735-40.
197. Yang, G., et al., *Cyclosporine reduces left ventricular mass with chronic aortic banding in mice, which could be due to apoptosis and fibrosis.* J Mol Cell Cardiol, 2001. **33**(8): p. 1505-14.
198. Teranishi, F., et al., *Phosphoinositide 3-kinase inhibitor (wortmannin) inhibits pancreatic cancer cell motility and migration induced by hyaluronan in vitro and peritoneal metastasis in vivo.* Cancer Sci, 2009. **100**(4): p. 770-7.
199. Zhang, H.X., et al., *HMR 1098 is not an SUR isotype specific inhibitor of heterologous or sarcolemmal K ATP channels.* J Mol Cell Cardiol, 2011. **50**(3): p. 552-60.